



<https://theses.gla.ac.uk/>

Theses Digitisation:

<https://www.gla.ac.uk/myglasgow/research/enlighten/theses/digitisation/>

This is a digitised version of the original print thesis.

Copyright and moral rights for this work are retained by the author

A copy can be downloaded for personal non-commercial research or study,  
without prior permission or charge

This work cannot be reproduced or quoted extensively from without first  
obtaining permission in writing from the author

The content must not be changed in any way or sold commercially in any  
format or medium without the formal permission of the author

When referring to this work, full bibliographic details including the author,  
title, awarding institution and date of the thesis must be given

Enlighten: Theses

<https://theses.gla.ac.uk/>  
[research-enlighten@glasgow.ac.uk](mailto:research-enlighten@glasgow.ac.uk)

# INTERNAL FRICTION IN IRON-ALUMINIUM ALLOYS.

by

L.J. Paterson B.Sc., A.R.C.S.T.

Summary of Thesis submitted to the University of Glasgow  
for the Degree of Doctor of Philosophy.

A series of iron-aluminium alloys, with aluminium contents varying from 0.015 to 0.3%, were manufactured and their relaxation characteristics examined after nitriding and carburising. The examination was carried out on a specially constructed torsion pendulum which made use of specimens 0.03 inches in diameter. A vacuum casting unit and heat-treatment furnaces were built to produce specimens of this nature and subject them to the necessary processes of annealing, nitriding and carburisation.

This apparatus has allowed the author to confirm most of the reported information to be gained from the study of the internal friction due to stress-induced diffusion of interstitial nitrogen in pure iron.

The iron-aluminium-nitrogen system has been investigated and a metastable damping peak discovered. This has been attributed to the interaction of nitrogen atoms with distortions in the lattice due to a coherent precipitate of iron-aluminium nitride. Otherwise the observation of J.D. Fast (Metaux Corr. Indus., 1961, 36, 383 and 431), that there is no damping peak due to the interaction of aluminium and nitrogen in fully homogenised iron specimens at equilibrium, is confirmed.

ProQuest Number: 10647345

All rights reserved

INFORMATION TO ALL USERS

The quality of this reproduction is dependent upon the quality of the copy submitted.

In the unlikely event that the author did not send a complete manuscript and there are missing pages, these will be noted. Also, if material had to be removed, a note will indicate the deletion.



ProQuest 10647345

Published by ProQuest LLC (2017). Copyright of the Dissertation is held by the Author.

All rights reserved.

This work is protected against unauthorized copying under Title 17, United States Code  
Microform Edition © ProQuest LLC.

ProQuest LLC.  
789 East Eisenhower Parkway  
P.O. Box 1346  
Ann Arbor, MI 48106 – 1346

The aluminium alloys were manufactured from material containing oxygen and were reduced by carbon additions. The subsequently formed aluminium carbide contributed to a lack of success in calculating the solubility of aluminium nitride in alpha-iron. The other factor in this failure was the fact that equilibrium was not achieved. Had equilibrium been fully achieved it is in fact doubtful if the internal friction technique would be sensitive enough to measure the very low solid solubilities of nitrogen in this case.

In view of the interference of carbon in the experiments of this work it would be advisable to deoxidise future alloys with hydrogen where there is the possibility of the formation of a stable carbide of the alloying element. However the interaction of nitrogen and carbon discovered in this work is of interest since the presence of carbon and nitrogen in solid solution are of great importance in determining the mechanical properties and in particular the high temperature creep properties, of steels. This interaction might usefully be studied using an internal friction technique.

Computer techniques were developed to analyse the complex damping curves found in this work. These techniques may prove to be of importance in future work in the field of internal friction studies.

INTERNAL FRICTION IN IRON-ALUMINIUM ALLOYS.

by

L.J. Paterson, B.Sc., A.R.C.S.T.

Thesis submitted to the University of Glasgow for the  
Degree of Doctor of Philosophy.

February, 1964.

# I N D E X.

Page No.

## PART 1. INTRODUCTION.

Section 1.1	Introduction.	1
Section 1.2	Review of Theory of Internal Friction.	5
Section 1.3	Review of Previous Work.	15

## PART 2. DESCRIPTION AND USE OF APPARATUS.

Section 2.1	Vacuum Casting Unit.	27
Section 2.2	Heat Treatment Furnaces.	33
Section 2.3	Internal Friction Apparatus: Torsion Pendulum.	38

## PART 3. USE OF APPARATUS.

Section 3.1	Manufacture of Alloys.	43
Section 3.2	Preparation of Specimens.	48
Section 3.3	Vacuum Annealing, Decarburisation, Nitriding and Carburisation	52
Section 3.4	Measurement of Internal Friction.	58
Section 3.5	Calculation and Computer Techniques.	64

## PART 4. APPENDICES, TABLES OF RESULTS.

Appendix 1.	Description of Computer Programmes	70
Appendix 2.	Description of Method of Nitrogen Analysis.	83
	Table of Results.	85
	Figures 1 to 37.	115

PART 5. DISCUSSION OF RESULTS.

Section 5.1	Introduction.	149
Section 5.2	The Snoek Peak in Iron-Nitrogen Alloys.	150
Section 5.3	Diffusion of Nitrogen in Alpha- Iron.	153
Section 5.4	Solid Solubility of Nitrogen in Alpha-Iron.	154
Section 5.5	Damping in Iron-Aluminium- Nitrogen Alloys.	161
Section 5.6	Mechanism for the Secondary Peak.	173
Section 5.7	Solubility of Aluminium Nitride in Iron.	183
Section 5.8	Summary of Conclusions.	187
Section 5.9	Bibliography.	190

## PART 1 - INTRODUCTION.

### Section 1.1 Introduction.

One of the most significant trends in the steel industry since the Second World War has been the ever increasing demands made by the consumer industries for mild steel strip. Over one third of the total tonnage of steel produced in the United Kingdom to-day goes to the making of wide strip and strip mills have become synonymous with a high standard of living, associated as they are with motor cars, refrigerators and a vast range of tinned goods. Trade returns seem to indicate that this trend will continue as mild steel has no serious competitors for packaging and light construction purposes.

The majority of the industries using these large quantities of strip steel are highly automated and invariably their products require that the strip should have good deep-drawing properties. As such they must necessarily have strip with uniform mechanical and chemical properties. Chemical segregation, variations in grain size and differences in rates of age-hardening are three factors which must be clearly controlled if an automated production line is to be kept in smooth continuous operation. The onus is on the steel-maker to furnish a product which has to be consistent from ingot to ingot and from cast to cast.

In the motor car industry especially the consistency of the strip is of great importance. Manufacturers have been introducing body styles which have demanded that mild steel sheet be subjected to draws of difficulty. Thus maximum ductility at the time of pressing

cont'd...

is essential and age-hardening must be kept to a minimum.

The phenomenon of ageing in steel has been well known if not well understood since the beginning of this century<sup>1</sup>. With respect to steel making it may be described as a move towards equilibrium from an unstable condition resulting mainly from the retention of nitrogen in solid solution in the ferrite. Morica<sup>2</sup> and Koster<sup>3</sup> in the early 1930's established that this nitrogen eventually precipitates and causes embrittlement of the metal. It would appear desirable therefore to produce a steel with no nitrogen in solid solution or alternatively to neutralise the effect of nitrogen. It is impracticable to produce nitrogen-free steel on a large industrial scale but it was found that additions of aluminium had the effect of reducing or even eliminating age-hardening due to nitrogen precipitation.

Aluminium had been used as an addition to steel for many years. Originally it was used, almost surreptitiously as a corrective for over-oxidised heats and was regarded as a means of compensating for poor furnace practice. At that time the view was held that any steel which contained aluminium was of inferior quality. In the 1930's reports of experimental work appeared which indicated that aluminium was effective in controlling grain size and in inhibiting ageing and the stigma associated with the use of aluminium as a deoxidant was finally removed.

cont'd...

It is now possible to produce steels by the use of oxygen, steam and the Linz-Donawitz process, to name three, whose nitrogen concentrations lie in the range  $4 \cdot 10^{-3}$  to  $8 \cdot 10^{-3}\%$ . At nitrogen levels in this range steels are still susceptible to age-hardening so that the grain refining and ageing inhibiting properties of aluminium are of importance.

It appears that if aluminium inhibits ageing in steels containing nitrogen in solid solution it must have a marked effect on the solubility of nitrogen in ferrite and on the rate of precipitation from ferrite. Some work has been done<sup>13,14,15,16</sup> on the effect of aluminium on the ageing, notch ductility and temper brittleness of steels containing nitrogen. The reports have often been conflicting and clouded with uncertainties. It would appear that the effectiveness of aluminium depends on the state of deoxidation of the metal and on what other alloying elements are present. It was decided therefore that this present work should be undertaken to study the interaction of aluminium and nitrogen atoms in iron in an attempt to help clarify the situation since these interactions are of obvious theoretical and practical importance.

An experimental technique which would yield an effective method of measuring the amount of nitrogen in solid solution as distinct from total nitrogen content is to be found in the anelastic effects, commonly known as internal friction, caused by the presence of interstitial solute atoms in body centre cubic lattices. It has been found<sup>11</sup> that nitrogen atoms in solid solution in alpha-iron produce

cont'd...

internal friction effects which are directly proportional to the amount of nitrogen in solid solution. Hence the measurement of internal friction phenomena provides a method of ascertaining the nitrogen in solid solution as nitrogen which has precipitated does not contribute towards internal friction. Further, the interaction of alloying elements and nitrogen has been found to produce internal friction effects distinguishable from those of nitrogen in iron alone<sup>54</sup> and the effect of alloy additions on the solubility of nitrogen in iron can also be studied by this method. A summary of the theoretical background of the study of internal friction due to solute atoms will be found in Section 1.2.

## Section 1.2

### Review of the Theory of Internal Friction.

The classical theory of elasticity implies a linear relationship between stress and strain. Such a relationship does not in fact exist for real metals. A well known example of the departure of metals from the classical theory is the elastic "after-effect" on loading and unloading or recoverable creep under constant stress. Internal friction is another example. It was Zener<sup>4</sup> in a definitive survey of these phenomena who coined the term "anelasticity". By his definition anelastic phenomena exist where strain is not a function only of stress. In fact where anelastic effects are present strain lags behind stress in time.

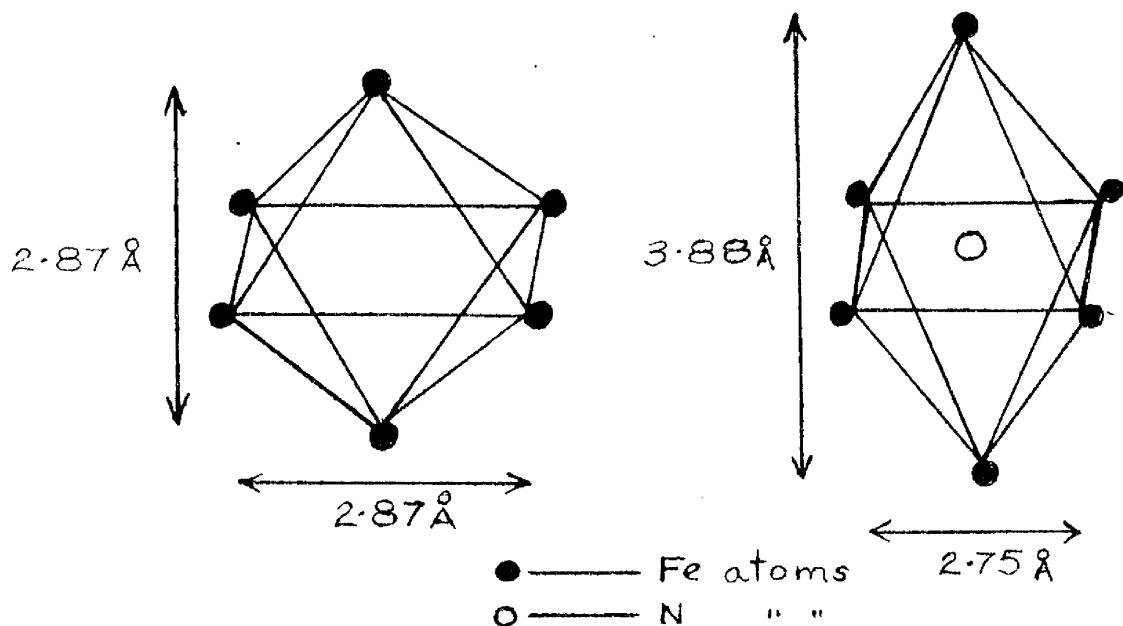
From the above definition it is apparent that any physical change in a metal produced by an applied stress will cause internal friction if the subsequent strain is out of phase with the applied stress. Such stress induced phenomena include intercrystalline thermal currents<sup>5,6</sup>, stress induced viscous slip<sup>7</sup> and stress induced diffusion of atoms. It is the last of these with respect to interstitial atoms in solid solution that makes the measurement of internal friction such a powerful tool in this present work.

It was Richter<sup>8,9</sup> who in 1937, first discovered an elastic after-effect in iron which had first exhibited a magnetic after-effect or magnetic hysteresis. His work was confirmed by Snoek<sup>10,11</sup> who discovered that the elastic after-effect was due to small amounts of carbon and nitrogen, but only when they were in solid solution.

cont'd...

The magnetic and elastic after-effects he postulated were merely different manifestations of the same phenomenon. It followed therefore that since only those atoms in solid solution contributed to internal friction the metallurgist had a unique method of determining the amount in solid solution and of following the course of precipitation of the interstitial from solid solution.

Snoek further postulated that this internal friction was due to stress induced diffusion of carbon and nitrogen atoms between interstitial positions in the body centre cubic alpha-iron. In alpha-iron nitrogen tends to occupy the interstitial position  $(\frac{1}{2}, \frac{1}{2}, 0)$  in the unit cell<sup>12</sup> and produces lattice distortion along the tetragonal axis as shown below:-



In a stress free specimen atoms will be distributed equally among interstices having their tetragonal axis parallel to any one of the three major axes of the cell. However when a stress is applied along the x - axis, for example, there will be a greater probability that the solute atoms will move to interstitial positions whose tetragonal symmetry is along the x - axis, than in the unstressed condition. Time is obviously required for the nitrogen atoms to diffuse back to their random positions after the stress has been removed. Hence the strain lags behind the stress giving rise to internal friction and other anelastic effects.

It becomes apparent from the above model that the process involves the diffusion of interstitial atoms over atomic distances. The relaxation time for atomic diffusion is given by the exponential equation,

$$\tau = \tau_0 \exp. \frac{dH}{RT} \dots\dots\dots (1)$$

where  $\tau_0$  is a constant, R, the gas constant, T, the temperature in degrees Kelvin and dH, the activation energy for the diffusion process. It is in supplying the activation energy for diffusion to the pre-stressed equilibrium that energy is dissipated. It is this dissipation of energy that gives rise to the best known phenomenon of relaxation processes; damping. The terms damping and internal friction are synonymous. In this present work, the damping of a freely oscillating system was used to determine the elastic after-effect and hence the amount of nitrogen in solid solution.

cont'd...

Snook used the tangent of the phase displacement between stress and strain to define the internal friction as a function of the relaxation time. He derived the expression,

$$\tan \phi = \frac{e_1}{e_0} \cdot \frac{w\tau}{1 + (w\tau)^2} \dots\dots\dots (2)$$

where  $\phi$  is the angle of displacement,  $w$  is the angular frequency of testing,  $e_0$  is an elastic constant of the metal and  $e_1$  is proportional to the amount of nitrogen in solid solution. The simplest way to measure internal friction is to divide the logarithmic decrement of a freely oscillating system by  $\pi$ . This is in fact equal to  $\tan \phi$  and is referred to as  $Q^{-1}$  by analogy with electrical oscillations. Hence we have the following expression:-

$$Q^{-1} = \frac{\tan \phi}{\pi} = \frac{e_1}{e_0} \cdot \frac{w\tau}{1 + (w\tau)^2} \dots\dots\dots (3)$$

When it is remembered that  $\tau = \tau_0 \exp. dH/RT$  it can be seen that the internal friction is strongly temperature dependent. At low temperatures the relaxation time is very large, for any given value of  $\tau_0$ . At these temperatures practically nothing has been relaxed in the period of the application of the stress and stress and strain are therefore practically in phase. As a result  $Q^{-1}$  is small. At high temperatures  $\tau$  is so small that relaxation will be complete well within the period of application of the stress. Again stress and strain will be virtually in phase and  $Q^{-1}$  will be small. Only at intermediate temperatures where the relaxation time is comparable with the period of the application of stress will there be relaxation and  $Q^{-1}$  will be large.

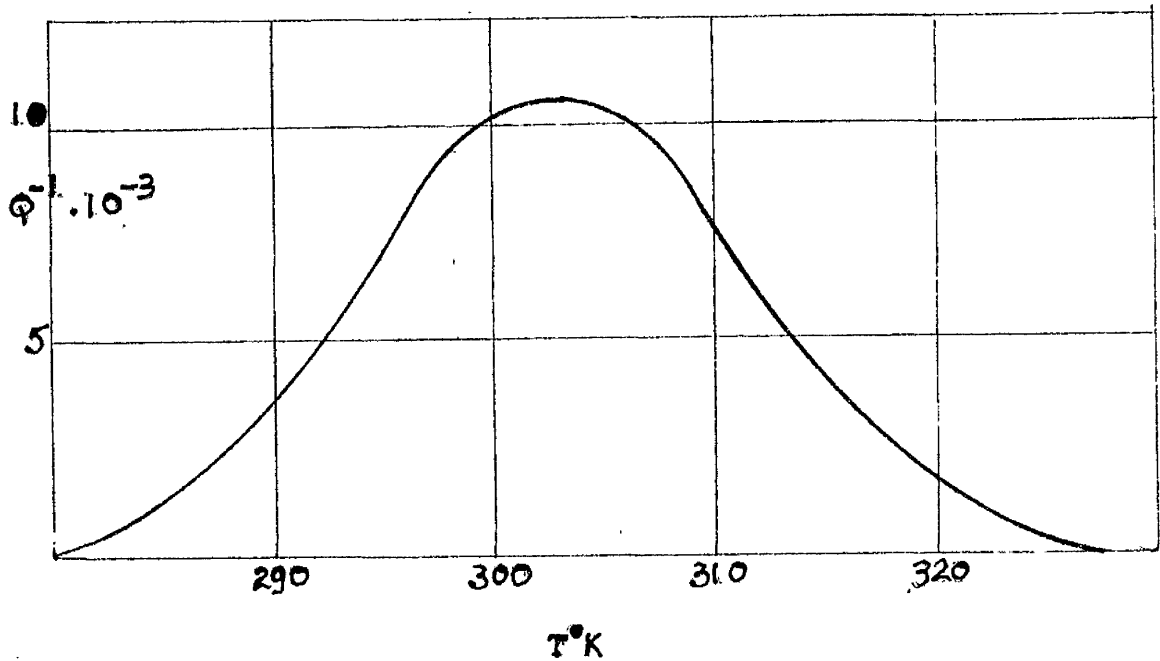
cont'd...

The conditions for maximum  $Q^{-1}$  value can be determined mathematically.  $Q^{-1}$  will be largest where the rate of change of  $Q^{-1}$  with  $w$  and  $\tau$  is zero. By differentiating equation (3) we find that  $Q^{-1}$  is a maximum where  $w\tau = 1.0$ . From this we obtain:

$$\tau = \frac{1}{w} = \frac{1}{2\pi f}$$

where  $f$  is the linear frequency of oscillation.

It also follows that a plot of  $Q^{-1}$  against temperature for a constant frequency will have a maximum at the temperature where  $w\tau$  is unity. An example of a damping curve due to interstitial nitrogen in iron is shown below:-



The value of  $Q^{-1}$  at this point,  $Q_m^{-1}$  is therefore given by the expression,

$$Q_m^{-1} = \frac{e_1}{e_0} \cdot \frac{1}{2} \text{ according to equation (3)}$$

from which it follows that,

$$Q^{-1} = \frac{2Q_m^{-1} w \tau}{1 + (w \tau)^2} \dots\dots\dots(4)$$

From equations (1) and (4) it is possible to calculate a theoretical curve knowing the maximum value of  $Q^{-1}$ , the value of  $dH$  and the temperature of the maximum. The use of the two equations is however cumbersome and they may be combined as shown below:-

For a given frequency the ratio of the maximum  $Q^{-1}$  value to the value of  $Q^{-1}$  at temperature  $T^{\circ}K$  is,

$$\frac{Q_m^{-1}}{Q^{-1}} = \frac{1 + (w \tau)^2}{2w \tau} = \frac{(w \tau)^{-1} + (w \tau)}{2}$$

Now since  $\cosh x = \frac{e^{-x} + e^x}{2}$

$$\frac{Q_m^{-1}}{Q^{-1}} = \cosh (\ln w \tau)$$

Given that  $T = T_0 \exp \frac{dH}{RT} \dots\dots\dots(1)$

then  $\ln \tau = \ln T_0 + \frac{dH}{RT}$

$\therefore \frac{Q_m^{-1}}{Q^{-1}} = \cosh (\ln w T_0 + \frac{dH}{RT})$

cont'd...

At the peak maximum,  $T = \frac{1}{\omega} \exp. \frac{-dH}{RT_m}$

$\therefore T_0 = \frac{1}{\omega}$

where  $T_m$  is the temperature at the maximum  $Q^{-1}$  value

$$\therefore \frac{Q_m^{-1}}{Q^{-1}} = \cosh \left( \frac{-dH}{RT_m} + \frac{dH}{RT} \right)$$

$$= \cosh \left\{ \frac{dH}{R} \left( \frac{1}{T} - \frac{1}{T_m} \right) \right\}$$

or  $Q^{-1} = \frac{Q_m^{-1}}{\cosh \left\{ \frac{dH}{R} \left( \frac{1}{T} - \frac{1}{T_m} \right) \right\}} \dots \dots \dots (5)$

Equation (5) allows the definition of a relaxation curve in terms of its three most important parameters, the height of the peak, the temperature of the occurrence of its peak and the activation energy of the process of atomic movement involved. Equation (5) was the one used throughout this work.

While equation (5) allows the calculation of the heat of activation from one single curve at one single frequency it is possible to calculate the value of  $dH$  from the shift in the temperature at which  $Q_m^{-1}$  occurs, with frequency.

At the peaks of two curves which occur at temperatures  $T_1$  and  $T_2$  for frequencies  $\omega_1$  and  $\omega_2$  we have,

cont'd...

$$v_1 \tau_1 = 1 = v_2 \tau_2$$

$$\therefore \frac{v_1}{v_2} = \frac{\tau_2}{\tau_1}$$

$$= \frac{\tau_0 \exp \frac{dH}{RT_2}}{\tau_0 \exp \frac{dH}{RT_1}}$$

$$\ln \frac{v_1}{v_2} = \frac{dH}{R} \left( \frac{1}{T_2} - \frac{1}{T_1} \right)$$

$$\ln \left( \frac{f_1}{f_2} \right) = \frac{dH}{R} \left( \frac{1}{T_2} - \frac{1}{T_1} \right)$$

$$dH = \frac{R \ln \left( \frac{f_1}{f_2} \right) T_2 \cdot T_1 \dots \dots \dots (6)}{T_1 - T_2}$$

Equation (6) yields yet another method of calculating the activation energy of the process of atomic movement.

The location of the peak of a plot of  $Q^{-1}$  against temperature in degrees Kelvin produces useful information about diffusion rates and diffusion coefficients. If the movement of atoms in the internal friction process is regarded as a random walk problem in a body centre cubic lattice we have  $D$ , the diffusion rate, given by the relationship,

$$D = \frac{\lambda^2}{6\tau} \dots \dots \dots (7)$$

where  $\lambda$  is the distance an atom jumps in the anelastic process and where  $\tau$  is the average time of stay in a given lattice site.

$\lambda$  is in fact half a unit cell of  $\frac{a}{2}$  where  $a$  is the lattice parameter. Wert<sup>20</sup> has shown that  $\tau^{-1}$  is related to the relaxation time  $\tau$ , thus  $\tau^{-1} = \frac{3}{2}\tau$

Thus equation (7) becomes  $D = \frac{a^2}{36\tau}$

At the peak  $w\tau = 1.0$  and so  $D$  is readily calculated and can be used for the evaluation of  $D_0$  in the classic diffusion equation  $D = D_0 \exp \frac{dH}{RT}$ , where  $D$  is the diffusion coefficient and  $D_0$  a constant.

As previously mentioned the actual value of the peak height,  $Q_m^{-1}$ , is of considerable importance. From equation (3) it can be seen that the peak value  $Q_m^{-1}$  is  $\frac{e_1}{2e_0}$  where  $e_0$  is an elastic constant and  $e_1$  is directly proportional to the amount of interstitial atoms in solid solution. Therefore a direct relationship exists between  $Q_m^{-1}$  and the number of atoms present and hence the weight percentage of interstitial element in solid solution. This may be expressed in the following way,

$$N(\text{wt}\%) = K Q_m^{-1} \text{ where } K \text{ is a constant.}$$

In the case of nitrogen in alpha-iron the average value of  $K$  from the results of several workers<sup>21,22</sup> is 1.28.

In summary the following information can be obtained from a single relaxation curve i.e. from a plot of  $Q^{-1}$  against temperature, for a given frequency;

- 1) The activation energy of the process of diffusion involved in the anelastic effect where the effect is due to interstitial solute atoms. In this present work this will be nitrogen in

cont'd...

in iron or iron-aluminium alloys.

- 2) The diffusion coefficient for the process.
- 3) The weight percentage of nitrogen in interstitial solid solution for any given set of conditions.

There is therefore considerable application for internal friction techniques to problems of solid solubility and precipitation. A review of the work previously done by the application of the technique to the behaviour of nitrogen in interstitial solid solution in iron will be found in the following section.

### Section 1.3

#### Review of Previous Work.

As indicated in the previous section the investigations and theories of Snoek<sup>10,11</sup> laid the foundations of all the internal friction work which has since been done on solid solutions of carbon and nitrogen in alpha-iron. What has since become known as the Snoek effect is caused by the redistribution, under an external force, of solute atoms among the interstices of a body centre cubic lattice and the subsequent diffusion of these solute atoms to re-establish equilibrium after the removal of the external force. Snoek's hypothesis indicated that the damping so caused was proportional to the number of solute atoms present and that it was an anisotropic property. Polder<sup>34</sup> worked out Snoek's theory in more detail and derived a formula for the elastic after-effect in terms of the elastic constants of the cubic crystal and the calculated components of strain due to an applied stress on a single crystal. This expression gave the same results as Snoek. Shortly afterwards Ke<sup>23</sup> provided additional corroborative evidence in that body centre cubic materials exhibited relaxation phenomena when carbon, nitrogen and oxygen were present in solid solution, indicating that such phenomena are characteristic of interstitial solid solutions of body-centre cubic metals.

The theory of interstitial damping was now well-substantiated and studies of low temperature diffusion, solid solubility and the related phenomena of precipitation could be investigated in a

unique manner.

Ke<sup>64</sup> investigated the damping characteristics produced in alpha-iron by nitrogen between room temperature and recrystallisation temperature at a frequency of one cycle per second. He found three internal friction peaks at 20, 225 and 490°C. The first is due to the Snoek effect, the second appeared after the specimen had been cold-worked and the third is caused by grain-boundary relaxation, according to Ke's analysis.

Using formula (6) of section 1.2,

$$\ln \left( \frac{f_2}{f_1} \right) = \frac{dH}{R} \left( \frac{1}{T_1} - \frac{1}{T_2} \right)$$

Ke calculated the activation energy for the diffusion of nitrogen whose peak was at 20°C to be 20 Kcals/mole, to an accuracy of ten per cent. This value is higher than the 16.4 Kcals/mole assumed by Snoek on the basis of his magnetic after-effect experiments.

Several workers have determined dH values and these are summarised in Table 1. Most workers have reported dH values in the region of  $18 \pm 2$  Kcals/mole and have placed the internal friction peak around 20°C at a frequency of one cycle per second. When using the values quoted in Table 1 in conjunction with equation (6) they do not produce consistent results when calculating the position of the peak for any given frequency. The data of Fast and Verrijp<sup>44</sup> was always closest to the average of the results of the calculations, as can be seen from Table 1(a). For this reason their data was used for predicting the peak temperature in the present work.

Equation (7) of the preceding section allows the calculation of the diffusion coefficient of the interstitial in the metal from an experimentally determined value of the relaxation time. This is found from the position of the maximum damping where  $\omega\tau$  is equal to unity. In this manner Bert<sup>42, 43</sup> studied the diffusion of carbon in alpha-iron between 25 and 200°C obtaining a value of  $D_0$  for the expression,

$$D = D_0 \exp. \frac{dH}{RT}$$

He found  $D_0 = 2 \times 10^{-3} \text{ cm}^2/\text{second}$  with a  $dH$  value of 20.1 Kcal/mole while Past and Verrijp<sup>44</sup> obtained a value of  $D_0 = 7 \times 10^{-3} \text{ cm}^2/\text{second}$  with a  $dH$  value of 18.6 Kcal/mole for nitrogen. Both agree well with values extrapolated from the results of conventional diffusion experiments at higher temperatures.

The determination of the solid solubilities of carbon or nitrogen from the peak heights of internal friction curves depends on the theories expounded in section 1.2. Once the peak height has been obtained the solubility can be found if the constant of proportionality is found. Forder's<sup>34</sup> work gives a theoretical value for this constant for single crystals and Smit and Van Gueren's<sup>36</sup> for polycrystalline solids. This latter gives the weight per-centage nitrogen as

$$\%N = \frac{\frac{1}{dH} \times T}{2.2 \times 10^{-2}}$$

which corresponds to 1.33 at 20°C. Most workers have preferred to determine this value experimentally by direct comparison of  $\frac{1}{dH}$  with chemical analysis and have found values of 1.26 to 1.30<sup>33,47,48,49</sup>.

cont'd...

Dijkstra<sup>21</sup> in following the course of precipitation of carbon and nitrogen from solid solution in alpha-iron discovered that nitrogen precipitated in two stages if ageing was carried out below 300°C. His suggestion of the formation of another iron-nitrogen phase apart from Fe<sub>4</sub>N was supported by X-ray investigations of Jeck<sup>48</sup> who designated the phase Fe<sub>3</sub>N.

Dijkstra's results gave the heat of solution of Fe<sub>4</sub>N in alpha-iron as 8 Kcal/mole and that of Fe<sub>3</sub>N as 10 Kcal/mole. Although these heats of solution did not agree with Koster's<sup>3</sup> they were supported by later work<sup>33</sup>. An extrapolation of Dijkstra's data gives a maximum solid solubility for nitrogen as 0.10% wt. at 590°C. and for carbon as 0.025% wt. at 723°C.

Using a method of isothermal calorimetry Borelius et al<sup>45</sup> had obtained solubility figures for nitrogen which differed from Dijkstra's<sup>21</sup> by a factor of two. In attempting to account for this Astrom and Borelius<sup>50</sup> repeated the calorimetric experiments. Though correcting the previous results they obtained new values which deviated from Dijkstra's to an extent that led them to suggest that in fact  $\frac{d\mu}{dN}$  was not directly proportional to the amount of dissolved nitrogen. Their calorimetric results were supported by relaxation measurements on a nitrated spring coil where the nitrogen was calculated by increase in weight. Their observations were a direct contradiction of the theories of Snoek<sup>10,11</sup> and Polder<sup>34</sup>. Support for Snoek and Polder was almost immediately forthcoming from the

cont'd...

independent studies of Fast and Verrijp<sup>33</sup> and Rawlings and Tambini<sup>48</sup>, all of whom used internal friction methods.

Fast and Verrijp were studying the solubilities of nitrogen in alpha-iron in equilibrium with the iron nitrides  $Fe_4N$  and  $Fe_8N$  and in equilibrium with gaseous nitrogen at one atmosphere pressure. They produced the following expressions for the solubility  $Q$ ,

$$Q(Fe_4N) = 12.3 \exp\left(\frac{-8300}{RT}\right) \text{ wt.}\%$$

$$Q(N_2:1 \text{ atm}) = 9.8 \cdot 10^{-2} \exp\left(\frac{-7200}{RT}\right) \text{ wt.}\%$$

$$Q(Fe_8N) = 3.3 \cdot 10^2 \exp\left(\frac{-2900}{RT}\right) \text{ wt.}\%$$

From the first two equations the dissociation pressure of  $Fe_4N$  is given by,

$$pN_2(Fe_4N) = 1.6 \cdot 10^4 \exp\left(\frac{-2200}{RT}\right) \text{ atm.}$$

which is in reasonable agreement with Bennett et al<sup>60</sup> who used methods of chemical analysis. Using Dijkstra's results in a similar calculation the solubility in equilibrium with  $Fe_4N$  is given by,

$$Q(Fe_4N) = 7.5 \exp\left(\frac{-7700}{RT}\right) \text{ wt.}\%$$

The results of Paranjpe et al<sup>51</sup> and Corney and Tarakdogan<sup>53</sup> show an even better agreement with Fast and Verrijp. Their equation of the solubility in equilibrium with gaseous nitrogen agrees well with the results of Sieverts et al<sup>52</sup>. Their heat of solution of  $Fe_8N$  is 10 Kcals/mole and is 2 Kcals/mole higher than that obtained by Dijkstra who found both  $Fe_4N$  and  $Fe_8N$  to have a heat of solution of

cont'd...

8 Kcal/mole.

Rawlings and Tambini<sup>48</sup> carried previous investigations to their logical conclusion and determined the alpha-iron/ $\text{Fe}_4\text{N}$  phase boundaries by internal friction methods and found excellent agreement between their results and previous work placing the eutectoid temperature at  $590^\circ\text{C}$  with a maximum solid solubility of 0.10% nitrogen by weight.

In summary, it may be said at this point that Snoek's theories had been substantiated and that the application of his theories to a study of the solubilities of carbon and nitrogen in alpha-iron had yielded results which were in good agreement with results obtained for these systems by other experimental methods. From this point onwards investigators concentrated on the effects of alloy additions on the solubility of nitrogen in iron as measured by internal friction methods.

Dijkstra and Sladek<sup>54</sup> discovered that additions of 0.5 atomic per cent of manganese, chromium, molybdenum and vanadium had a marked effect on the characteristics of the iron-nitrogen damping curve. The shape of the damping versus temperature curve was modified in the case of manganese and chromium and with molybdenum and vanadium two distinct peaks were observed. In each case the curve was resolved into two component peaks one of which had the characteristics of the normal Snoek peak for an iron-nitrogen system. The second peak, which in each case was at a higher temperature than the iron-nitrogen, was claimed by Dijkstra and Sladek to be due to the presence of atoms of the alloying element. The Snoek peak is due to the diffusion of nitrogen atoms between iron-iron interstices and the other, it is

suggested is due to diffusion of nitrogen atoms between an iron-iron interstice and an iron-manganese interstice, for example. They postulated that one of the atoms of the tetrahedron of iron atoms surrounding the interstitial nitrogen is replaced by a manganese atom and that this system has a lower free energy level for a nitrogen atom. The nitrogen atom therefore finds it easier to diffuse to such an interstice. This theory implies that there is another relaxation time and a different activation energy associated with diffusion of this nature.

This work of Dijkstra and Sladek had been done to investigate a report by Fast<sup>55</sup> that manganese broadened the internal friction peak and inhibited the precipitation of nitrogen from saturated solid solution. It is implied by Dijkstra and Sladek that quantities of dissolved nitrogen are associated with the alloying elements and that by studying the peak caused, their presence and their effect on the solubility of nitrogen can be qualitatively and perhaps quantitatively ascertained.

Work on an iron alloy containing 0.5 atomic per cent vanadium by Fast and Meijering<sup>56</sup> confirmed the effects, found by Dijkstra and Sladek. They obtained the Snoek peak at 21.5°C and a second peak in the region of 80-90°C, for a frequency of one cycle per second. On progressively increasing the time of nitriding the second peak rose higher than the normal Snoek peak. It reached a maximum after several hours after which the Snoek peak began to rise. Fast later<sup>57</sup> concluded that the second peak was due to vanadium solubility in gamma-iron

although initially he had attributed the effect to the presence of vanadium nitride. He finally concluded that there was no peak due to diffusion between iron-iron and iron-vanadium interstices at lower temperatures as nitrogen combined preferentially to form vanadium nitride and caused no damping.

Leak et al.<sup>50</sup> undertook a study of an iron-silicon-nitrogen system (containing 2.83 weight per cent silicon) by internal friction techniques. They found two reproducible peaks, with the existence of a third suspected. The peak at 22°C had the activation energy value of 10 Kcal/mole corresponding to the normal iron-nitrogen peak. The second peak which occurred at 37°C had a value of 12 Kcal/mole. The diffusion coefficient of nitrogen associated with the second peak was calculated and found to be the same as that of nitrogen in pure iron. No data was reported for the problematical third peak. The silicon addition was found to have lowered the solubility, as compared with that in pure iron by a factor of ten. Below 700°C the amount of nitrogen associated with purely iron sites, as indicated by the height of the Snoek peak, was negligible, indicating a preference of nitrogen for silicon. Their solubility results compare well with those of Corney and Turkdogan<sup>53</sup>.

Leak et al postulated that the energy barrier for a nitrogen atom going from iron-silicon sites to iron-iron sites is greater than for movement in the opposite direction. In other words they suggest that diffusion from iron-silicon to iron-iron requires a larger activation energy than the diffusion of nitrogen through pure iron. The

activation energies calculated for the peaks due to manganese etc. in Dijkstra's work<sup>54</sup> are of the order of 18 Kcals/mole and their own activation energy of 12 Kcals/mole for their silicon peak are therefore, according to their theory, incompatible with movement of nitrogen from iron-iron sites to iron-silicon sites, or in Dijkstra's case from iron-iron to iron-manganese. A value of 12 Kcals/mole is compatible however with the iron-silicon to iron-iron process that Leak et al claim for the second peak at 37°C.

Rawlings and Robinson<sup>59</sup> examined an iron/silicon/nitrogen system with silicon contents from 0.5 to 1.1 per cent silicon at one cycle/sec. They discovered three peaks at 25°C, 35°C and 62°C in addition to two others found only when the specimens were quenched from the gamma range. The first was the normal Snoek peak with an activation energy of 18.3 Kcals. The peak at 35°C corresponds to the second peak of Leak et al<sup>58</sup> for which they find an activation energy of 10 Kcals/mole by using equation (6).

$$\ln \left( \frac{f_2}{f_1} \right) = \frac{dH}{R} \left( \frac{1}{T_1} - \frac{1}{T_2} \right)$$

and a value of 30 Kcals/mole, for the same peak, from "the shape of the curve". The peak of 62°C, for which they offered no explanation has a dH value of 8.5 Kcals/mole from equation (6) and 80 Kcals/mole from the "shape of the curve". The values calculated from the shift in peak with frequency using equation (6) correspond with Leak et al but seem rather low to the author and their disparity with the values calculated from the shape of the curve (a method which they do not explain) are very surprising. Low dH values are characteristic of

cont'd...

very broad peaks which are often composed of more than one relaxation process and the possibility exists that peaks with values of 8.5 and 10 Kcals/mole can be further resolved into two or more components.

Laxar et al<sup>24</sup> in an investigation of ageing in low carbon steels found that the number of peaks increased as the aluminium content increased from 0.04 to 2.36 weight per cent. The internal friction results indicated the presence of three peaks in addition to the normal iron-carbon peak at 40°C. These abnormal peaks were found at 24, 67 and 87°C, at one cycle/second, and increased in size at the expense of the normal peak as the aluminium content increased. The activation energies found were 19, 21.8 and 23 Kcals/mole for the peaks at 24, 67 and 87°C respectively. The mechanism ascribed, by Laxar et al<sup>24</sup>, to the peak at 24°C is that of diffusion between iron-iron and iron-aluminium interstices on the basis that the lowest energy jump would be of this nature and would occur more easily than diffusion between iron-iron and iron-iron sites. The other peaks above the normal peak could be attributed to iron-aluminium to iron-iron diffusion or even to iron-aluminium to iron-aluminium diffusion where the aluminium concentration is high enough to introduce the possibility of aluminium atoms occupying adjacent lattice sites. However no information is available of the relative energy states of such sites and so there is no sound basis for deciding which process is responsible for which peak.

By comparison it would appear that more than two abnormal peaks should occur in an iron-silicon-nitrogen of comparable silicon composition and that activation energies of the order of 20 Kcals/mole and not

the 10 Kcal/mole obtained by Leak et al<sup>58</sup> and Rawlings and Robinson<sup>59</sup> This is what leads the author to believe that the peaks obtained in the iron-silicon-nitrogen systems could be further resolved. Certainly if more peaks of a higher activation energy were discovered in the case of Leak et al the objections of these workers to Dijkstra's mechanism would be removed.

When this present work was undertaken in 1960 it could be said that the basic mechanism of the theory of internal friction in the iron-nitrogen system was well understood. There was good agreement on such matters as the activation energy of nitrogen diffusion in iron, the diffusion coefficients for the process and the position of the internal friction peak for any given frequency and the solubility of nitrogen in alpha-iron. Investigations had been made in to the internal friction curves of ternary systems with iron-nitrogen as the basis and attempts had been made to resolve the resulting complex curves and ascribe mechanisms to them. As far as the author was aware no study had been made on the effects of aluminium on the solid solubility of nitrogen in iron apart from the work of Kula and Josefsson<sup>61</sup> and Flament<sup>62</sup> all of whom were working on iron-carbon-manganese-nitrogen-aluminium systems from which the effect of aluminium could not be isolated.

The work of Laxer et al<sup>24</sup> in their investigations on carbon had shown that the iron-aluminium-nitrogen system might also be of interest. From a purely thermodynamic point of view the appearance of abnormal peaks is rather unexpected. Aluminium carbide is a very stable compound and the chemical affinity of aluminium for carbon is much larger than that of iron for carbon, for example.

On these grounds it might be supposed that in a carbonised specimen the aluminium would be present as precipitated aluminium carbide and as such would make no contribution to damping. Aluminium nitride being an even more thermodynamically stable compound it might be expected that no damping other than the Snoek effect would be observed were it not for the fact that the aluminium-carbon system did exhibit abnormal damping. Fast in December 1961<sup>57</sup> indicated that in previously unpublished work he had failed to detect any other peak except the normal iron-nitrogen one in alloys containing 0.5 atomic per cent of titanium and aluminium. Now effects that are found with carbon are usually found with nitrogen and vice versa e.g. Collette's abnormal peak in iron-molybdenum-carbon<sup>63</sup> and Dijkstra's<sup>54</sup> in iron-molybdenum-nitrogen. Laxar's work had shown abnormal peaks with carbon and it was surprising that Fast found no abnormal ones with nitrogen. Because of these conflicting views it was considered that further investigation might substantiate or disprove these findings. This then was the background against which this present work was undertaken.

PART 2 - DESCRIPTION AND USE OF APPARATUS.Section 2.1 Vacuum Casting Unit.

Since an investigation of this nature was a new departure for the Metallurgy Department of the Royal College of Science and Technology all of the apparatus described in the following sections had to be designed, constructed and, in certain cases, calibrated before experimental work could proceed.

It was important that the alloys produced for this work should be free of gaseous impurities such as oxygen and nitrogen. Oxygen would combine with any aluminium added and nitrogen would give a false impression of the quantity of nitrogen added experimentally. The removal of both these gases from molten iron can be efficiently carried out under vacuum, either by physical or chemical methods.

The unit is shown in Figs.1 and 4. Basically it consists of a cylindrical vessel eighteen inches high and two feet in diameter which is evacuated by a three stage oil diffusion pump(r) backed by a single stage rotary pump(s). The diffusion pump (supplied by Vacuum Industrial Appliances Ltd.) has a pumping capacity of 800 litres per minute at a pressure of  $10^{-4}$  m.m. mercury and the Edwards' High Vacuum Rotary Pump a capacity of 700 litres per minute. The top of the vessel is detachable and is sealed by screws and an O-ring seal when the unit is in operation. In the top is a six inch diameter port over which an eighteen inch high silica sleeve (b) is fitted by a O-ring seal. The top of the sleeve was closed off from atmosphere by a water cooled metal cap, the seal again being made effective by

cont'd...

O-ring. Round the outer diameter of this sleeve is the copper coil from an induction heater. During melting of the metal the crucible (m) containing the charge was wound up in the sleeve into the region of the coil by means of a rack and pinion arrangement (1).

The crucible containing the charge is placed in the metal basket(K) illustrated in Fig.1, on top of the ratchet in its fully lowered position. The cylinder is then sealed off and evacuated. After the crucible is raised into the region of the induction coil the heater is switched on. When the charge is molten the crucible is returned to the basket and alloy additions made before the basket is tilted and the metal poured into a previously positioned mould. The cast is allowed to cool under vacuum before the system is opened to atmosphere.

The heating power was supplied by a Radyne medium frequency induction heater which operated at a frequency of about five Kilocycles per second. This heater was purchased after considerable difficulty had been experienced with glow discharge when using a high frequency (440 Kilocycles/second) induction heater. The discharge is caused by electrical breakdown of gas by the high frequency electromagnetic field of the induction coil. The effect becomes pronounced below 0.5 m.m. mercury and causes severe power losses. Burden<sup>29</sup> reported that the only adequate solution to the problem was to silver plate the inner walls of the furnace water cooling system. In the design used here this was not applicable and the problem was obviated by the use of a low frequency generator. This worked satisfactorily and the charge could usually be melted in approximately fifteen minutes.

cont'd...

The alloy additions are made by means of a small chute arrangement (u, in Fig.1). Four small conical containers are filled prior to sealing the cylinder. The containers are actually open at the bottom but since they rested on a plate they were effectively closed. The bottom plate has drilled in it a hole over the entrance to the chute. The containers are rotated by means of a handle (d, in Fig.1) and when they are over the entrance to the chute they discharge their loads into the lowered crucible.

The mould mentioned above was drilled from a cast iron block and produced an ingot one inch in diameter and six inches long. The ingot, complete with feeder head weighed just over two pounds. The mould is always preheated prior to casting by a nichrome resistance winding enclosed between two alumina sheaths. It was hoped to avoid the piping, and porosity to which a casting of such small dimensions was undoubtedly susceptible. These defects could usually be avoided by heating the mould to between 250°C and 300°C.

Measurement of pressure within the vessel is obtained by using an Edwards' High Vacuum Gauge in conjunction with a Pirani discharge tube and a Penning cold emission gauge. The Pirani is useful down to pressures of 0.05 m.m. of mercury and the Penning to lower than  $10^{-5}$  m.m. With the mould heater on to aid degassing, it is possible to reach pressures of  $10^{-5}$  m.m. mercury, without the aid of cold traps, approximately thirty minutes after sealing the vessel.

The crucibles used are six inches high with an internal diameter of two inches. The actual choice of refractory was arrived at only

after some initial difficulty. The refractoriness of magnesia seemed to indicate that it would be a good material to use and attempts were made to slip cast crucibles of this material. However, there were many failures due to the difficulty of separating crucibles of this size from the mould and the failure rate by cracking while drying and firing was also high.

Several trial runs were then made using recrystallised alumina crucibles. Any pick-up from these crucibles would be aluminium and for that reason and their good high temperature strength they were chosen. All of the crucibles tested failed soon after the melt out of the iron probably due to thermal shock.

Crucibles were then made with Zircosil ramming mixture, supplied by Associated Lead Development. Zircosil is a mixture of zirconium silicate with an ammonium phosphate bonding agent. The grey powder form in which it is supplied is simply mixed with water and pressed into a mould. It is dried overnight at a temperature of 200°C and fired to a white heat for an hour under vacuum in the vacuum casting unit using a carbon susceptor. This has the effect of driving off ammonia and forming a refractory complex of zirconium silico-phosphate. These crucibles proved very satisfactory in operation and had the advantage of being cheaper than any of the others previously used. They had however one serious disadvantage. Chemical analysis of the casts produced in the crucibles showed that the phosphorus content had risen from 0.001% in the original iron to 0.10% probably due to partial decomposition of the phosphate complex. Other

cont'd...

possibilities had therefore to be examined.

Associated Lead Development then produced a high-temperature sintered zirconium silicate crucible, but this was found to spall very easily. A pure zirconia crucible was then supplied by Associated Lead. These crucibles had none of the faults of their other products and in addition could not be reduced by aluminium, since zirconia has a higher negative free energy of formation at 1600°C than alumina. The solution finally reached was to use zirconia crucibles with an outer jacket of rammed Zircosil. This combination proved highly satisfactory and all casts referred to in the next section were made in these crucibles.

It was found necessary to use the outer jacket referred to above because of the initial difficulty experienced in melting the charge. This was due to an undesirable feature of the vacuum-unit which allowed excessive heat losses from the crucible by radiation through the walls of the silica sleeve. The design of the furnace was less than ideal in other respects. The whole unit had to be stripped down and disconnected from the induction heater to get the cast out so that the system did not lend itself to speed of operation.

Although the use of a medium frequency induction heater obviated the problem of glow discharge it created another problem. It appeared that there was a critical size for the pieces of Swedish iron used in the charge. The heater appeared incapable of melting pieces which differed greatly from a standard size of one and half inches square by half an inch thick.

cont'd...

Much helpful advice and practical aid in finally producing casts came from Vacuum Industrial Appliances Ltd., of Wishaw, to whom due acknowledgement is made.

## Section 2.2

### Heat Treatment Furnaces.

The alloys produced in the vacuum casting unit had to undergo three types of thermal treatment before use in the torsion pendulum. Firstly the alloys required annealing during their reduction to the 0.03 inches diameter needed for the pendulum. It is important that the specimens should not suffer oxidation when the cross-sectional area becomes quite small. Secondly since it was planned to use carbon as a deoxidant, decarburisation treatments with hydrogen would be required to remove any residual carbon. Finally, once the wires had been decarburised, nitrogen had to be introduced into solid solution, presumably by a gaseous reaction. It followed therefore that furnaces had to be designed which could operate under vacuum or with controlled gaseous atmosphere. Furnaces were built to meet these various demands and are shown in Figs. 2 and 5.

The furnaces were constructed in pairs, one pair horizontal and another pair vertical, to economise on pumping equipment. Each vertical furnace consists of a three and a half foot long glazed silica tube of two inches internal diameter. Heat is supplied by the Joule energy from a 22 s.w.g. nichrome wire winding covered by a layer of alumina cement. The silica tube is housed in a Sindanyo asbestos board cylindrical case (h) in Fig.2 which is packed with asbestos wool for insulation. Particular care was taken in spacing the turns of the nichrome winding to ensure that there was an evenly heated zone of at least twelve inches in the central part of the

furnace. A tolerance of  $\pm 5^{\circ}\text{C}$  was allowed on either side of the middle of the furnace length for at least six inches in each direction. Temperature measurement is by chrome/alumel thermocouple placed on the outside of the nichrome winding with its tip at the point corresponding to the middle of the hot zone. A thermocouple so placed would obviously not indicate the temperature extant in the furnace. Each furnace was therefore calibrated by determining the actual temperature within the furnace in the middle of the hot zone and graphing that against the temperature indicated by the thermocouple on the winding. Temperature control is by Kelvin Hughes Proportional Controller with a quoted accuracy of  $\pm 2^{\circ}\text{C}$ .

The top of the furnace was sealed from the atmosphere by an O-ring sandwiched between a brass ring round the circumference of the silica tube and a brass cap with a gas port and valve.

A detachable brass quenching tank (p) is attached to the bottom of the tube by a similar O-ring seal provision also being made for a connection to the pumping system. Specimens are suspended in the carrier (m) as illustrated in Fig.2. This holder hangs from a small piece of fuse wire (l) placed across two terminals in the cap at the top of the furnace. Quenching is effected by applying a high current across the terminals to melt the fuse wire. The carrier and specimens then plunge into the quenching tank. When quenching was being carried out after a vacuum heat treatment the quenching tank contains a low vapour pressure oil. The quenching medium after a nitriding or carburising treatment was water.

The pumping system consists of a three stage oil diffusion pump(s) of twenty-five litres per second capacity backed by a single stage rotary pump(t) of twenty-eight litres per second pumping capacity. (Both were supplied by N.G.N. Electrical Ltd.). The specifications of the two pumps quoted ultimate pressures  $5.10^{-6}$  m.m. and 0.1 m.m. of mercury respectively. The vacuum is indicated by a Geisler tube which blacks out at a pressure of  $10^{-3}$  m.m. and better. The system is designed so that the two furnaces can be used independently or in conjunction with each other.

Purification trains and metering systems were required for the gases used in the nitriding and decarburising treatments. The gases used are high purity hydrogen, nitrogen, argon and ammonia. All are dried by passing them over anhydrous magnesium perchlorate. In order to avoid carbon pick-up the hydrogen is passed through activated granular charcoal at the temperature of solid carbon dioxide (Circa -  $70^{\circ}\text{C}$ ) to absorb hydrocarbon impurities. It was later found that molecular sieve material (aluminium calcium silicate) was very effective in removing hydrocarbons from hydrogen and this replaced the activated charcoal whose efficiency fell off quite rapidly. In addition the hydrogen and nitrogen were deoxidised by passing them through a Deoxo tube, a platinum catalytic purifier supplied by Engelhard Industries Ltd.

Control of the flow of the gas is accomplished by calibrating the normal type of capillary flow-meter against the volume of gas flowing. In the case of hydrogen this was done physically by a rotary gas flow-meter. The ammonia flow was determined by titration.

cont'd...

Ammonia was passed into an acid solution of known strength for a given time and the excess acid titrated against a base.

When specimens were being nitrated by the use of hydrogen and ammonia mixtures precautions were taken to ensure that they were properly mixed. They were not led separately and directly into the furnace but to a series of mixing vessels (v). Since the ammonia used was never more than 6% of the total volume at any one time the nozzle which fed it to the first vessel was much narrower than that for hydrogen. The resulting increase in pressure of the ammonia entering the vessel ensured that this gas could mix more efficiently with the greater volume of hydrogen. The gases were then led into a large vessel to allow further mixing before being passed through a bed of glass beads and then to the furnace. This combination was found by titration methods to mix the gases thoroughly.

Where specimens were to be carburised this was done by passing the previously dried hydrogen through a vessel containing toluene at room temperature to allow it to entrain some of the hydrocarbon vapour and carry it to the furnace.

In addition to the two vertical furnaces described above two horizontal furnaces of very similar design were constructed. They were intended for vacuum annealing and decarburisation treatments where subsequent quenching to retain nitrogen in solid solution was unnecessary. The horizontal arrangement was used as it permitted easier insertion and removal of specimens than in the vertical furnaces. The only difference in design is that these furnaces are

at right angles to the pumping system and not directly above as  
is the case with the vertical furnaces.

### Section 2.3

#### Internal Friction Apparatus - Torsion Pendulum.

Since the internal friction peak caused by nitrogen in interstitial solid solution in alpha-iron occurs at room temperature for a linear frequency of one cycle per second it was decided to use a torsion pendulum for the measurement of internal friction.

This decision was taken for several reasons. Firstly the apparatus is simple to construct and frequency of one cycle per second is obtainable within the working range of this type of apparatus. The cylindrical shape of the specimen used in this type of apparatus means that frictional losses between the surface of the specimen and air are very small.

The apparatus itself is shown in Figs. 3 and 6 and is a modification of that used by Ke<sup>23</sup>. The actual pendulum consists of a steel frame to which the top grip (d) for the wire specimen was attached. The inertia member consists of a steel grip brazed to a brass rod and a cross-member of thin steel rod on which are two brass weights. The frequency of testing can be varied by altering the distance of these weights from the centre of the cross-member. The frequency range, with the weights (j) used, is one to four cycles per second.

Also attached to the inertia member is a small square mirror(h) which reflects the beam from a light source to a drum with a photographic paper on which the course of damping is recorded as

cont'd...

shown in Fig. 3. To facilitate the placing of the light spot on the drum, the pendulum is constructed so that there are three methods of adjusting the mirror with respect to the light source and drum. Firstly the top grip can be moved vertically by means of a screw and spring arrangement (i and v) through the top of the frame. The top grip can also be rotated through a semi-circle in the plane of the drum by a ratchet and screw mechanism. Finally the mirror itself can be tilted through a small angle by means of screws fixed top and bottom. The bottom of the inertia member is immersed in a dashpot of oil (m and k) to damp out lateral movement to ensure that it moves only in torsional vibration. The torsional force is applied to the wire specimen by activating two small electromagnets (p). These are positioned facing in opposite directions to apply a torque. The size of this torque is of considerable importance with regard to the elastic and anelastic effects it can produce. This will be dealt with later in Section 3.

The optical system is a simple one. The experiments are conducted in normal dark room safety-light conditions. The light source (z) is a twelve volt, twenty-four watt bulb shining through a rectangular slit 10 m.m. x 1 m.m. The image of this slit is focussed on to the mirror of the inertia member. This in turn is reflected through a convex lens (x) of one dioptre to a plane focussing lens which produced a very sharp highly intense and narrow spot four m.m. in length when the light was focussed on the paper on a drum. The drum (y) is a cylinder ten inches long and six inches in diameter which is driven by a small synchronous electric motor (z) at a

speed of one revolution every two minutes. Even at the highest frequency of four cycles per second where this speed gives four hundred and eighty cycles over a length of approximately nineteen inches of photographic paper, each cycle is easily resolved from its neighbours.

The photographic paper is supplied in rolls of twenty five feet by twenty inches, and is a hard grade of bromide paper to give maximum contrast. This paper was found to be sensitive to the light spot without pre-sensitising. Several workers<sup>64,54,56</sup> had depended partly or entirely on human observation of the damping to calculate the internal friction. This in the view of the author is subject to too many errors even at low frequencies and becomes well-nigh impossible at a frequency of two cycles per second. A photographic trace, although slower than methods of visual observation, yields a permanent, easily measured record of the course of damping and has the advantage that deviations from purely torsional movement, such as lateral movement of the inertia member, can be readily detected by a study of the pattern produced.

Ke's apparatus was designed primarily to study internal friction over a range of several hundred degrees and for that purpose a carefully wound electrical resistance furnace was constructed. For this present work a much shorter range of testing temperatures was indicated by the literature. The work of Laxar et al<sup>24</sup> indicates that in the range of aluminium compositions intended for investigation here the possibly relevant parts of the relaxation

cont'd...

curve would lie between 10°C and 70°C. For this reason, allied to the fact that Ke's apparatus does not lend itself to ease of manipulation with respect to loading and unloading the specimen, an alternative method of heating the specimen over a shorter range, was sought.

The possibility of heating the specimen by passing electricity through it was considered. Ang and Wert<sup>25</sup> adopted this method with an inverted pendulum system where the specimen was heated by the resistance heat of a current supplied by a low voltage source. However since they admitted to an unspecified rapid falling off of temperature towards the grips of the pendulum and since their method of temperature measurement (by welding a thermocouple to the specimen) did not recommend itself because of the dangers of specimen deformation and welding heat on precipitation of nitrogen, this approach was not adopted.

It was decided to build a wooden cabinet (b) to surround the pendulum apparatus, and to heat the atmosphere enclosed within, to the desired temperature. This is achieved by suspending four vertical coils of 20 s.w.g. nichrome wire (s), connected in series, within the framework of the pendulum. The heating current is supplied from the normal two hundred and fifty volt mains and controlled by a Variac transformer. Circulation of the air within the cabinet is produced by a small electrically driven fan in the roof of the cabinet. It was found that by having more turns of the coils nearer

the base of the pendulum and by increasing the speed of the fan, the natural tendency of hot air to rise to the top of the cabinet could be corrected to control the temperature gradient over the length of the wire from the coldest bottom to the hottest top. The gradient achieved is  $3^{\circ}\text{C}$  and can in fact be improved upon by further increasing the speed of the fan. However the subsequent air turbulence is such that the free decay of the vibrations of the oscillating cross-member is interfered with. A temperature gradient of  $\pm 1.5^{\circ}\text{C}$  about a mean temperature near the middle of the wire specimen is difficult to improve upon under the circumstances described above. It is not considered that this gradient is excessive and the mean temperature at the middle of the specimen is that quoted throughout this work.

The control of the temperature within the chamber to any specific value is achieved by the use of an adjustable be-metal thermostat (Type T.S.I. as supplied by Associated Electrical Industries Ltd.) in conjunction with a Sunvic controller. (Type F.102 supplied by the same company). Together these instruments can regulate the temperature to  $\pm 0.5^{\circ}$  of any required value. Temperature measurements are actually made with N.P.I. graduated mercury thermometers which were considered to be as accurate as any other method of temperature measurement in the range from  $10^{\circ}\text{C}$  to  $70^{\circ}\text{C}$ .

PART 3 - USE OF APPARATUS.Section 3.1 Manufacture of Alloys.

Additions of aluminium to steel seldom exceed a few pounds per ton even for fully-killed fine grained steels. Common additions in the semi-killed and fully killed range are three to five pounds per ton representing compositions of the order of  $10^{-2}$  weight per cent. For this reason the decision was made to aim for alloys between 0.02 and 0.2 weight per cent, being equivalent to half-pound per ton and five pounds per ton respectively. Such a range would more than account for the maximum solid solubility of nitrogen in alpha iron on a stoichiometric basis and will give an indication of the effects of aluminium contents of the order of those in commercial steels.

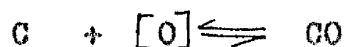
The compositions of the alloys produced are shown in Table 2. The alloys were made from high purity Swedish iron which was kindly donated by the British Iron and Steel Research Association. The analysis of this material is shown in Table 2 .

From the point of view of determining the effect of aluminium on nitrogen it essential the iron be fully deoxidised. The most troublesome impurity in the iron supplied by B.I.S.R.A. was therefore the oxygen content of 0.15%. Unless eliminated it would combine with the aluminium additions to form alumina. The conditions for this reaction are favourable since alumina has a high negative free energy of formation<sup>41</sup> at the melting point of iron. The oxygen therefore had to be removed before aluminium

cont'd...

additions were made.

There are three possible methods of deoxidation (a) by carbon (b) by hydrogen or (c) by an element whose oxide would not be reduced by aluminium. This latter was rejected on the grounds that it would tend to leave non-metallic inclusions in the metal. Deoxidation by carbon and hydrogen would proceed according to the equations:-



$H_2 (g) + [O] \rightleftharpoons H_2O(g)$  where the square brackets denote that the substance is in solution in the iron. At  $1600^{\circ}C$  the negative free energy of the carbon reaction is 19.3 Kcals/mole while that of the hydrogen reaction is  $4.4^{41}$ . Thermodynamically therefore the carbon reaction is the more effective remover of oxygen. There are two further advantages. In a vacuum system where the carbon monoxide evolved is being continuously pumped off by the vacuum system the equation will go far to the right as written and the resultant oxygen will be very low indeed. On the other hand the controlling factor in the hydrogen reaction is to ratio of the partial pressure of water to that of hydrogen.  $K$ , the equilibrium constant is given by,

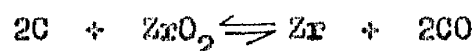
$$K = \frac{p.H_2O}{p.H_2} \cdot \frac{1}{[O\%]}$$

Since there is no change in volume of gas produced the reaction derives no special benefit from taking place in a low pressure chamber. There are also greater technical difficulties associated

cont'd...

with the introduction of hydrogen into the melt than with carbon.

There are however two disadvantages attendant on the use of carbon as a deoxidant. Although quicker and safer to use than hydrogen it is bound to leave a carbon residual in the metal, which could only be removed by lengthy decarburisation treatments. There is also the possibility of carbon attacking the refractory of the crucible thus,



conditions being favourable because of the rapid removal of carbon monoxide by the pumps. By and large, however concern for this possibility was unjustified as the zirconium analysis in the finished alloys demonstrates in Table 2.

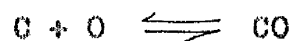
On weighing the pros and cons it was decided that the chemical efficiency of carbon as a deoxidant out weighed the disadvantages involved in its use.

Of major concern, however, was the possible loss of aluminium due to volatilisation. The temperature of the molten iron is approximately 1600°C and at this temperature the vapour pressure of aluminium, which melts at 660°C is 4.6 m.m. of mercury at a pressure of one atmosphere<sup>41</sup>. At the low pressures involved in this present work the vapour pressure would be much higher. If the partial pressure of aluminium is reduced by the introduction of an inert gas such as argon then losses will be reduced. By the adding the aluminium additions just before casting losses will

cont'd...

also be kept to a minimum. The technique adopted therefore was to introduce argon to a pressure of about 20 m.m. before adding aluminium. The crucible was then returned to the heating zone for approximately one minute to allow the induction stirring action to mix the alloy thoroughly before casting. The recovery of aluminium in alloys made in this manner was usually about seventy per cent of that added.

The procedure followed was to evacuate the vessel to  $10^{-4}$  to  $10^{-5}$  m.m. mercury and melt the charge of 900 gms. of iron. During this period the metal is effectively purged of hydrogen and nitrogen. (Residual nitrogen and hydrogen are  $4 \cdot 10^{-4}\%$  and  $2 \times 10^{-5}\%$  respectively according to Laganberg<sup>32</sup>). It was found that the addition of carbon to remove the oxygen produced such a violent reaction at this pressure that considerable amounts of metal were lost due to boiling and splashing. In some isolated cases bridging across the mouth of the crucible resulted. The pressure was therefore increased to 20 m.m. of mercury by the addition of argon immediately prior to the addition of carbon. The pressure was then slowly reduced to its former level and in this way the carbon boil was moderated. The amount of carbon added was the stoichiometric amount calculated from the equation,



and was added in small graphite chips. From Table 2 it can be seen that the average carbon residual is approximately 0.01%.

Thermodynamic calculations indicate that this would result in

cont'd...

an oxygen residual of the order of  $10^{-8}\%$ <sup>41</sup>. It is doubtful if this level was in fact obtained but there is every indication that the final oxygen was very low. With the precautions mentioned above the aluminium additions were then made. The aluminium was supplied by the British Aluminium Co. Ltd. and was quoted as 99.99% pure. The alloys were cast at a pressure of 20 m.m. of mercury and the vessel was again evacuated to a pressure of  $10^{-5}$  m.m. mercury as the cast cooled.

### Section 3.2 - Preparation of Specimens.

It has been shown in Section 1.3 that the internal friction peak due to nitrogen interstitially dissolved in alpha iron occurs at room temperature at a linear frequency of one cycle per second. Without exception previous investigators who have adopted internal friction techniques for measuring nitrogen solubilities have used the torsion pendulum. This apparatus requires a specimen of small physical dimensions to give a frequency of one cycle per second since the frequency at which a specimen can be induced to vibrate in torsion is closely related to the size and length of the specimen. The specimens have usually been about one foot in length and 0.03 inches in diameter. This has advantages in experiments of this nature as such wires can be readily nitrated and homogenised because of their small cross-sectional area. All the specimens used in this investigation conformed to the type used by previous workers.

The task was therefore one of reducing the two pound cast produced by vacuum casting to wire 0.030 inches in diameter. The casts when deprived of feeder heads and dressed on the outer surface were six inches long and just under one inch in diameter. Initial attempts to cold roll the casts had caused surface cracking so that eventually all casts were hot-rolled to bar 0.5 inches in diameter. Cold swaging and drawing followed until the diameter of the wire was reduced to the requisite 0.03 inches. The rolling mill, swager and drawing bench are shown in Figs. 7 & 8.

cont'd...

Such a reduction was not carried out without intermediate anneals and these were carried out in vacuum at  $600^{\circ}\text{C}$  in the furnaces described in Section 2.2. No predetermined limit was set on the degree of cold work to which the wire was submitted. Annealing was only carried out when the reduced cross-sectional area of the swaged part of the wire broke in tension during drawing. This allowed the wire to be reduced to the required size with a minimum number of anneals and obviated the problem of the combination of insufficient cold work and frequent anneals causing the growth of large grains. The presence of large grains is undesirable as they would have lowered the tensile strength and caused frequent fracture of the wires at the lower diameters. Several investigators have obtained experimental results which are relevant when considering the effect of such working and annealing as was carried out here.

Polder<sup>34</sup> worked out Snoek's theory in more detail and derived a formula for the elastic after effect in terms of the elastic constants of the cubic crystal and the calculated components of strain due to an applied stress on a single crystal. This expression gave the same results as Snoek when the stress is applied in the  $\langle 100 \rangle$  direction and gave after-effect as zero when the stress is applied in the  $\langle 111 \rangle$  direction. This again is as predicted by Snoek. Experimental corroboration was forthcoming in the form of work by Dijkstra<sup>18</sup> who confirmed the dependence of damping on solute concentration and found that the damping in the  $\langle 111 \rangle$  direction was less than 5% of that in the  $\langle 100 \rangle$  direction for single crystals

and polycrystalline specimens. It follows therefore that internal friction is anisotropic and that any procedure which will cause the torsion pendulum specimens to have directional properties will be troublesome. The fact that swaging and wire drawing produces preferred orientation of grains in the finished wire is well established. In the case of iron it consists of grains having the crystallographic direction  $\langle 110 \rangle$  parallel to the wire axis<sup>35</sup>. Directional properties of this nature can produce different damping results for the same quantity of dissolved nitrogen as was found by East and Verrijp<sup>33</sup>. What is required then is a fine-grained metal with grains orientated at random which will possess identical properties in all directions and give reproducible results. Smit and Van Bueren<sup>36</sup> in fact demonstrated that greater internal friction for the same nitrogen content was found in wires with random crystal orientation than in wires with a  $\langle 110 \rangle$  texture. Further it has been reported<sup>33</sup> that reproducible results could only be obtained with wires where in addition to random orientation the grain size was one tenth of the wire diameter. These conditions were produced by recrystallising the cold drawn wires above the alpha-gamma transformation point at  $950^{\circ}\text{C}$  as the indications were that iron retained its cold-worked texture on annealing up to  $800^{\circ}\text{C}$ <sup>37</sup>.

On the other hand Lagerberg and Josefsson<sup>38</sup> claim that the grain size influences the internal friction caused by carbon in solution but not that due to nitrogen. This they explain by the

cont'd...

fact that carbon forms a grain boundary film while nitrogen does not. A small grain size would increase the grain-boundary surface and hence the amount of carbon in solid solution.

In the case of the wires produced for this investigation they showed that average grain size was small varying from  $2 \cdot 10^{-3}$  to  $5 \cdot 10^{-3}$  inches across. Several samples from each cast were examined for preferred orientation by the Laue transmission X-ray method. In no case was there the preference for a  $\langle 110 \rangle$  texture reported previously<sup>33</sup> as can be seen from the uniform intensity all round the circumference of the Debye rings in Fig.9 - Both the microscopic and X-ray examinations were made after the wires had undergone long decarburisation treatments at  $600^{\circ}\text{C}$ . This is in agreement with Lagerberg and Josefsson<sup>38</sup> who also report that X-ray diffraction did not reveal any preferred orientation in wires recrystallised in the alpha-range. Since the wires used in this investigation were of a uniform grain size throughout it is not possible to comment on the relative merits of the findings of Fast and Verrijp<sup>33</sup> and of Lagerberg and Josefsson, except to state that with the grain size described above, the results of internal friction from wires having had the same nitriding treatment and hence containing the same quantity of nitrogen, were similar to within  $\pm 5 \cdot 10^{-4}$  of each other.

Section 3.3 Vacuum Annealing, Decarburisation, Nitriding  
and Carburisation.

As pointed out in the previous Section it was realised that intermediate annealing after swaging and drawing would have to be carried out in such a manner as to prevent oxidation of the wire. It is particularly important that oxidation should be avoided as the wire becomes thinner since an oxide layer even a few thousands of an inch thick represents an increasingly higher proportion of the cross-sectional area.

Regarding the oxidation of the wire as the reaction

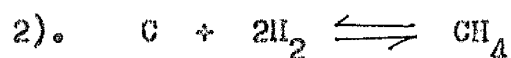
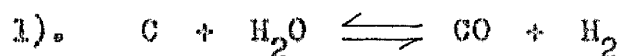
$$\text{Fe} + \frac{1}{2} \text{O}_2 \rightleftharpoons \text{FeO}$$
 it can be seen that it depends entirely on the partial pressure of oxygen present. Thermodynamic data<sup>41</sup> indicates that at 600°C oxidation will not occur if the partial pressure is less than  $10^{-3}$  m.m of mercury. Such a pressure is within the capabilities of the pumping system installed as described in Section 2.2 and in practice it was discovered that the wires annealed under vacuum at 600°C showed no trace of oxide afterwards.

The procedure followed in intermediate anneals was to clean the wires of all lubricants used in the drawing process and anneal for half an hour to an hour depending on thickness. The wires were then soft enough to undergo considerable reductions of area without any difficulty.

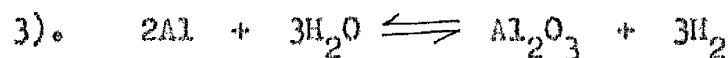
Analysis of the casts produced showed that the wire specimens could be expected to contain approximately 0.01 per cent of carbon

cont'd...

as a residual from the deoxidation process. A quantity of carbon such as this could be expected to produce an internal friction peak which would interfere quite markedly with a damping peak due to nitrogen since the two are only 18°C apart. This carbon had therefore to be removed. Perhaps the most common method of decarburisation of iron is to pass wet hydrogen over it at 720°C, the temperature of maximum solid solubility of carbon in iron. There are two reactions involved,



At 720°C these have negative free energy values of -32 Kcals/mole and -4.6 Kcals/mole respectively<sup>41</sup>. It is apparent that the first reaction is the more efficient as a decarburiser. However in alloys containing aluminium in substitutional solid solution the following reaction is possible,



Again at 720°C the negative free energy value is 186 Kcals/mole<sup>41</sup> and hence reaction (3) is the most likely of the three to occur. This excludes the use of wet hydrogen for the alloys used in this investigation (since it will result in the loss of aluminium in solution during the decarburisation treatment).

It only remains to be seen if conditions can be controlled to ensure that a dry hydrogen treatment involving only reaction (1) will decarburise the metal. For the reaction the equilibrium constant,  $K$ , is equal to the ratio of the partial pressures of

hydrogen and methane thus,

$$K = \frac{p_{CH_4}}{p_{H_2}^2}$$

Calculating K from the free energy data for 720°C yields the answer that  $K = 10^{-1}$ . Assuming that the partial pressure of hydrogen is unity (a reasonable assumption),  $p_{CH_4}$  becomes equal to 1/10 of an atmosphere. In other words decarburisation is possible if the partial pressure of methane can be maintained below one tenth. If the hydrogen used flows through the furnace at a high linear velocity then the system should be flushed clear of methane. Reaction (2) is in fact more efficient at 600°C and at this temperature all the carbon present should be in solid solution. The procedure adopted therefore was to decarburise at 600°C under hydrogen flowing at 150 c.c. per minute for ninety-six hours.

According to Sievert's Law the solubility of a diatomic gas, such as nitrogen, in a metal is proportional to the square root of the pressure. This statement is expressed as,

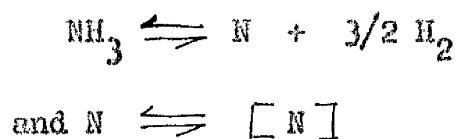
$$\%N = K(p_{N_2})^{1/2}$$

For a solid solubility of 0.1% nitrogen in alpha-iron 600°C Sievert's Law indicates that this quantity of solid solution would be in equilibrium with nitrogen gas at a pressure of about ten thousand atmospheres. Since the negative free energy is -11.6 Kcal/mole<sup>41</sup> this gives a K value of  $10^{-3}$  and hence a  $(p_{N_2})$  value of  $10^4$ . It follows therefore that nitriding by the use of pure nitrogen is out of the question.

cont'd...

Hydrogen has been shown to have a catalysing effect on the solution of pure nitrogen in alpha-iron<sup>33</sup> due to the formation of some intermediate hydrides on the metal surface but the reaction appears to be slow below 900°C which effectively limits the amount of nitrogen which can be taken up to the solubility limit at that temperature.

Since none of the above methods is satisfactory it was decided to use the cracking of ammonia, which iron catalyses, to introduce nitrogen into solid solution. The reactions are:-



where the square brackets denote nitrogen in solution in the metal. It is possible that hydrogen is taken into solution in the same way as nitrogen but it has been reported that a smooth metal surface, such as results from drawings and a large gas flow minimise this reaction<sup>40</sup>.

Considering, in the meantime, only the reaction for the cracking of ammonia, the equilibrium constant is,

$$K = (p\text{N})^{\frac{1}{2}} \times \frac{(p\text{H}_2)^{\frac{3}{2}}}{p\text{NH}_3}$$

It follows that the partial pressure of nascent nitrogen and hence the nitrogen available for solid solution is proportional to the ratio of the partial pressures of hydrogen and ammonia.

The data of Lehrer<sup>66</sup> indicates that for equilibrium at the eutectoid temperature of 600°C the ratio of ammonia to hydrogen

should be one tenth on a volume basis. Experience quickly showed however that this was too high an ammonia potential and tended to give a substantial nitride layer on the surface of the specimens. Fig. 10 gives an example of over-nitriding in this way. A definite triplex structure is evident. The outer layer is iron nitride, the second an iron-iron nitride eutectoid and the inner section is alpha-iron with nitrogen in solid solution. This specimen gave rise to anomalous results. Continued nitriding treatments gave decreasing solid solubility as indicated by the internal friction peak instead of increasing solubility, for treatments with a ten per cent ammonia mixture. In fact as iron nitride was formed there were fewer interstices for interstitial nitrogen to occupy and contribute to internal friction and so the damping peak decreased. This indicated that the equilibrium amount of nitrogen at 600°C for ten per cent ammonia was in excess of the eutectoid composition.

Calculations from known diffusion data<sup>20,33</sup> show that at 600°C a period of eight hours would elapse before nitrogen would diffuse to the centre of 0.03 inch diameter wire specimen. Eight hours nitriding with ten per cent ammonia mixture would lead to gross over-nitriding and so the technique developed was to nitride for a short period, say thirty minutes or an hour, with a six per cent ammonia mixture and then homogenise for eight hours. In this way it was possible to dissolve quantities of nitrogen up to the eutectoid limit of 0.1% without forming iron nitride.

The usual procedure was to nitride the specimens in a six per cent ammonia, hydrogen/ammonia atmosphere and then quench the

specimens to retain the nitrogen in solid solution. The furnaces were always flushed out with argon before being opened to atmosphere to prevent the possible formation of explosive mixtures. Specimens were then stored in liquid nitrogen until they were required.

A few specimens were carburised for comparison with the work of Laxax et al.<sup>24</sup> whose technique was used for the sake of comparison. It consisted of heating the wires in a furnace containing toluene introduced by passing hydrogen through a vessel containing that liquid.

### Section 3.4 Measurement of Internal Friction.

In the measurement of internal friction the applied stress should be so small that it should not exceed the elastic limit of the material being tested and the internal friction should be independent of the amplitude of vibration during testing<sup>4</sup>.

It has been shown<sup>65</sup> that so long as the maximum strain amplitude in a specimen is below  $10^{-5}$  or  $10^{-6}$  damping is independent of amplitude. The maximum amplitude of vibration usually observed on the four photographic traces was 5 cm at a distance of metres from the mirror on the pendulum. With a specimen 0.030 inches in diameter and ten inches in length the maximum shear stress on the outer diameter of the wire is  $2.10^{-5}$  p.s.i. This is calculated from the equation:-

Stress =  $\frac{r\theta}{l}$  where  $r$  is the radius of the specimen,  $l$  the length of the specimen and  $\theta$  the angle, in radians subtended by the amplitude of the trace produced on the drum four metres from the specimen. This is well below the yield point of iron which is of the order of  $10^4$  p.s.i. and is equivalent to a maximum shear strain below the required limit. The total weight of the bottom grip, inertia-member, mirror and brass weights is 65.36 gms. This corresponds to a tensile stress of two hundred p.s.i. on a specimen 0.03 inches in diameter, which again is far below the yield point of iron at room temperature. From these two calculations it was concluded that there should be no permanent change in the wire specimen during measurement of internal friction.

To test further the independence of internal friction from the amplitude of vibration a plot of the amplitude against the number of vibrations was made for several cases. As can be seen from Fig. 10, a straight line relationship is always found. This demonstrates that under the conditions described above the torque on the wire was sufficiently small for the logarithmic decrement and hence the internal friction to be independent of the strain amplitude. The different gradients in Fig. 11 illustrate different rates of decay of the free vibrations of the specimen i.e. different rates of damping.

At least nine different units have been used to express internal friction or damping capacity in a quantitative manner. The most common however are the dimensionless ratios independent of the size of the specimen. They are the logarithmic decrement, and the resonance-curve breadth factor  $Q^{-1}$ . These two are inter-related.

The logarithmic decrement is defined in terms of the maximum amplitude of successive cycles of freely decaying vibrations.

$$\delta = \ln \left( \frac{A_n}{A_{n+1}} \right)$$

where  $A_n$  and  $A_{n+1}$  are successive amplitudes. Usually the decrease in amplitude between two successive cycles is too small to be measured with any accuracy and so the decrease over a large number of cycles is noted. The formula is rewritten thus:-

$$\delta = \frac{1}{n} \ln \left( \frac{A_0}{A_n} \right)$$

where  $A_0$  is the amplitude of the first cycle,  $A_n$  the amplitude of the  $(n+1)$ th cycle and  $n$  the number of intervening cycles.

$Q^{-1}$  is essentially a unit used in electrical terminology but can be applied to anelastic effects by analogy and is related to  $\delta$  thus,

$$\delta = \pi Q^{-1}$$

and hence  $Q^{-1} = \frac{1}{\pi n} \ln \left( \frac{A_0}{A_n} \right)$

This was the measure of internal friction used in this work.

Another method of determining  $Q^{-1}$  is to find the time or number of cycles for the amplitude to fall to half an arbitrary initial value. The equation for  $Q^{-1}$  then reduces to

$$Q^{-1} = \frac{\ln 2}{\pi n} \quad \text{or} \quad Q^{-1} = \frac{\ln 2}{f \pi t_{\frac{1}{2}}}$$

where  $f$  is the linear frequency and  $t_{\frac{1}{2}}$  is the time for the amplitude to fall to half its initial value.

These latter formulae are generally used by those investigators who calculated the internal friction by human observation i.e. without making a permanent record, as referred to in Section 2.3. However the observer can easily make mistakes in counting or timing and has no means of checking his results without repeating the whole experiment. In addition it is often the case that no two complete cycles fall exactly within the ratio 1:2. These methods are therefore not quite as accurate as the methods described below. It was for these reasons that it was decided to make a permanent record of the damping in the form of a photographic trace, although the method is slower, involving as it does developing and fixing.

Typical photographic traces are shown in Fig.12. Type (a) is classed as acceptable as it shows none of the defects of

trace (b). Trace (b) is an example of lateral movement of the inertia-member caused by the air turbulence of too high a fan speed. This trace is obviously not an acceptable measure of damping as more than pure torsional movement is involved.

The procedure followed was to measure the width in centimetres of one of the wider amplitudes near to the top of the trace and to count down from that perhaps 26, 51 or 101 cycles as the nature of the trace allowed. The amplitude of the nth cycle, be it 26, 51 or 101 was then measured. A small correction equal to the width of the light spot was subtracted from each measurement and the equation,

$$Q^{-1} = \frac{1}{\pi n} \ln \left( \frac{A_0}{A_n} \right)$$

was applied.

At this point it is relevant to discuss the question of background damping. Obviously any damping value obtained from a specimen with nitrogen in solid solution is not attributable solely to the presence of nitrogen. There will be contributions from damping due to residual elements such as hydrogen and carbon dissolved in the metal. Magnetic and sonic after-effects not to mention friction between the surfaces of the specimen and the inertia-member and the air will also contribute to the damping as measured. Inter-crystalline damping will also be present as part of the measured value. It is however possible to reduce these effects to an acceptable minimum by choosing the experimental conditions carefully.

It is known<sup>4</sup> that the spectrum for relaxation effects extends from  $10^{-12}$  to  $10^4$  cycles per second<sup>4</sup>. Relaxation effects due to

cont'd..

grain boundary movement occur at frequencies of the order of  $10^{-10}$  to  $10^{-6}$  and those due to intercrystalline thermal currents above  $10^4$ . It can be seen therefore that in the frequency range of one to four cycles per second used here contributions from these two effects will be very small. Even damping due to interstitial solute atoms is to be found over a range of  $10^{-2}$  to 10 cycles per second. Within this range it has been found<sup>26</sup> that for a frequency of one cycle per second the internal friction peak due to hydrogen in alpha-iron lies at  $-173^{\circ}\text{C}$ . Again the contribution to damping at room temperature where the nitrogen peak occurs will be negligible from any dissolved hydrogen in the specimens.

Snock<sup>11</sup> in his experiments applied a longitudinal magnetic field of forty oersteds to suppress the damping caused by magneto-mechanical hysteresis effects. With the strain amplitudes described above without a magnetic field background damping values on pure iron specimens freed of carbon by prolonged hydrogen treatment as previously described were found to be as low as  $5 \cdot 10^{-4}$ . Since this value included air losses due to friction it would appear that Snock's fears would not have been justified under the conditions used for this work. It was decided therefore not to take the measures adopted by Snock. Since the background damping was so low it became apparent that it would in no way obscure the damping due to nitrogen which was expected to be of the order of  $10^{-2}$ . Fine<sup>27</sup> and Pearson<sup>28</sup> have obtained background dampings of  $10^{-4}$  with pure iron by streamlining the oscillating inertia member, eliminating oil damping and by operating in vacuo. However the additional

operational complications hardly justify the expense and inconvenience for this present investigation. It was also found that the depth to which the inertia-member was dipped into oil to damp out lateral vibrations had a slight effect on the background damping. This was adjusted to give maximum suppression of lateral movement with minimum increase in background damping. This was found to be a depth of quarter of an inch and the inertia-member was always immersed to this depth.

The linear frequency of vibration was always measured directly from a photographic trace. The synchronous motor driving the drum was very accurately constructed to revolve once every two minutes without vibration. The number of cycles in one complete revolution of the drum was found and simply divided by one hundred and twenty to give the linear frequency in cycles per second.

### Section 3.5 Calculations and Computer Techniques.

As already indicated in Section 1.2 the usual manner in which the heat of activation,  $dH$ , of the diffusion process is calculated is by application of the formula,

$$\ln \frac{f_1}{f_2} = \frac{dH}{R} \left( \frac{1}{T_2} - \frac{1}{T_1} \right)$$

to the data obtained from two complete curves obtained by plotting  $Q^{-1}$  against temperature at different frequencies. In the above equation  $T_1$  is the temperature of the peak of the curve obtained at frequency  $f_1$ . The symbols  $T_2$  and  $f_2$  have a similar significance. The equation may be slightly modified and rearranged thus,

$$dH = \frac{R \ln \left( \frac{f_1}{f_2} \right) T_2 \cdot T_1}{(T_1 - T_2)}$$

when it becomes apparent that the value of  $dH$  depends largely on the difference between  $T_1$  and  $T_2$ . The values of frequencies can be calculated very accurately from the photographic traces and the error induced here is almost negligible. The accuracy of the temperatures however is quite another matter. In the system of controlling and measuring the temperature at which the individual points on the curve are determined there is an error of  $\pm 0.5^\circ\text{C}$ . The position of the peak of the curve is determined by inspection of the completed curve on the graph. This can probably be done to an accuracy of  $\pm 1^\circ\text{C}$ . When it is considered that within the frequency range of the torsion pendulum i.e. one to four cycles per second the shift of the peak is only  $14^\circ\text{C}$  it can be seen that the error induced

cont'd...

of the order of ten per cent at the best. With peaks which are separated by a smaller temperature interval the error becomes correspondingly larger.

Alternatively the  $dH$  value can be calculated from individual points on the curves. The theory indicates that the relaxation time of a process should be constant for any given fraction of the peak irrespectively of the peak height. That is to say that the relaxation time at 80% of the maximum value of  $Q^{-1}$  should be the same no matter what the actual value of the maximum  $Q^{-1}$ . Mathematically this fact can be stated,

$$w\tau = K \text{ (a constant)}$$

$$\text{Now } \tau = \tau_0 \exp. \frac{dH}{RT}$$

$$\therefore \frac{k}{w} = \tau_0 \exp. \frac{dH}{RT}$$

$$\text{Hence } \ln K = \ln w = \ln \tau_0 + \frac{dH}{RT}$$

$$\therefore \ln w = \ln \frac{K}{\tau_0} = \frac{dH}{RT}$$

$$\therefore \ln 2\pi f = \frac{\ln K}{\tau_0} = \frac{dH}{RT}$$

$$\therefore \ln f = \frac{\ln K}{2\pi\tau_0} = \frac{dH}{RT}$$

From this equation it follows that plotting the reciprocal of the temperature corresponding to 80% of the peak height against the natural logarithm of the frequencies at which the peak occurs should yield a straight line whose gradient is  $dH$ . The procedure can be repeated for any fraction of the peak height. For accuracy this method requires at least three curves to establish the straight line relationship. It is a more cumbersome method of calculation but

cont'd...

experience has shown that it is possible to determine the height of the peak to a much higher degree of accuracy than the actual peak position. The previous statement with regard to the accuracy of temperature measurement still holds good but the accuracy of the method does not depend at all on the temperature difference between peak heights. The accuracy of this method is higher than that of the previous method.

Two methods have been evolved for calculating the dh value from a single peak. One is a graphical method and the second is essentially one of trial and error which involved the use of a computer.

The first method makes use of the equation derived by Snook<sup>11</sup> first discussed in Section 1.2 namely,

$$Q^{-1} = \frac{Q_0^{-1}}{Q_0} \cdot \frac{wT}{1 + (wT)^2} \quad (3)$$

It was also demonstrated that this expression could be modified thus,

$$Q^{-1} = 2Q_M^{-1} \frac{wT}{1 + (wT)^2} \quad \text{where } Q_M^{-1} \text{ is the}$$

value of  $Q^{-1}$  at the peak height.

$$\text{Hence } Q^{-1} + Q^{-1}(wT)^2 = 2Q_M^{-1} \cdot Tw$$

$$\text{or } Q^{-1}(wT)^2 - 2Q_M^{-1} \cdot Tw + Q^{-1} = 0$$

This is a quadratic in  $T$  and its solution is given

$$T = \frac{2Q_M^{-1} \pm \left\{ (2Q_M^{-1})^2 w^2 - 4(Q^{-1})^2 w^2 \right\}^{1/2}}{2Q_M^{-1} \cdot w^2}$$

cont'd...

$$\therefore \tau = \frac{2Q_m^{-1} \pm \left\{ (2Q_m^{-1})^2 - 4(Q^{-1})^2 \right\}^{\frac{1}{2}}}{2Q_w^{-1}}$$

X That is to say  $\tau$  is now expressed in terms of a single value of  $Q^{-1}$ , the frequency  $w$  and the peak maximum  $Q_m^{-1}$ . Remembering that  $\tau = \tau_0 \exp \frac{dH}{RT}$  it can be seen that if the values of the natural logarithm of  $\tau$  so found are plotted against the reciprocal of the temperature of the  $Q^{-1}$  value used in the quadratic the result will be a straight line whose gradient is  $dH$ .

Y Two solutions are yielded by the quadratic and two straight lines are found which intersect at right angles. That is to say the two sets of values for  $\tau$  give the same numerical result for  $dH$  but the sign differs. This method is basically similar to the previously mentioned graphical method but has the advantage that only one relaxation curve need be determined.

The computer method uses the formula, also developed in Section 1.2 giving  $Q^{-1}$  in terms of the maximum  $Q_m^{-1}$  value its temperature and the  $dH$  thus,

$$Q^{-1} = \frac{Q_m^{-1}}{\cosh \left\{ \frac{dH}{R} \left( \frac{1}{T} - \frac{1}{T_m} \right) \right\}} \quad (5)$$

All of the experimental results found were fed into the computer which produced a curve in terms of the three variables  $Q_m^{-1}$ ,  $T_m$  and  $dH$  which was the best mathematical description of the curve found experimentally. The method of least squares was used to determine this "best-fit" curve.

A range of values of  $dH$ ,  $T_m$  and  $Q_m$  was obtained from an

cont'd...

inspection of the experimental results and it was by testing these in conjunction with each other that the combination of all three which best described the experimental curve was found. If the results indicated that either the lower or the upper limit of any of the three variables to be the best then the range was extended beyond that limit and the results retested. This ensured that there was series of values both above and below that indicated as best which gave a poorer fit with the experimental results. This is important in assessing the accuracy of the method as will be shown below.

By working to the eighth decimal place the computer is able to distinguish between mean square deviations of  $1.371 \cdot 10^{-5}$  and  $1.423 \cdot 10^{-5}$  to quote two examples. For the eleven experimental results involved in this case the average deviation is  $2.2 \cdot 10^{-4}$  per result. Since the reproducibility of values of  $Q^{-1}$  is  $\pm 5 \cdot 10^{-4}$  it is clear that the mathematical distinction made by the computer is not justified on the ground of experimental accuracy. Working on the basis of an experimental reproducibility of  $\pm 5 \cdot 10^{-4}$  it can be calculated that tolerances of  $\pm 25x \cdot 10^{-8}$  where  $x$  is the number of experimental results should be applied in accepting the mean square deviation quoted by the computer.

Several workers have shown that it is possible to obtain relaxation peaks which can be characterised by no one relaxation time. These have usually been due to the combined effects of two interstitials or of an interstitial and an alloying element.

cont'd...

It is possible to analyse these curves by making the following assumptions:

- 1) That the peak is due to at least two relaxation process and the experimental curve is the sum of these.
- 2) That these processes do not alter such characteristics as the  $\Delta H$ ,  $T_m$  and  $Q_m$  values of each other.
- 3) That the characteristics of one process are well known.

Thus if nitrogen is introduced into an iron alloy and the resultant relaxation peak does not have the characteristics of a single relaxation process, an analysis can be made by assuming that the normal peak due to nitrogen in iron is present. By knowing the frequency of testing the peak temperature can be calculated. Making use of assumption (2) the curve for the iron-nitrogen process can be calculated theoretically and subtracted from the experimental results leaving one or more unexplained peaks. A computer programme working on the same trial and error basis as that described above was developed which gave the best mathematical description of the experimental results in terms of two or more relaxation peaks.

The computer used was the Ferranti Sirius model and descriptions and details of the programmes used are given in the Appendix to Section 4 together with the programme instructions in Sirius Autocode.

PART 4 - APPENDICES TABLES OF RESULTS AND FIGURES.

Appendix 1. Description of Computer Techniques.  
 APPENDIX 1. DESCRIPTION OF COMPUTER TECHNIQUES.

There were in fact three computer programmes used in this investigation. Two were concerned with finding the best mathematical explanation of a set of experimental results and the third was a straight forward calculation from an established formula.

As explained in Section 3.5 it is possible to obtain a value of the activation energy of a diffusion process,  $dH$ , in conjunction with two other factors from experimental results. The method used is essentially one of trial and error based on the method of least squares. Here the "best-fit" of a theoretical curve to the experimental one was found by varying the three parameters of equation (5) of Section 3.2. The equation is:-

$$Q^{-1} = \frac{Q_m^{-1}}{\cosh \left\{ \frac{dH}{R} \left( \frac{1}{T} - \frac{1}{T_m} \right) \right\}}$$

where the three parameters are  $Q_m^{-1}$ , the peak maximum which occurs at a temperature of  $T_m$  °K and  $dH$  is the heat of activation.  $Q^{-1}$  in this expression is an experimental value found at temperature  $T$  °K.

The basis of the programme is as follows. A set of experimental results, describing a complete curve is fed into the computer together with a range of values of  $Q_m^{-1}$ ,  $T_m$  and  $dH$  which are obtained from an inspection of experimental results. At the temperature of one of the experimental results a theoretical value of  $Q^{-1}$  is calculated from the lowest value each of the given

cont'd...

values of  $dH$ ,  $Q_m^{-1}$  and  $T_m$ . This theoretical value of  $Q^{-1}$  is subtracted from the experimental value and the difference between the two is squared and stored by the computer. The same process is repeated for each experimental result fed into the computer until every experimental result has been so treated and the sum of the squares of all the deviations has been obtained. This total is stored by the computer as the mean square deviation.

The whole cycle is then repeated using the same experimental results and the same  $dH$  and  $T_m$  but with a different value of  $Q_m^{-1}$ . The mean square deviation is evaluated for this cycle and compared with that of the first. If it is smaller then it is retained by the computer as it represents a closer fit between the theoretical and experimental curves than the previous value which is now rejected. If however the second value is the bigger then it is rejected. This cycling process is repeated until the whole range of values of  $dH$ ,  $T_m$  and  $Q_m^{-1}$  have been used. Hence if there are five values of  $dH$ , four of  $T_m$  and three of  $Q_m^{-1}$  there would be sixty cycles ( $5 \times 4 \times 3$ ) and sixty values of the mean square deviation tested to find the smallest. These variables are given regular increments over the range of values to be tested. The programme is completed by the computer printing out the combination of  $dH$ ,  $T_m$  and  $Q_m$  which have given the smallest mean square deviation i.e. the closest fit between the theoretical and experimental curves. The programme is given below in the Autocode used in the Sirius computer.

cont'd...

PROGRAMME 1.

Jv1

v70=TAPE 3

v1=TAPE 6

v73=v3

v74=v5

v10=TAPE\*

n1=n0

v60=100

10)v55=100

7)v7=100

4)v8=0

n0=0

1)v51=v3-v(11+n0)

v51=v1Xv51

v51=v51/1.987

v51=v51/v3

v51=v51/v(11+n0)

v52=EXPv51

v53=1/v52

v51=v52+v53

v51=v51/2

v51=v5/v51

v51=v(10+n0)-v51

v51=v51Xv51

v8=v8+v51

$$n0=n0+2$$

$$\rightarrow 1, n1/n0$$

$$\rightarrow 2, v7 \geq v8$$

$$\rightarrow 3$$

$$2)v7=v8$$

$$v9=v5$$

$$\rightarrow 3$$

$$3)v5=v5+v72$$

$$\rightarrow 4, v6 \geq v5$$

$$v5=v74$$

$$\rightarrow 5, v55 > v7$$

$$\rightarrow 6$$

$$5)v55=v7$$

$$v56=v3$$

$$v57=v9$$

$$\rightarrow 6$$

$$6)v3=v3+v71$$

$$\rightarrow 7, v4 \geq v3$$

$$v3=v73$$

$$\text{PRINT}v55, 3008$$

$$\text{PRINT}v1, 4100$$

$$\text{PRINT}v56, 4062$$

$$\text{PRINT}v57, 4005$$

$$\rightarrow 8, v60 > v55$$

$$\rightarrow 9,$$

$$8)v60=v55$$

v61=v1

v62=v56

v63=v57

→ 9

9) v1=v1+v70

→ 10, v2 ≥ v1

TEXT

H	T	Q	RESIDUAL
---	---	---	----------

PRINT v61, 3100

PRINT v62, 4062

PRINT v63, 4005

PRINT v61, 4008

TEXT

RESIDUAL	Q	T
----------	---	---

n0=0

11) v51=v62=v(11+n0)

v51=v61\*xv51

v51=v51/1.987

v51=v51/v62

v51=v51/v(11+n0)

v52=EXP v51

v53=1/v52

v51=v52+v53

v51=v51/2

v51=v63/v51

```

v51=v(10+n0)-v51
PRINTv51,3005
PRINTv(11+n0),4062
n0=n0+2
->11,n0/n1
(→o)

```

The data for this programme has to be arranged in a definite sequence to fit the construction of the programme. If, for example, the test was being made for  $\Delta H$  values from 16 Kcals/mole to 20 Kcals/mole at intervals of 0.5 Kcals/mole, for  $T_m$  values of 312 to 317°K with increments of 1°K and  $Q_m^{-1}$  values from  $2.5 \cdot 10^{-2}$  to  $2.7 \cdot 10^{-2}$  at intervals of  $2 \cdot 10^{-4}$  then the data would be made out as follows:-

```

500
1
0.0002
16000
20000
312
317
0.0250
0.0270

```

This would be immediately followed by the experimental values of  $Q_m^{-1}$  and their temperatures thus:-

cont'd...

0.0086

290

0.0098

293

etc. etc.

Possibly one point of explanation remains. The Sirius Autocode does not contain instructions which will allow the computer to calculate hyperbolic cosines as is required by equation (5). The procedure followed was to calculate the value of the bracket,

$$\frac{dH}{R} \left( \frac{1}{T} - \frac{1}{T_m} \right)$$

and put this equal to  $x$ . The cosh value was then found by addition of the exponential value of  $x$  according to the expression,

$$\cosh x = \frac{e^x + e^{-x}}{2}$$

It is appreciated that Programme 1 does not calculate the "best" value of  $dH$  alone but the best value of  $dH$  in conjunction with the "best" values of  $T_m$  and  $Q_m^{-1}$ . Experience has shown however that it was always on the basis of the  $dH$  value that the "best-fit" was decided. The programme was designed such that at the end of each cycle, it printed out each mean square deviation with the value of  $dH$ ,  $T_m$  and  $Q_m^{-1}$  which produced it. Hence the trend towards the best combination could be observed. Generally speaking the best values of  $T_m$  and  $Q_m^{-1}$  were picked within the first few cycles and thereafter the issue was settled on the basis of the  $dH$  value. This is readily understood when it is realised that changes in  $T_m$  would produce a lateral movement in the position of the theoretical

curve which would result in large deviation between it and the experimental curve. Equally changes in  $Q_m^{-1}$  would produce large vertical movement in the height of the curve which would be equally unacceptable in terms of the programme. The  $\delta H$  however is more intimately connected with the shape and especially the breadth of the curve and is the most important factor in deciding the "best fit" Programme 1 can therefore be taken as a method of calculating activation energy values.

In the cases where the damping curve obtained was a combination of two or more independent peaks a slightly different technique had to be employed.

At first it was thought possible to design a computer programme which would solve the experimental values into the most likely combination of peaks. For this purpose a reiterative programme based on a system of successive approximations was drawn up. The procedure followed was to feed in approximate values for the three parameters,  $\delta H$ ,  $T_m$  and  $Q_m^{-1}$  for the number of peaks thought to be present and to allow the computer to vary these values with respect to each other until the parameters settled down to constant values. In actual fact the programme showed numerical instability which indicated that there was no unique solution of the experimental results, to be obtained in this fashion. It became apparent that allowing the parameters of all the peaks to vary, even that whose parameters are known, could not produce results which fitted the experimentally derived curve. The problem could be solved by giving the computer specific information with

cont'd...

regard to one of the processes present, in this case the well established iron-nitrogen damping curve. That is to say it was assumed that the normal iron-nitrogen peak was present and that it could be subtracted from the experimental results as a first step to resolving the experimental curve into its components.

As a preliminary step the  $T_m$  for the iron-nitrogen peak was calculated from equation (6) using Fast and Verrijp's data<sup>33</sup>. An activation energy of 18.2 Kcals/mole was assigned to the process and the computer calculated the theoretical curve for these two constants over a range of  $Q_m^{-1}$  values. These theoretical curves were then subtracted from the experimentally established curve and the difference for each experimental temperature was printed out. Originally a programme had been designed which chose a value of  $Q_m^{-1}$  from a range arrived at by inspection of the experimental results. It almost always chose the upper limit of the range because the programme operated on the "best-fit" principle described above. This meant that this particular programme attempted to explain the complex curve in terms of the iron-nitrogen curve alone and hence at the expense of the secondary curve or curves. For this reason this second programme was not used. On the other hand the first programme gives a series of deviations of the experimental from theoretical iron-nitrogen curves of various peak heights. The initial assumption was then made that only one abnormal peak would be present so that one side of the complex curve should fit almost exactly with the iron-nitrogen curve theoretically calculated. The experimental results were taken

as the yardstick and no  $Q_m^{-1}$  value which produced negative deviations was accepted as a possible value. A  $Q_m^{-1}$  value was selected which gave positive deviations of no more than  $10^{-3}$  at one side of the experimental curve. The remainder on the other side of the curve was taken as the abnormal peak and its values were processed in Programme 1 to evaluate the activation energy for the diffusion involved. The values of  $dH$ ,  $Q_m^{-1}$  and  $T_m$  obtained in this manner were then processed in Programme 2 such that the remainder in the case became the iron-nitrogen curve. This curve was compared with original iron-nitrogen curve to see what measure of agreement was obtained. This cycling procedure involving use of both Programmes 1 and 2 was continued until the theoretical curves gave a good mathematical explanation of the experimental curve. Programme 2 is given below:-

PROGRAMME 2.

```

Jv1
v1=TABLE 5
v10=TABLE*
X4)v6=0
n1=0
PRINTv3,3005
1)v51=v2*v(11+n1)
v51=v1Xv51
v51=v51/1.987
v51=v51/v2
v51=v51/v(11+n1)
v52=EXPv51

```

```

v53=1/v52
v51=v52+v53
v51=v51/2
v51=v3/v51
v51=v(10+n1)-v51
PRINTv51,3005
PRINTv(11+n1),4061
v51=v51Xv51
v6=v6+v51
n1=n1+2
→1,n1/n0
PRINTv6,4005
v3=v3+v5
→4,v4 ≥ v3
(→0)

```

The data for Programme 2 has to be laid out as follows:-

```

18200
310
0.0200
0.0250
0.0005
0.0090
290 etc.etc.

```

which in this case would mean that a theoretical curve with a  $\Delta H$  value of 18.2 Kcal/mole and a  $T_m$  of  $310^{\circ}\text{K}$  would be calculated between a  $Q_m^{\text{cal}}$  range of  $2.10^{-2}$  and  $2.5.10^{-2}$  at intervals of

cont'd...

$5 \cdot 10^{-4}$ . The experimental value of  $Q^{-1}$  at  $290^{\circ}\text{K}$  is  $9 \cdot 10^{-3}$ .

As mentioned above the position of the peak maximum for the iron-nitrogen process in a complex curve was calculated from the data of Fast and Verrijp<sup>33</sup>. This consisted of a straightforward use of equation (6),

$$\ln \left( \frac{f_1}{f_2} \right) = \frac{dH}{R} \left( \frac{1}{T_2} - \frac{1}{T_1} \right)$$

where  $T_1$  and  $T_2$  are the peaks for tests at frequencies of  $f_1$  and  $f_2$  respectively. In the case of iron-nitrogen  $dH$  was taken as 13.2 Kcals/mole,  $f_1$  as 0.89 cycles per second and  $T_1$  as  $295^{\circ}\text{K}$ . The experimental frequency for which it was desired to calculate  $T_2$ , is  $f_2$ . The programme is given below in Sirius Autocode.

PROGRAMME 3.

```

Jv1
v1= TAPN5
1)v6=1/v1
v7=v4/v2
v7=LOGv7
v7=1.987Xv7
v7=v7/v3
v6=v6-v7
v6=1/v6
PRINTv4,3022
PRINTv6,4062
v4=v4+0.05
→1, v5 ≥ v4

```

cont'd...

(→0)

For Programme 3 the data was made out as follows,

295

0.89

18,200

1.0

4.0

That is to say from a frequency of 0.89 cycles per second and a temperature of 295<sup>0</sup>K (Fast and Verrijp's data<sup>33</sup>) the temperature of the peak maximum would be calculated over a frequency range of one to four cycles per second. The frequency was increased in stages of 0.05 cycles per second by an instruction written into the programme.

Appendix 2.Description of Method of Nitrogen Analysis, etc.

The method employed was essentially that laid down by British Chemical Standards along with Standard No.230.

The sample is dissolved in 5 ml. of sulphuric acid in 20 ml of deionized water. When the specimen is dissolved approximately 5 ml. of 30% hydrogen peroxide is added and the solution evaporated to fuming, after which it is cooled, diluted and transferred to a 250 ml. graduated flask. To this is added 40 ml. of 20% sodium hydroxide care being taken to keep the solution cool. The bulk is made up to 250 ml., well shaken and the precipitate is allowed to settle. It is then filtered. The first filling of the filter paper is rejected to dispose of any ammonia in the filter paper. This is preferable to acid washing which would upset the pH and cause some resolution of the precipitate. Fifty ml. of the filtrate is transferred to a 50 ml. Nessler cylinder together with one ml. of standard Nessler reagent. The method requires an addition of one ml. of a 5% solution of Gum Arabic to be added at this stage. The best Gum Arabic obtainable contained some ammonia which would have given a high nitrogen result. The ammonia was removed by the use of a cation exchange resin and all the Gum Arabic used here was so treated. A blank of all reagents treated in exactly the same manner and put into another 50 ml. Nessler cylinder. The depth of colour in the two cylinders is compared in a Nesslerizer with that of a standard ammonia discs. Three discs were used covering the range

cont'd.../

ten to one hundred parts per million. The weight of the sample is chosen to give a depth of colour within the range of the disks. Generally a sample weight of 0.1 to 0.2 gm. was used but if the resulting colour was outwith the above mentioned range the sample weight was adjusted.

The nitrogen content of the sample is given by the following equation:-

$$\text{Weight \% Nitrogen} = \frac{\text{Disk reading} \times .82 \left( \frac{\text{NH}_3}{3} - \frac{\text{N}_2}{2} \right) \times 100 \times \frac{250}{50}}{\text{Weight of sample} \times 10^6}$$

With each batch of tests a one gramme sample of B.C.S.265 was analysed. This low carbon standard for nitrogen (0.020%) was used as a check on conditions and manipulation.

TABLES OF RESULTS.

TABLE 1.

Comparison of the  $dH$  and  $T_m$  values found for the diffusion of nitrogen in alpha-iron by various workers.

	Ref. No.	$dH$ Value Kcals/mole	$T_m$ °C	Frequency cycles/sec.
Leak et al	58	18 ± 1	22.5	1.0
Ke	23	20 ± 2	30	1.8
Fast & Verrijp	44	18.6	22	0.77
Wert	42	17.7 ± 0.4	-	-
Dijkstra	21	18.2	20	1.0
Rawlings & Robinson	59	18.2	17	0.56

TABLE 1(a).

$T_m$  values at various frequencies calculated from the data of several workers. A  $dH$  value of 18.2 Kcals/mole was used as a basis for comparison in conjunction with the equation  $\ln \frac{f_1}{f_2} = \frac{dH}{R} \left( \frac{1}{T_2} - \frac{1}{T_1} \right)$

Reference	Ref. No.	Frequency, cycles/sec		
		1.0	2.0	3.0
Leak et al	50	295.5°K	302.3°K	306.4
Ke	23	297.3°K	304°K	308.2°K
Rawlings & Robinson	60	296.9°K	303.7°K	307.8°K
Dijkstra	21	293°K	299.6°K	303.8°K
Fast & Verrijp	44	296.2°K	303°K	307.1°K
Average		295.8°K	302.5°K	306.6°K

cont'd...

TABLE 2.

Analysis of aluminium alloys and of the pure Swedish iron from which they are made expressed as weight per cent.

Cast	C	Al	Si	S	P	Mn	Ni	Cr	Mo	V	Ti
Swedish Iron	.02	.0018	.005	.009	.001	.0027	.0067	.0025	.003	.0004	.0009
L17	.006	Trace	.005	.013	.008	-	-	-	-	-	-
L18	.011	.015	.007	.013	.009	-	-	-	-	-	-
L23	.004	.044	.009	.011	.010	-	-	-	-	-	-
L19	.007	.068	.011	.011	.009	-	-	-	-	-	-
L20	.008	.090	.011	.012	.007	-	-	-	-	-	-
L27	.002	.30	.007	.013	.012	-	-	-	-	-	-

TABLE 3.

The amplitude independence of damping. Values of amplitude of vibration and  $\log_{10}$  of the amplitude for given numbers of cycles as plotted in Fig.11.

$Q^{-1} = 1.63 \cdot 10^{-2}$			$Q^{-1} = 9.45 \cdot 10^{-3}$			$Q^{-1} = 5.3 \cdot 10^{-3}$		
No. of Cycles	Amp. cms.	$\log_{10}$ Amp.	No. of Cycles	Amp. cms.	$\log_{10}$ Amp.	No. of Cycles	Amp. cms.	$\log_{10}$ Amp.
5	9.2	.964	10	8.4	.924	10	11.5	1.06
10	7.1	.851	20	5.85	.767	20	9.35	.980
15	5.55	.744	30	4.1	.613	30	7.55	.878
20	4.3	.634	40	2.9	.462	40	6.2	.792
25	3.3	.518	50	2.0	.030	50	5.1	.708
30	2.55	.407	-	-	-	60	4.2	.623
35	1.95	.290	-	-	-	70	3.55	.550
40	1.50	.176	-	-	-	80	3.0	.477

cont'd...



TABLE 5.

$\Delta H$  values calculated from the equation  $\ln \left( \frac{f_2}{f_1} \right) = \frac{\Delta H}{R} \left( \frac{1}{T_1} - \frac{1}{T_2} \right)$  using the values of Table 4.

$f_1$ cycles/sec	$f_2$ cycles/sec	$T_1$ °K	$T_2$ °K	$\Delta H$ Kcals/mole
1.10	3.29	297	308	18,280
1.10	1.76	297	302	16,922
1.76	3.29	302	308	19,394
			Average	19,199

TABLE 6.

Comparison of values of  $\Delta H$  and  $T_m$  found by computer for pure iron with and without allowances for background damping.

Frequency cycles/sec.		$\Delta H$ Kcals/mole	$T_m$ °K
1.10	Background	17000	297
	Subtracted		
1.76	Background	16000	297
	Not Subtracted		
1.76	Background	17400	303
	Subtracted		
3.29	Background	16000	302
	Not Subtracted		
3.29	Background	18400	308
	Subtracted		
3.29	Background	17600	309
	Not Subtracted		

cont'd...

TABLE 7.

Diffusion of nitrogen in alpha-iron. Values of D calculated from the equation  $D = \frac{D^2}{18} f$  for various frequencies, as plotted in Fig.14.

Frequency cycles/sec	$T_m$ °K	$10^3/T_m$	D. $10^{-16}$	$\log_{10} D.$
1.10	297	3.36	1.58	-15.80
1.11	298.5	3.34	1.59	-15.80
1.76	301.5	3.32	2.53	-15.60
2.23	307	3.26	3.20	-15.49
3.17	309	3.24	4.55	-15.33
3.29	308	3.25	4.61	-15.34

TABLE 8.

Approach to equilibrium solid solubility value at  $215^{\circ}\text{C}$  from both higher and lower temperatures.  $Q_m^{-1}$  values for various times as plotted in Fig.15.

Heat Treatment	Time in Hrs	1	3	5	7	9
Nitrided, Quenched and aged. Heated from ambient temperature to $215^{\circ}\text{C}$ and held for increasing periods till a maximum $Q^{-1}$ was found.	$Q_1^{-1} \times 10^{-3}$	3.15	3.15	4.45	4.27	4.25
	$Q_2^{-1} \times 10^{-3}$	2.9	3.52	4.45	4.22	4.06
Nitrided and furnace cooled to $215^{\circ}\text{C}$ and held for increasing periods until a minimum $Q^{-1}$ was found.	Time in Hrs	1	2	4	5	
	$Q_1^{-1} \times 10^{-3}$	5.2	4.21	4.2	4.2	
	$Q_2^{-1} \times 10^{-3}$	5.0	4.18	4.2	4.2	

cont'd...

TABLE 9.

Values of  $\log_{10} Q^{-1}$  with corresponding temperatures as plotted in Fig.16. Value of  $Q^{-1}$  are corrected for background damping.

Temperature $^{\circ}K$	$\frac{10^3}{T^{\circ}K}$	$Q^{-1} \cdot 10^{-3}$	$\text{Log}_{10}(Q^{-1})$
488	2.05	0.425	-2.60
573	1.75	0.712	-2.15
623	1.61	1.12	-1.95
673	1.49	2.32	-1.63
723	1.42	3.22	-1.50
773	1.30	4.72	-1.30
973	1.03	3.91	-1.45
998	1.00	3.28	-1.52
1023	0.98	2.74	-1.56
1073	0.93	1.88	-1.73
1123	0.89	1.25	-1.90

cont'd...

TABLE 9(a).

Weight per cent of nitrogen in solid solution as reported  
by various workers.

Temp °C.	Weight % Nitrogen			
	Dijkstra <sup>21</sup>	Paranjpe et al. <sup>51</sup>	Rawlings & Tambini <sup>48</sup>	This work. (0.1 x 1.28)
200	0.003	-	-	-
215	-	-	-	0.0054
250	0.005	-	0.009	-
300	0.010	-	0.0115	0.0091
350	0.015	-	0.02	0.0143
400	0.025	-	0.031	0.0297
450	-	0.033	0.0453	0.0412
500	0.050	-	0.0646	0.0604
550	-	0.070	0.087	-
575	0.075	-	-	-
590	-	0.10	-	-
650	-	0.086	-	-
675	-	-	0.0701	-
700	-	0.070	0.0605	0.050
725	-	-	-	0.042
750	-	-	0.0443	0.0351
800	-	-	0.0286	0.0241
850	-	-	-	0.0160

cont'd...

TABLE 10.

Damping values for Fig. 20. Theoretical peak at 315°K with  $\Delta H = 18.2$  Kcals/mole and  $Q_m^{-1} = 9.9 \cdot 10^{-3}$ .

Temperature °K	$Q_m^{-1} \cdot 10^{-3}$ Experimental	$Q_m^{-1}$ Theoretical $\cdot 10^{-3}$	$3 = (1 - 2)$ $10^{-3}$
	1	2	3
293	4.4	2.8	1.6
298	6.59	4.2	2.39
300	7.68	4.8	2.88
302.5	8.48	5.8	2.68
305	8.67	6.8	1.87
307	9.21	7.7	1.51
309	9.68	8.6	1.08
313	9.88	9.3	0.58
316	9.76	9.8	"
319	9.82	9.3	0.52
321	9.74	8.6	1.14
325	8.57	6.8	1.77
331	6.72	4.5	2.22
336	5.90	3.8	2.10

cont'd...

TABLE 11.

Damping Values for Fig. 21. Theoretical peak 306°K with  
 $\Delta H = 18.2$  Kcals/mole and  $Q_m^{-1} = 8.5 \cdot 10^{-3}$ .

Temperature °K	$Q^{-1} \times 10^{-3}$ Experimental	$Q^{-1} \times 10^{-3}$ Theoretical	$3 = (1-2) \cdot 10^{-3}$
	1	2	3
293	4.4	4.36	0.4
298	6.59	6.54	0.5
300	7.68	7.63	0.5
302.5	8.48	8.43	0.5
305	8.67	8.64	0.3
307	9.21	9.13	0.8
309	9.68	8.23	1.45
313	9.88	6.88	3.00
316	9.76	5.70	4.06
319	9.82	4.64	5.18
321	9.74	4.00	5.74
325	8.57	2.74	5.83
331	6.72	1.77	4.95
336	5.9	1.17	4.73

cont'd...

TABLE 12.

$\Delta H$  values calculated from the equation  $\ln \left( \frac{f_2}{f_1} \right) = \frac{\Delta H}{R} \left( \frac{1}{T_1} - \frac{1}{T_2} \right)$   
 for the subsidiary peaks exemplified in Fig. 21.

$f_1$ cycles/sec.	$f_2$ cycles/sec.	$T_1$ °K	$T_2$ °K	$\Delta H$ Kcals/mole
1.29	2.68	318	325	21,420
1.29	3.72	318	330	23,250
2.68	3.72	325	330	13,920
Average				19,530

TABLE 12 (a)

Comparison of values of  $\Delta H$  and  $T_m$  found by graphical and computer methods for the subsidiary peaks exemplified in Fig. 21.

Frequency cycles/sec	$T_m$ °K Graphical	$T_m$ °K Computer	$\Delta H$ Kcals/ mole Computer	$\Delta H$ Equation (6) Average	$\Delta H$ Kcals/ mole Computer Average
1.29	318	317	19.2	19.53	21.07
2.68	325	324	22.0		
3.72	330	327	22.0		

cont'd...

TABLE 13.

Damping values for Fig.22. Theoretical peak at 303°K with  
 $\Delta H = 18.2$  Kcals/mole and  $Q_m^{-1} = 13 \cdot 10^{-3}$ .

Temperature °K	$Q_m^{-1} \cdot 10^{-3}$ Experimental	$Q_m^{-1} \cdot 10^{-3}$ Theoretical	$3\pi(1-\alpha) \cdot 10^{-3}$
	1	2	3
290.5	8.3	7.1	1.2
297	11.2	11.1	0.1
300.5	13.0	12.9	-0.1
305	12.7	12.9	-0.2
309	10.8	10.9	-0.1
313.5	8.1	8.0	0.1
319.5	5.7	5.2	0.5
324	4.5	3.7	0.8
329	3.1	2.4	0.7
331.5	2.4	2.0	0.4
336	1.7	1.5	0.2

cont'd...

TABLE 14.

Damping values taken from Iaxan et al for an Fe - Al - C alloy containing 0.36% Al. Theoretical peak at  $313^{\circ}\text{K}$  with  $\Delta H = 20.0$  Kcals/mole and  $Q_m^{-1} = 12.7 \cdot 10^{-3}$  (Fig. 23).

Temperature $^{\circ}\text{K}$	$Q^{-1} \times 10^{-3}$ Experimental	$Q^{-1} \times 10^{-3}$ Theoretical	$\beta = (1-3)10^{-3}$
	1	2	3
290	3.0	2.2	0.8
293	3.6	2.8	0.8
296	5.3	3.9	1.4
301	8.2	6.5	1.7
303	9.6	7.8	1.8
305	10.9	9.2	1.7
308	12.0	11.1	0.9
310	12.4	12.1	0.3
312.5	12.7	12.7	0.0
317	11.6	11.5	0.1
320	10.8	10.1	0.7
322.5	9.8	8.6	1.2
325	8.7	7.1	1.6
330.5	6.8	4.5	2.3
333	5.9	3.6	2.3
339	4.3	2.1	2.2
342	3.6	1.6	2.0
345	3.0	1.3	1.7
350	2.0	0.8	1.2

cont'd...

TABLE 15.

Damping values for Fig. 24. Theoretical peak at  $313^{\circ}\text{K}$  with  
 $\Delta H = 20.0 \text{ Kcal/mole}$  and  $Q_m^{\ddagger} = 11.9 \cdot 10^{-3}$ .

Temperature $^{\circ}\text{K}$	$Q^{-1} \cdot 10^{-3}$ Experimental	$Q^{-1} \cdot 10^{-3}$ Theoretical	$3 = (1-2) \cdot 10^{-3}$
	1	2	3
293	4.2	3.9	0.3
297	5.6	5.0	0.6
300	7.9	6.7	1.2
305	10.5	9.9	0.6
310	11.8	11.6	0.2
314	11.8	11.8	0.0
318	10.3	9.5	0.8
323	7.8	6.9	0.9
327	6.3	5.0	1.3
332	4.5	3.5	1.0
337	3.3	2.5	0.8

cont'd...

TABLE 16.

Damping values for Fig. 25. Theoretical peak at 305°K with  $\Delta H = 18.2$  Kcals/mole and  $Q_m^{-1} = 14 \cdot 10^{-3}$ .

Temperature °K	$Q_m^{-1} \times 10^{-3}$ Experimental	$Q_m^{-1} \times 10^{-3}$ Theoretical	$\beta = (1-2) \cdot 10^{-3}$
	1	2	3
291	24.4	7.3	17.1
292.5	27.6	8.2	19.4
295	30.4	9.2	21.2
299	31.1	11.7	19.4
302	29.3	13.1	16.2
307.5	20.1	13.5	6.6
311.5	11.7	11.6	0.1
317	8.1	8.0	0.1
321	5.9	5.7	0.2
326	4.95	4.0	0.95
330.5	3.2	2.9	0.3
336	2.6	2.4	0.2

cont'd...

TABLE 17.

Damping values for Fig.26. Theoretical peak at 305°K  
with  $dH = 18.2$  Kcals/mole and  $Q_m^{-1} = 5.5 \cdot 10^{-3}$ .

Temperature °K	$Q_m^{-1} \times 10^{-3}$ Experimental	$Q_m^{-1} \times 10^{-3}$ Theoretical	$\beta = (1-2) \times 10^{-3}$
	1	2	3
290	10.8	2.6	8.0
292	13.3	3.3	10.0
294	15.0	3.8	11.2
298.5	15.6	4.0	10.8
301	12.3	5.3	7.0
304.5	9.8	5.5	4.3
309	7.0	5.3	1.7
313	5.1	4.2	0.9
319	4.0	3.6	0.4
324	2.5	2.2	0.3
333	1.6	1.3	0.3

cont'd...

TABLE 18.

Damping values for Fig. 27. Theoretical peak at  $306^{\circ}\text{K}$   
 with  $dH = 18.2$  Kcals/mole and  $Q_m^{-1} = 30.0 \cdot 10^{-3}$ .

Temperature $^{\circ}\text{K}$	$Q^{-1} \times 10^{-3}$ Experimental	$Q^{-1} \times 10^{-3}$ Theoretical	$3 = (1-2) \times 10^{-3}$
	1	2	3
293.5	18.3	13.1	5.2
297	21.9	17.9	4.0
301	30.0	24.0	6.0
306	35.0	29.4	5.6
311	32.0	28.8	3.2
316	24.9	23.1	1.8
321	18.6	16.5	2.1
326	11.2	11.2	0.0
330.5	7.9	7.3	0.6
336	5.3	5.0	0.3

cont'd...

TABLE 19.

Damping values for Fig. 28. Theoretical peak at 300°K with  $\Delta H = 18.2$  Kcals/mole and  $Q_m^{-1} = 35.0 \cdot 10^{-3}$ .

Temperature °K	$Q_m^{-1} \times 10^{-3}$ Experimental	$Q_m^{-1} \times 10^{-3}$ Theoretical	$3 = (1-2) \times 10^{-3}$
	1	2	3
293	17.6	15.2	2.4
297	24.6	21.4	3.2
300.5	33.4	27.9	5.5
306	37.0	35.0	2.0
310	35.0	34.5	0.5
317	26.3	25.5	0.8
321	21.0	20.4	0.6
326	15.5	15.0	0.5
330	11.1	10.9	0.2
336	8.0	7.6	0.4

cont'd...

TABLE 20.

Damping values for Fig.29. Theoretical peak at 308°K with  $\Delta H = 18.2$  Kcals/mole and  $Q_m^{-1} = 33.5 \cdot 10^{-3}$ .

Temperature °K	$Q_m^{-1} \times 10^{-3}$ Experimental	$Q_m^{-1} \times 10^{-3}$ Theoretical	$3=(1-2) \times 10^{-3}$
	1	2	3
294	20.5	17.0	3.5
297	26.9	20.3	6.6
301	38.4	27.4	11.0
306	39.5	32.9	6.6
311	36.6	32.6	4.0
316	29.4	26.4	3.0
320	21.6	19.6	2.0
325	14.2	13.6	0.6
330	9.3	9.1	0.2
336	6.3	6.0	0.3

cont'd...

TABLE 21.

Damping values for Fig.30. Theoretical peak at 309<sup>o</sup>K with  $\Delta H = 18.2$  Kcal/mole and  $Q_m^{\ddagger} = 34.10^{-3}$ .

Temperature <sup>o</sup> K	$Q_m^{\ddagger} \times 10^{-3}$ Experimental	$Q_m^{\ddagger} \times 10^{-3}$ Theoretical	$3=(1-2) \times 10^{-3}$
	1	2	3
294	17.0	14.5	2.5
297	22.6	19.3	3.3
300	28.7	23.9	4.8
305	36.0	31.7	4.3
310	37.2	34.0	3.2
315	33.3	31.7	1.6
320	22.0	21.9	0.1
325	15.0	13.5	1.5
329	11.2	11.0	0.2
335	6.6	6.5	0.1

cont'd...

TABLE 22.

Damping values for Fig.31. Theoretical peak at 309<sup>0</sup>K  
with  $\Delta H = 18.2$  Kcal/mole and  $Q_m^{-1} = 13.0 \cdot 10^{-3}$ .

Temperature °K	$Q_m^{-1} \times 10^{-3}$ EXPERIMENTAL	$Q_m^{-1} \times 10^{-3}$ THEORETICAL	$3 \cdot (1-2) \times 10^{-3}$
	1	2	3
293	18.6	5.5	13.1
296	24.7	6.9	17.8
300	30.4	9.0	21.4
305	35.0	12.2	22.8
309	30.0	13.0	17.0
316	18.6	10.4	8.2
320	10.9	8.0	2.9
325	6.1	5.5	0.6
331	3.2	3.0	0.2

cont'd...

TABLE 23.

Damping values for Fig.32. Theoretical peak at 309°K  
with  $dH = 18.2$  Kcal/mole and  $Q_m^{-1} = 36.0 \cdot 10^{-3}$ .

Temperature °K	$Q_m^{-1} \times 10^{-3}$ Experimental	$Q_m^{-1} \times 10^{-3}$ Theoretical	$\Delta = (1-2) \times 10^{-3}$
	1	2	3
292	12.5	13.1	-0.6
297	19.7	20.2	-0.5
301	28.3	27.0	1.3
305	35.2	34.5	0.5
311	35.8	35.8	0.0
316	30.2	29.1	1.1
320	21.9	21.7	0.2
326	14.2	14.2	0.0
330	10.2	10.2	0.0
334	7.0	7.0	0.0

cont'd...

TABLE 2A.

Damping values for Fig.35(a) and Fig.35(b). Theoretical peak at 309<sup>0</sup>K with  $dH = 18.2$  Kcals/mole and  $Q_m^{-1}$  equal to  $14.0 \cdot 10^{-3}$  and  $12.5 \cdot 10^{-3}$  respectively.

Fig.35(a)

Temperature °K	$Q_m^{-1} \times 10^{-3}$ Experimental	$Q_m^{-1} \times 10^{-3}$ Theoretical	$\delta = (1-2) \times 10^{-3}$
	1	2	3
293	8.3	5.3	3.0
297	12.4	7.7	4.7
301	16.1	10.8	5.3
306	19.1	13.6	5.3
311	16.7	12.9	3.8
316	12.0	10.4	1.6
320	9.0	8.5	0.5
326	4.6	4.5	0.1
336	2.0	1.9	0.1

cont'd...

TABLE 24.

Fig. 35(b)

Temperature °K	$Q_m^{-1} \times 10^{-3}$ Experimental	$Q_m^{-1} \times 10^{-3}$ Theoretical	$3=(1-2) \times 10^{23}$
	1	2	3
295	7.0	6.2	0.8
298	10.5	7.8	2.7
301	13.7	9.5	4.2
306	15.8	12.2	3.6
311	14.6	12.3	2.3
316	11.2	9.8	1.4
320	8.6	7.7	0.9
326	5.5	5.0	0.5
330	4.2	3.6	0.6
336	3.1	2.5	0.6

cont'd...

TABLE 26

Solubility product ( $K = [Al\%][N\%]$ ) for nitrided Al

Alloys at various temperatures as plotted in Fig.37.

Temp °C		0.3% Al	0.09% Al	0.068% Al	0.044% Al	0.015% Al
590	Wt.%N	$13.9 \cdot 10^{-2}$	$5.6 \cdot 10^{-2}$	$4.6 \cdot 10^{-2}$	$3.4 \cdot 10^{-2}$	$2.6 \cdot 10^{-2}$
	N	$2.04 \cdot 10^{-2}$	$2.64 \cdot 10^{-2}$	$2.74 \cdot 10^{-2}$	$1.73 \cdot 10^{-2}$	$1.79 \cdot 10^{-2}$
	Al	$8.8 \cdot 10^{-2}$	$3.29 \cdot 10^{-2}$	$2.68 \cdot 10^{-2}$	$1.18 \cdot 10^{-2}$	$1.3 \cdot 10^{-3}$
	K	$1.8 \cdot 10^{-3}$	$8.7 \cdot 10^{-4}$	$7.34 \cdot 10^{-4}$	$2.04 \cdot 10^{-4}$	$2.33 \cdot 10^{-5}$
500	Wt.% N	$13.6 \cdot 10^{-2}$	$4.3 \cdot 10^{-2}$	$5.4 \cdot 10^{-2}$	$3.9 \cdot 10^{-2}$	$2.3 \cdot 10^{-2}$
	N	$1.42 \cdot 10^{-2}$	$1.83 \cdot 10^{-2}$	$1.87 \cdot 10^{-2}$	$2.54 \cdot 10^{-2}$	$1.54 \cdot 10^{-2}$
	Al	$6.5 \cdot 10^{-2}$	$4.23 \cdot 10^{-2}$	$2.52 \cdot 10^{-2}$	$1.21 \cdot 10^{-2}$	$2.2 \cdot 10^{-3}$
	K	$9.23 \cdot 10^{-4}$	$5.34 \cdot 10^{-4}$	$4.71 \cdot 10^{-4}$	$3.07 \cdot 10^{-4}$	$3.39 \cdot 10^{-5}$
400	Wt.% N	$12.9 \cdot 10^{-2}$	$6.1 \cdot 10^{-3}$	$3.4 \cdot 10^{-2}$	$5 \cdot 10^{-3}$	$1.1 \cdot 10^{-2}$
	N	$2 \cdot 10^{-3}$	$3 \cdot 10^{-3}$	$5.5 \cdot 10^{-3}$	$1.6 \cdot 10^{-3}$	$5.6 \cdot 10^{-2}$
	Al	$5.5 \cdot 10^{-2}$	$8.42 \cdot 10^{-2}$	$3.95 \cdot 10^{-2}$	$3.74 \cdot 10^{-2}$	$4.58 \cdot 10^{-3}$
	K	$1.1 \cdot 10^{-4}$	$2.53 \cdot 10^{-4}$	$2.18 \cdot 10^{-4}$	$5.74 \cdot 10^{-5}$	$2.56 \cdot 10^{-5}$
300	Wt.% N	$13.6 \cdot 10^{-2}$	$4.52 \cdot 10^{-2}$	$3.04 \cdot 10^{-2}$	$2.05 \cdot 10^{-2}$	$4.47 \cdot 10^{-3}$
	N	$10^{-3}$	$4.2 \cdot 10^{-3}$	$4 \cdot 10^{-3}$	$8.5 \cdot 10^{-3}$	$1.1 \cdot 10^{-3}$
	Al	$3.7 \cdot 10^{-2}$	$7.9 \cdot 10^{-2}$	$5.1 \cdot 10^{-2}$	$2.32 \cdot 10^{-2}$	$6.5 \cdot 10^{-3}$
	K	$3.7 \cdot 10^{-5}$	$3.3 \cdot 10^{-5}$	$2.04 \cdot 10^{-5}$	$1.97 \cdot 10^{-5}$	$7.15 \cdot 10^{-6}$

cont'd...

TABLE 26

Solubility product ( $K = [Al\%][N\%]$ ) as found by various workers between 300 - 590°C.

Reference	K Values			
	300°C	400°C	500°C	590°C
Darken <sup>17</sup>	$10^{-11}$	$1.1 \cdot 10^{-10}$	$2.2 \cdot 10^{-8}$	$2.24 \cdot 10^{-7}$
Leslie <sup>39</sup>	$6.03 \cdot 10^{-11}$	$1.18 \cdot 10^{-10}$	$5.25 \cdot 10^{-8}$	$6.76 \cdot 10^{-7}$
This Work	$2.32 \cdot 10^{-5}$	$1.34 \cdot 10^{-4}$	$4.52 \cdot 10^{-4}$	$7.25 \cdot 10^{-4}$

cont'd...

TABLE 27.

Damping values for Figs. 36(a) and Fig. 36(b). Theoretical peak at 309°K with  $\Delta H = 18.2$  Kcals/mole and  $Q_m^{-1}$  equal to  $12.0 \cdot 10^{-3}$  and  $11.5 \cdot 10^{-3}$  respectively.

Fig. 36(a)

Temperature °K	$Q_m^{-1} \times 10^{-3}$ Experimental	$Q_m^{-1} \times 10^{-3}$ Theoretical	$\beta = (1-2) \times 10^{-3}$
	1	2	3
292	5.0	4.5	0.5
296	7.3	6.4	0.9
301	11.1	6.8	2.3
306	13.3	11.3	2.0
311	12.5	11.6	0.9
316	11.2	9.7	1.5
320	8.0	7.6	0.4
326	4.8	4.6	0.2
330	3.6	3.2	0.4
336	2.2	2.2	0.0

cont'd...

TABLE 28.

Fig. 36 (b)

Temperature °K	$Q_m^{-1} \times 10^{-3}$ Experimental	$Q_m^{-1} \times 10^{-3}$ Theoretical	$3 = (1-2) \times 10^{-3}$
	1	2	3
293	4.8	4.6	0.2
297	6.8	6.6	0.2
301	9.5	9.0	0.5
306	12.1	11.1	1.0
311	11.4	11.4	0.0
316	9.0	9.3	-0.3
320	8.2	7.6	0.6
326	5.2	5.0	0.2
336	2.0	2.0	0.0

cont'd...

CODE FOR FIG. 1.

- a - Thermocouple port.
- b - Silica tube.
- c - Copper coil from induction heater.
- d - Handle for alloy additions.
- e - Port for introducing alloy additions to receptacle, (u).
- f - Handle for rotating crucible basket.
- g - Springs.
- h - Outer casing for rack and pinion.
- i - Rack.
- j - Stand.
- k - Crucible basket.
- l - Refractory alumina.
- m - Crucible.
- n - O-rings.
- o - Water-cooling tube.
- p - Observation port.
- q - Flanges.
- r - Oil diffusion pump.
- s - Rotary pump.
- t - Valves.
- u - Receptacle for alloy additions.
- v - Flap valve

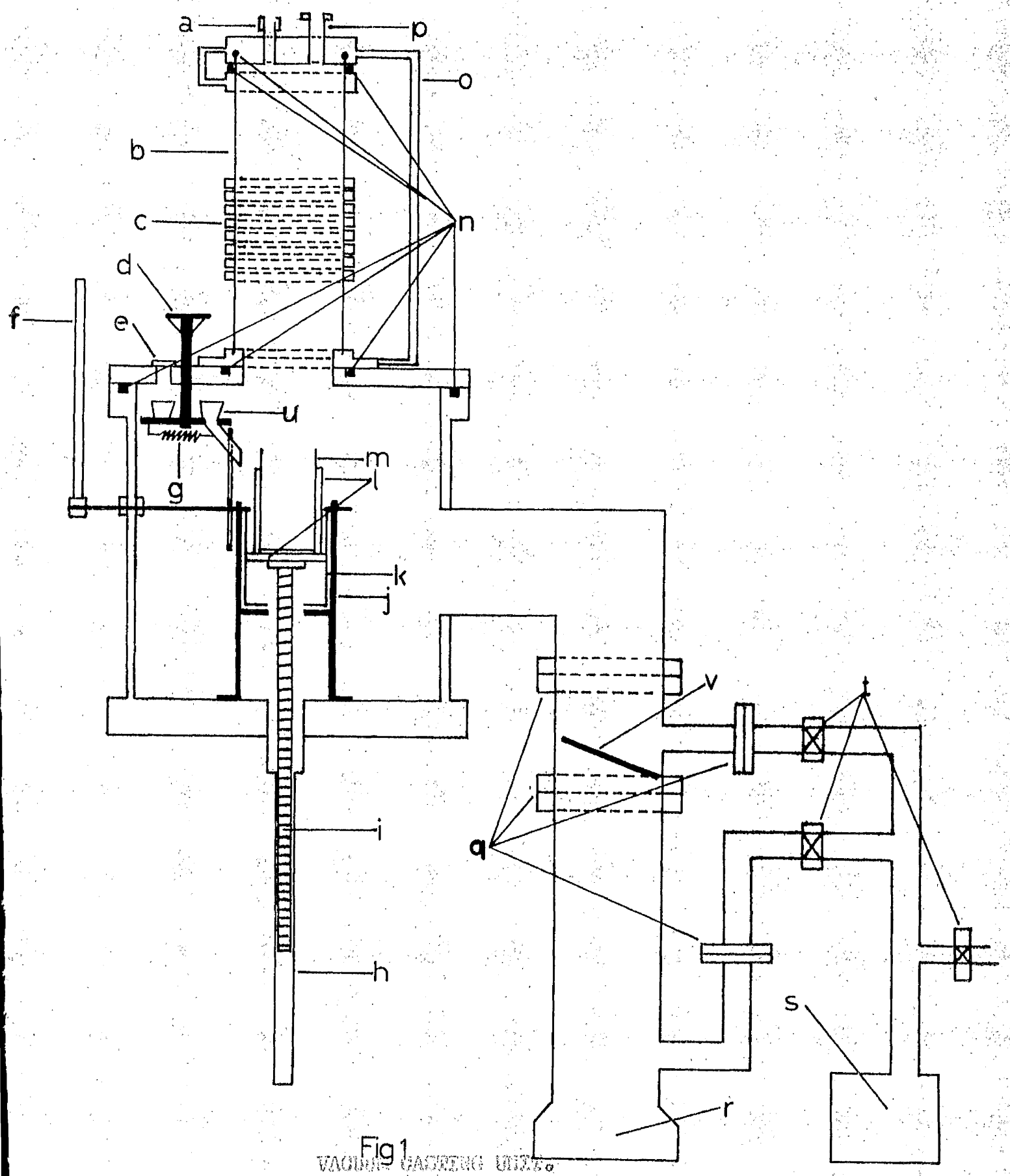


Fig 1  
VACUUM GAS WELDING APPARATUS

CODE FOR FIG. 2.

a	"	Manometer.
b	"	Stopcock.
c	"	Dewar flask.
d	"	Solid carbon dioxide.
e	"	Activated charcoal or molecular sieve material in a large test tube.
f	"	Toluene in glass bottle.
g	"	Asbestos wool.
h	"	Sindanyo ether.
i	"	Thermocouple.
j	"	Valve.
k	"	Terminals.
l	"	Fuse wire.
m	"	Specimen carrier.
n	"	O-rings.
o	"	Water, as quenching medium.
p	"	Detachable Quenching tank.
q	"	Geisler tube.
r	"	Flange.
s	"	Oil diffusion pump.
t	"	Rotary pump.
u	"	Brass flanges.
v	"	Gas-mixing vessels.

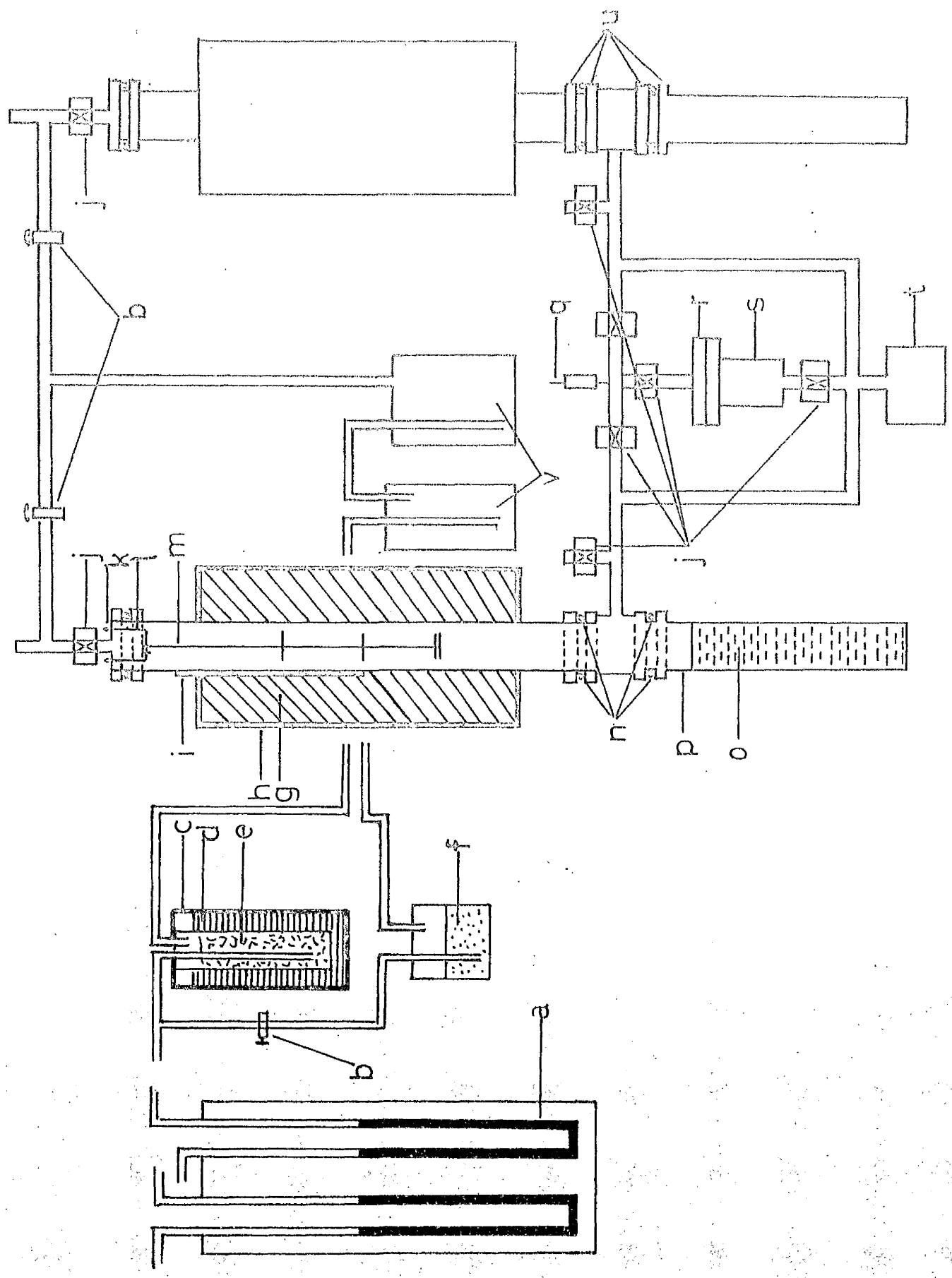


FIG. 2.

DEPARTMENT OF COMMERCE

CODE FOR FIG. 3 (cont'd).

Y - Drum.  
S - Light source.  
Z - Drum motor.

CODE FOR FIG. 3.

- a    "    Electrical fan motor.
- b    "    Wooden case.
- c    "    Gear wheel.
- d    "    Upper specimen grip.
- e    "    Thermocouple.
- f    "    Specimen.
- g    "    Lower specimen grip
- h    "    Mirror.
- i.   "    Springs.
- j    "    Brass weights of inertia member.
- k    "    Oil.
- l    "    Adjustable fest.
- m    "    Dashpot.
- n    "    Stands for electromagnets.
- o    "    Cross-wire of inertia member.
- p    "    Electromagnets.
- q    "    Sunvic Controller.
- r    "    Sunvic Controller.
- s    "    Coils of Nichrome wire.
- t    "    Screw for rotating specimen.
- u    "    Pendulum stand.
- v    "    Screw for adjusting height of specimen.
- w    "    Fan.
- x    "    Lenses.
- y    "    Drum stand.

cont'd...



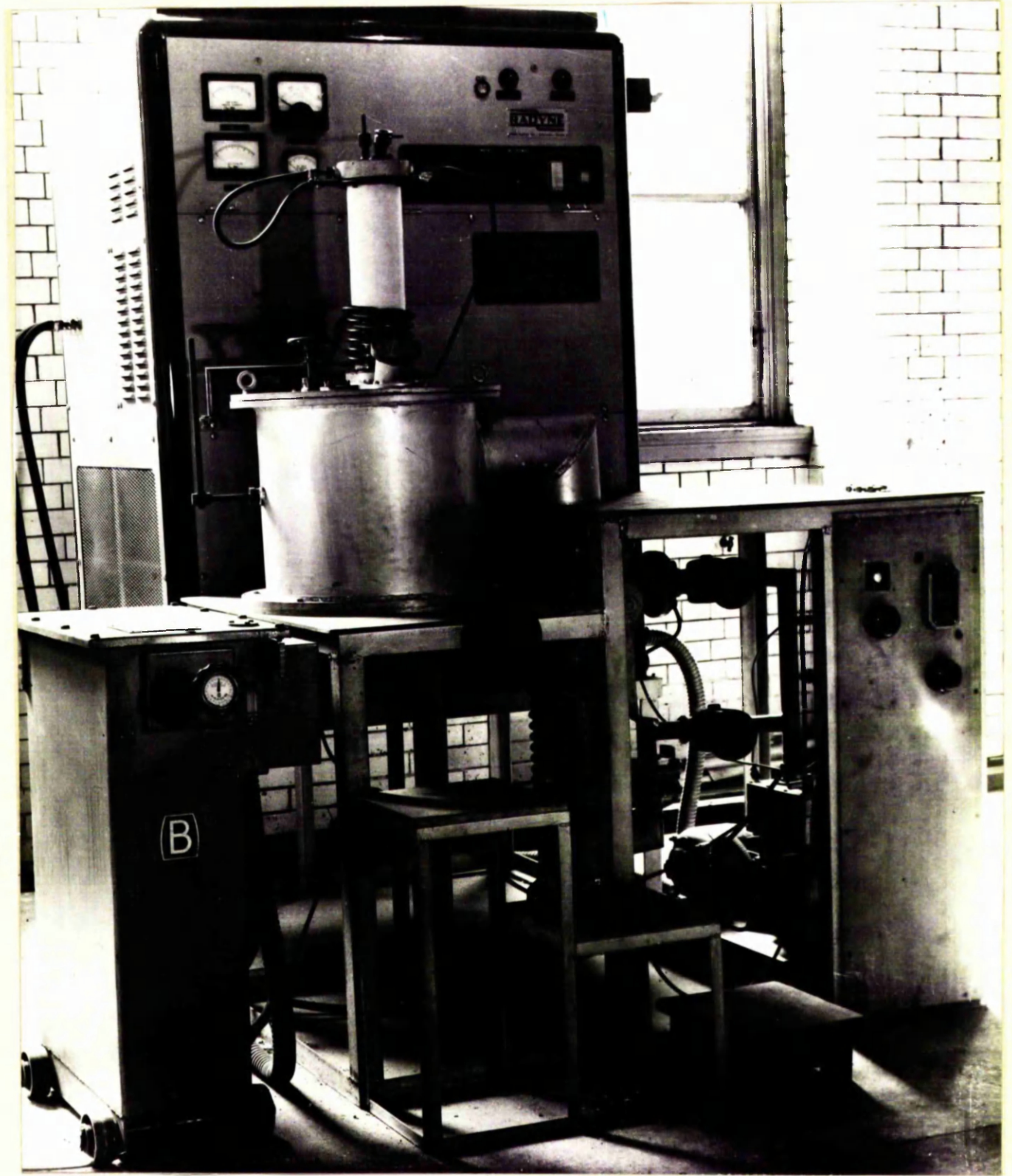


FIG.4.

VACUUM CASTING UNIT.

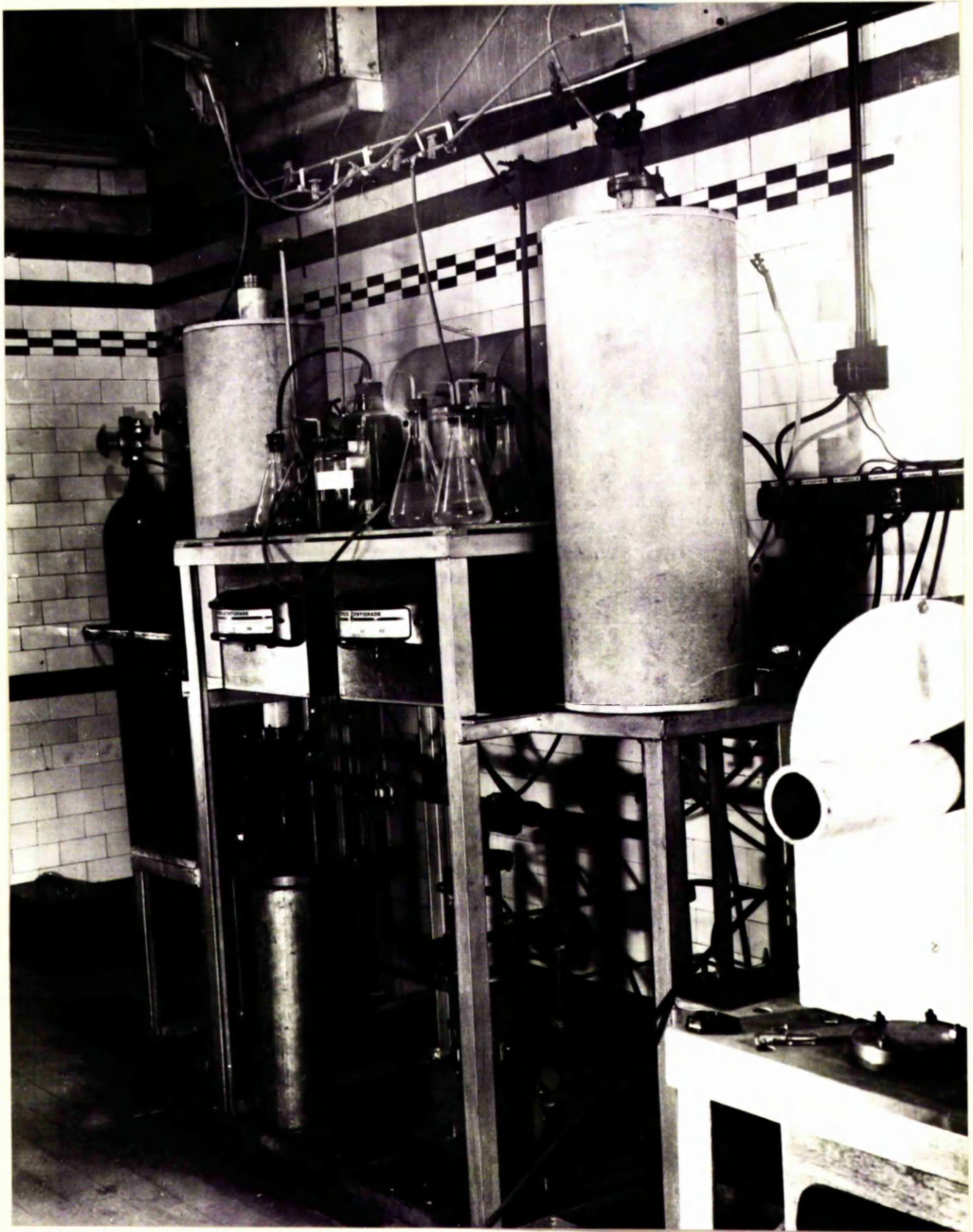


FIG.5.

HEAT TREATMENT FURNACES.

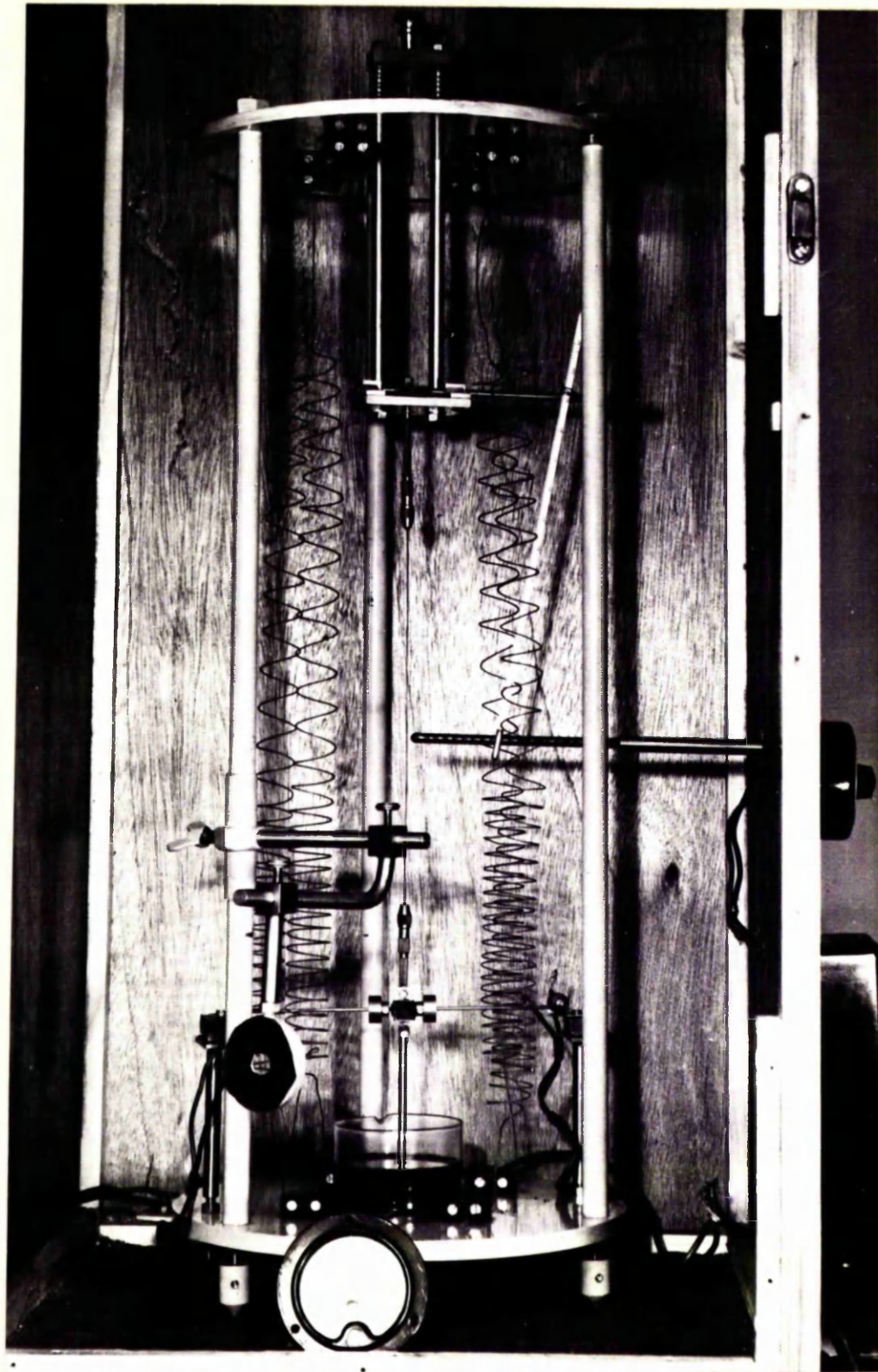


FIG.6.

TORSION PENDULUM.

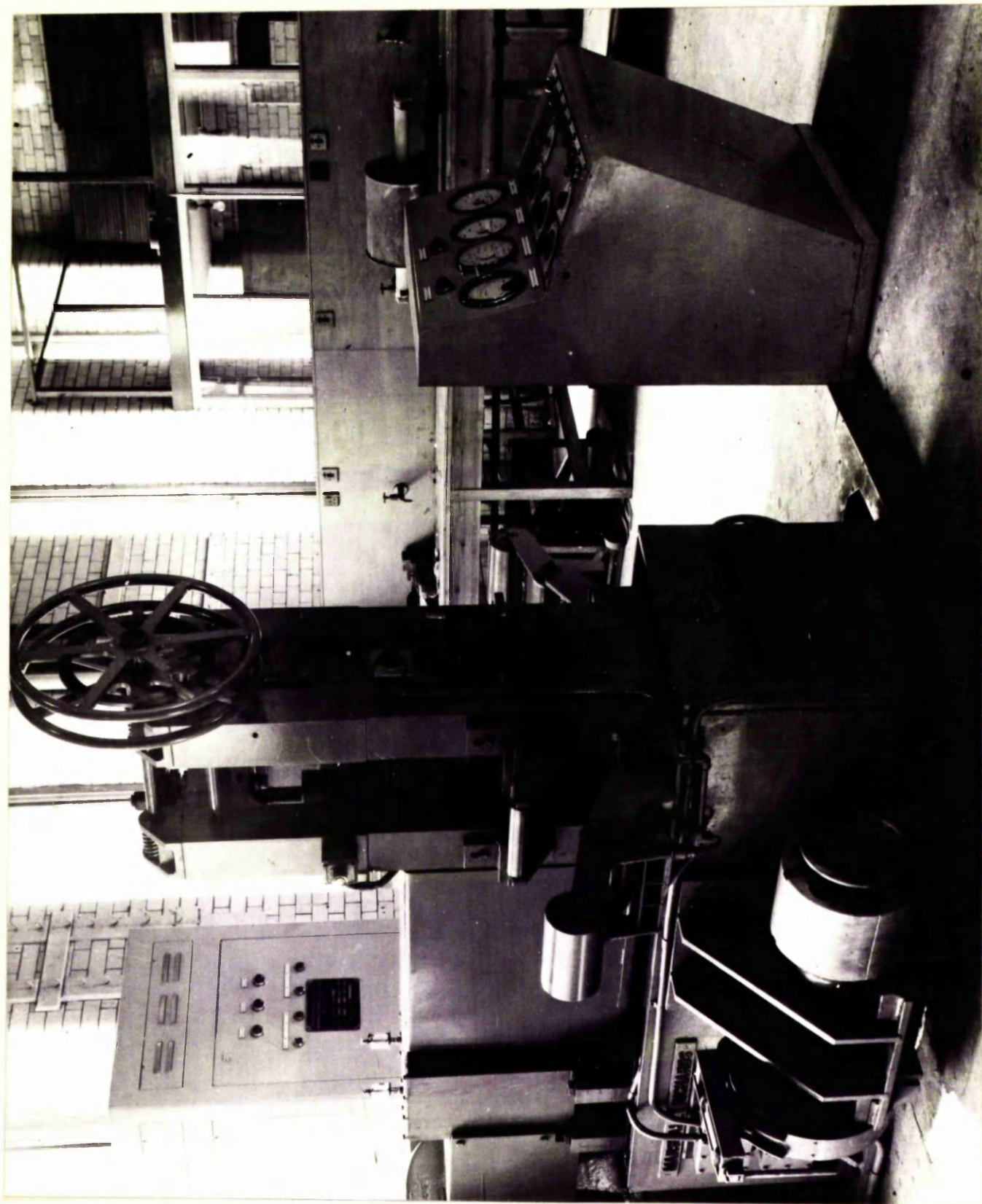


FIG.7.

MARSHALL-RICHARDS ROLLING MILL.

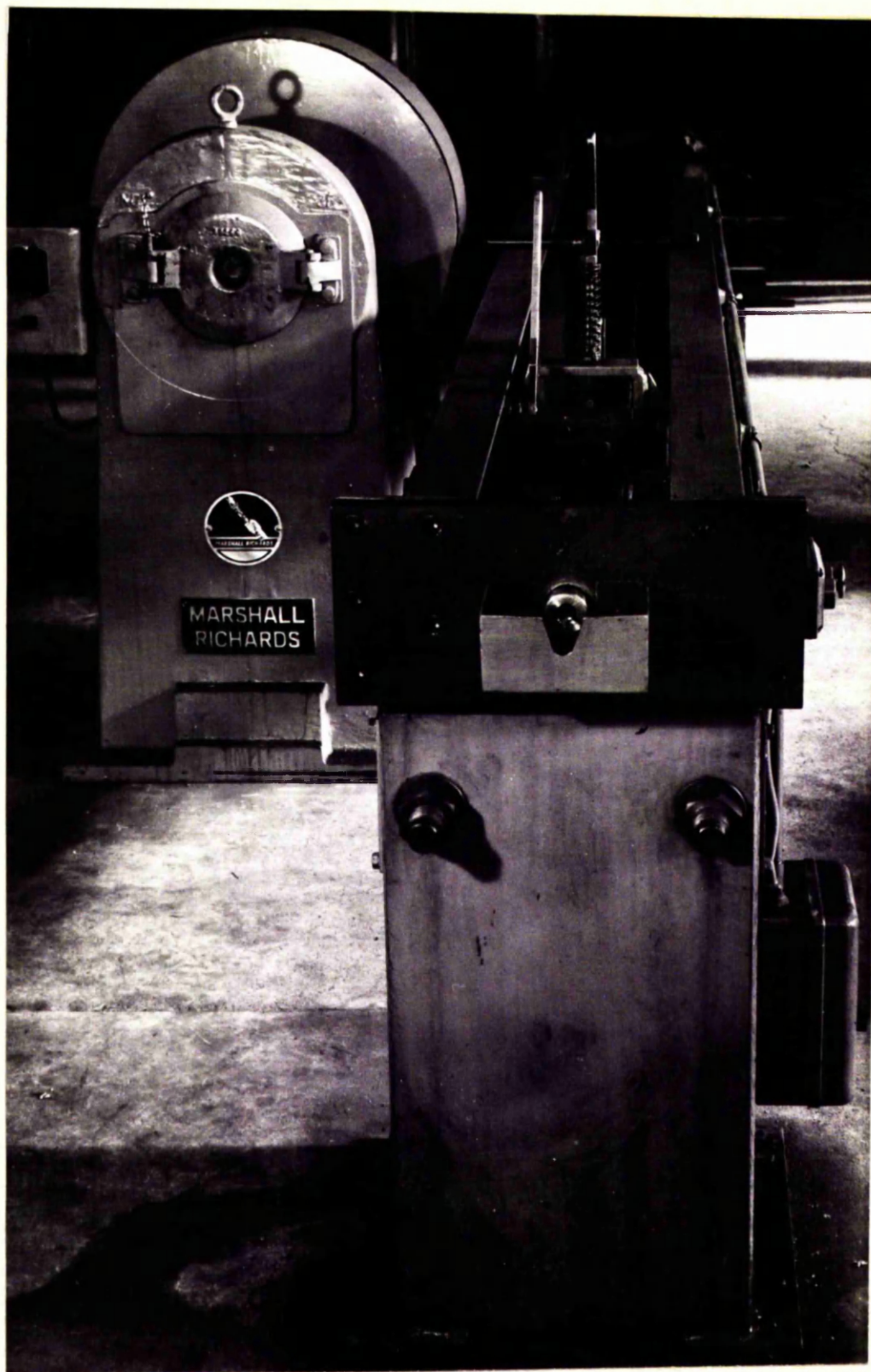


FIG. 8.

MARSHALL-RICHARDS DRAW-BENCH AND SWAGER.

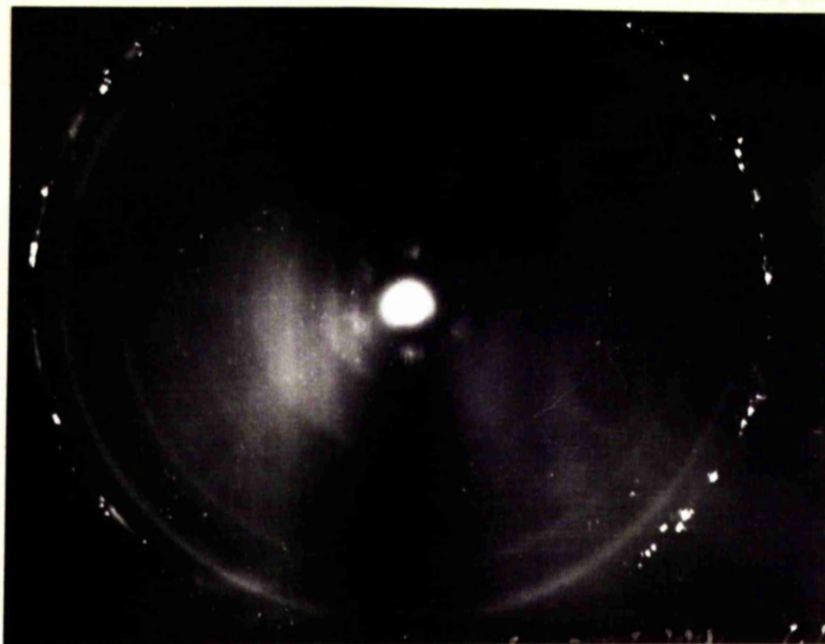


FIG. 9.

Laue Transmission Photograph of cold drawn and annealed wire specimen. No preferred orientation is evident as can be seen from the complete nature of the Debye rings.

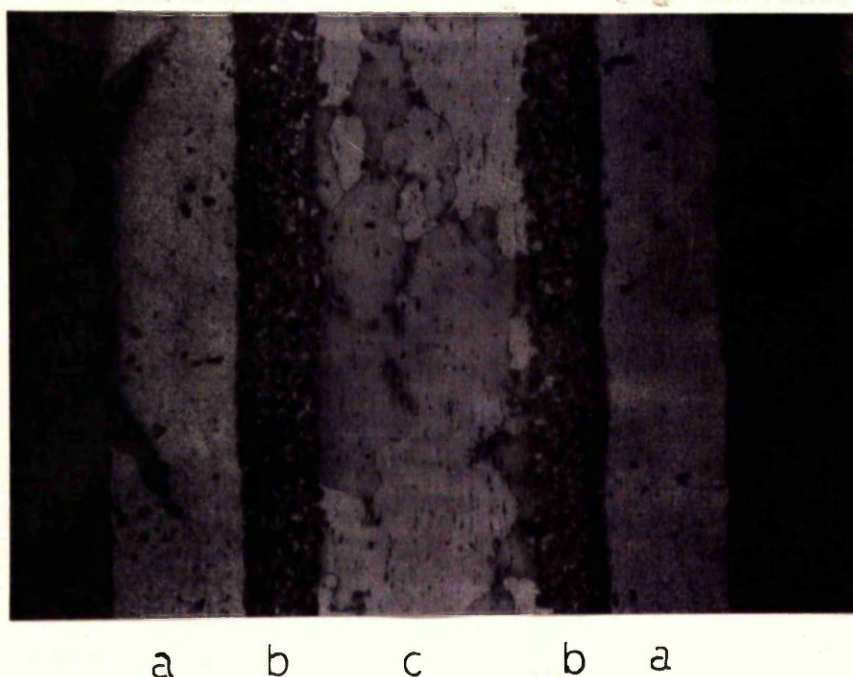
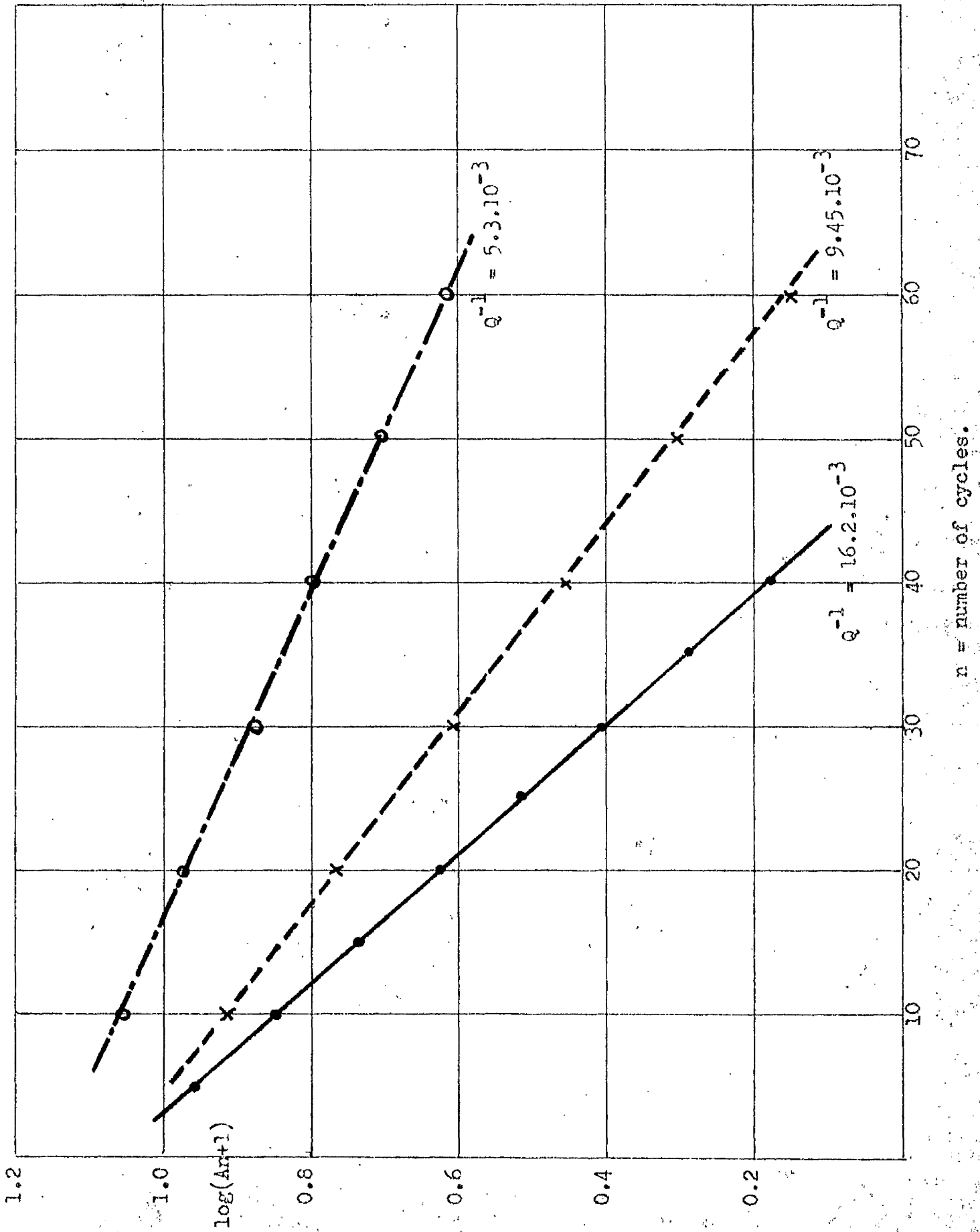
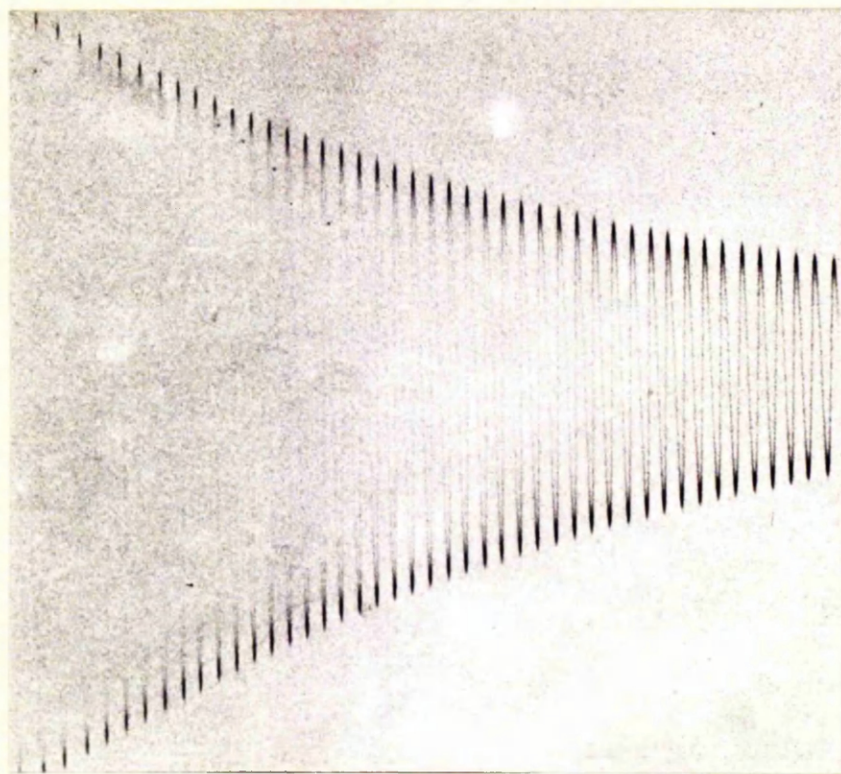


FIG.10.

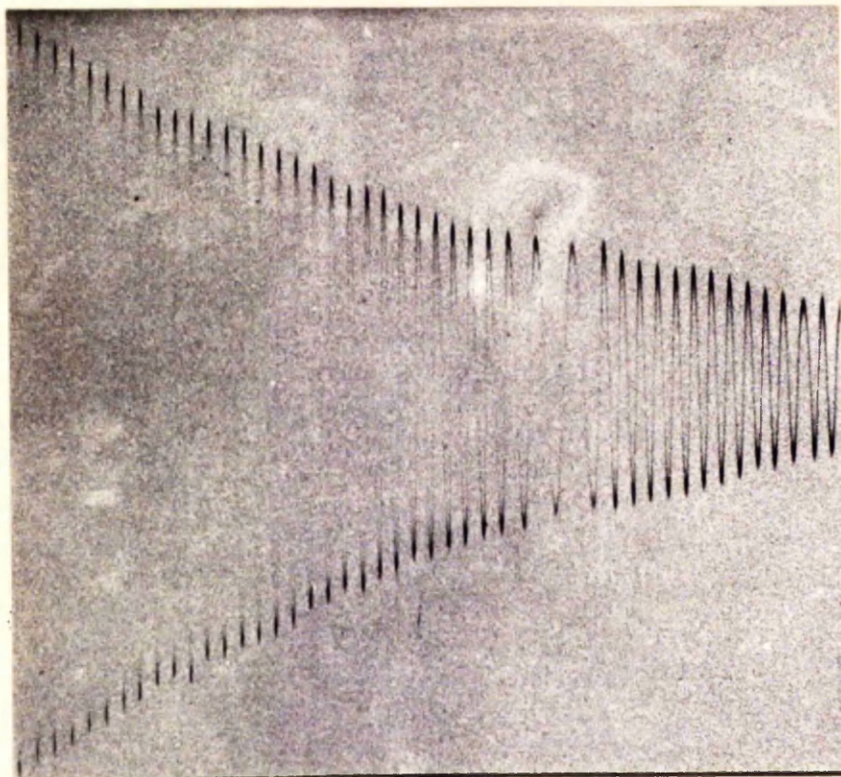
Triplex structure of over-nitrided pure iron specimen nitrided in 6% ammonia, ammonia/hydrogen mixture for eight-hours. (a) is  $Fe_4N$ , (b) iron/ $Fe_4N$  eutectoid and (c) alpha-iron with nitrogen in solid solution. (Etchant 2% Nital. Magnification X100).

FIG.11. Independence of damping from the amplitude of vibration.





(a)



(b)

FIG.12.

Example of traces produced with torsion-pendulum apparatus. (a) is acceptable, (b) is not acceptable.

FIG.13. Damping curves of pure iron specimens,  
nitrided 30 minutes in 6% ammonia mixture.

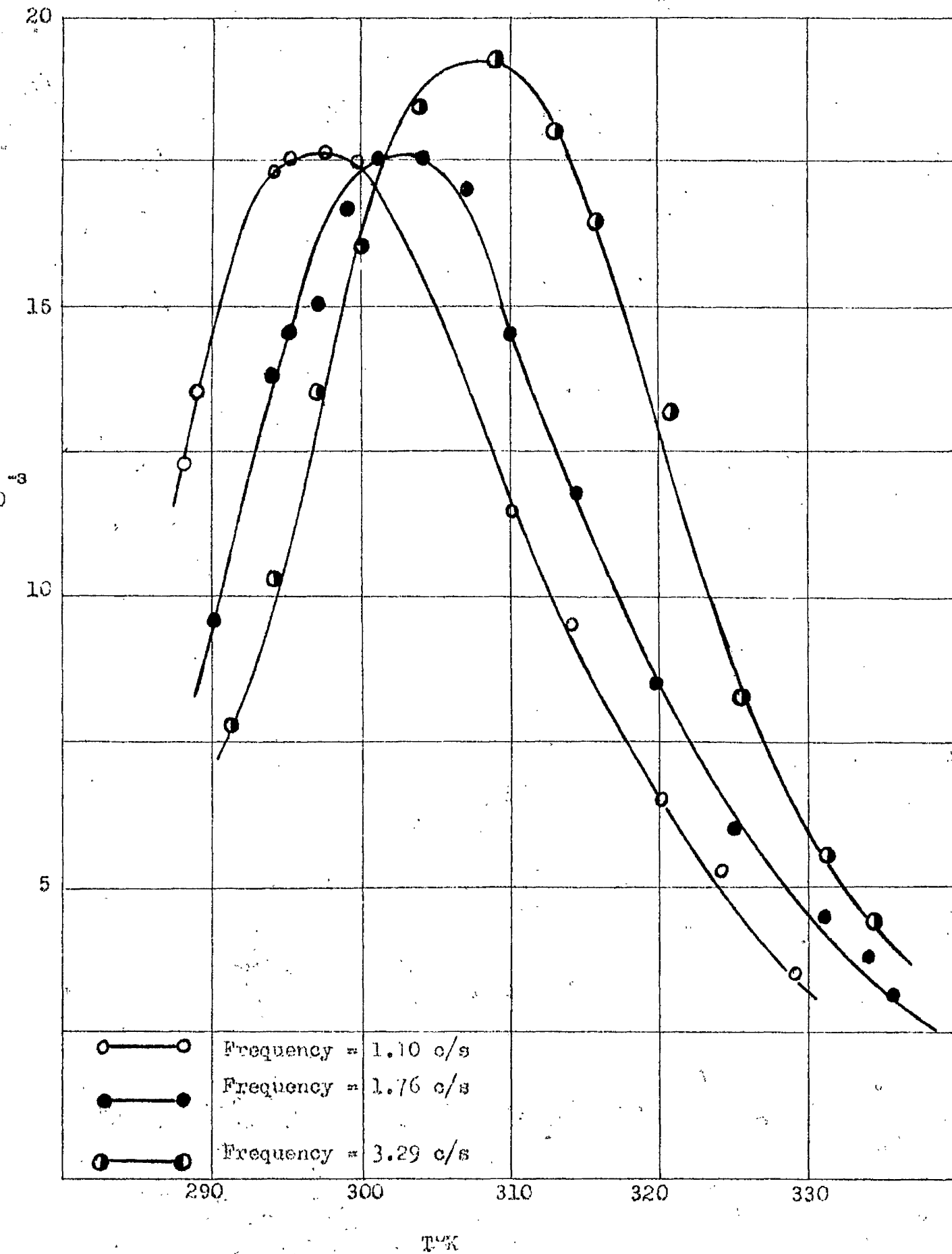


FIG.14. Variation of diffusion coefficient, D,  
with absolute temperature.

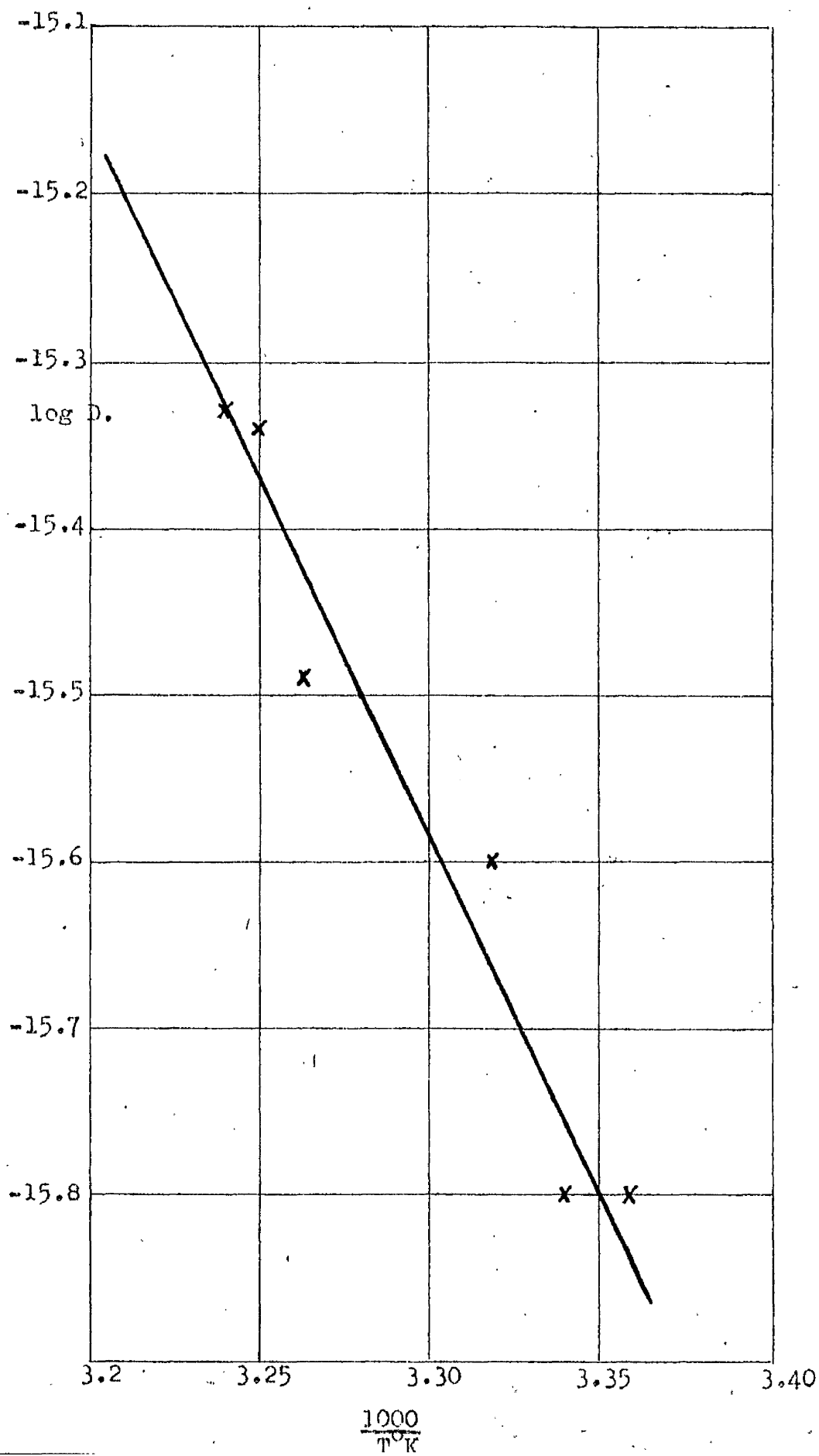


FIG.15. Approach to equilibrium at 215°C

(a) furnace cooled from 590°C

(b) heated from room temperature.

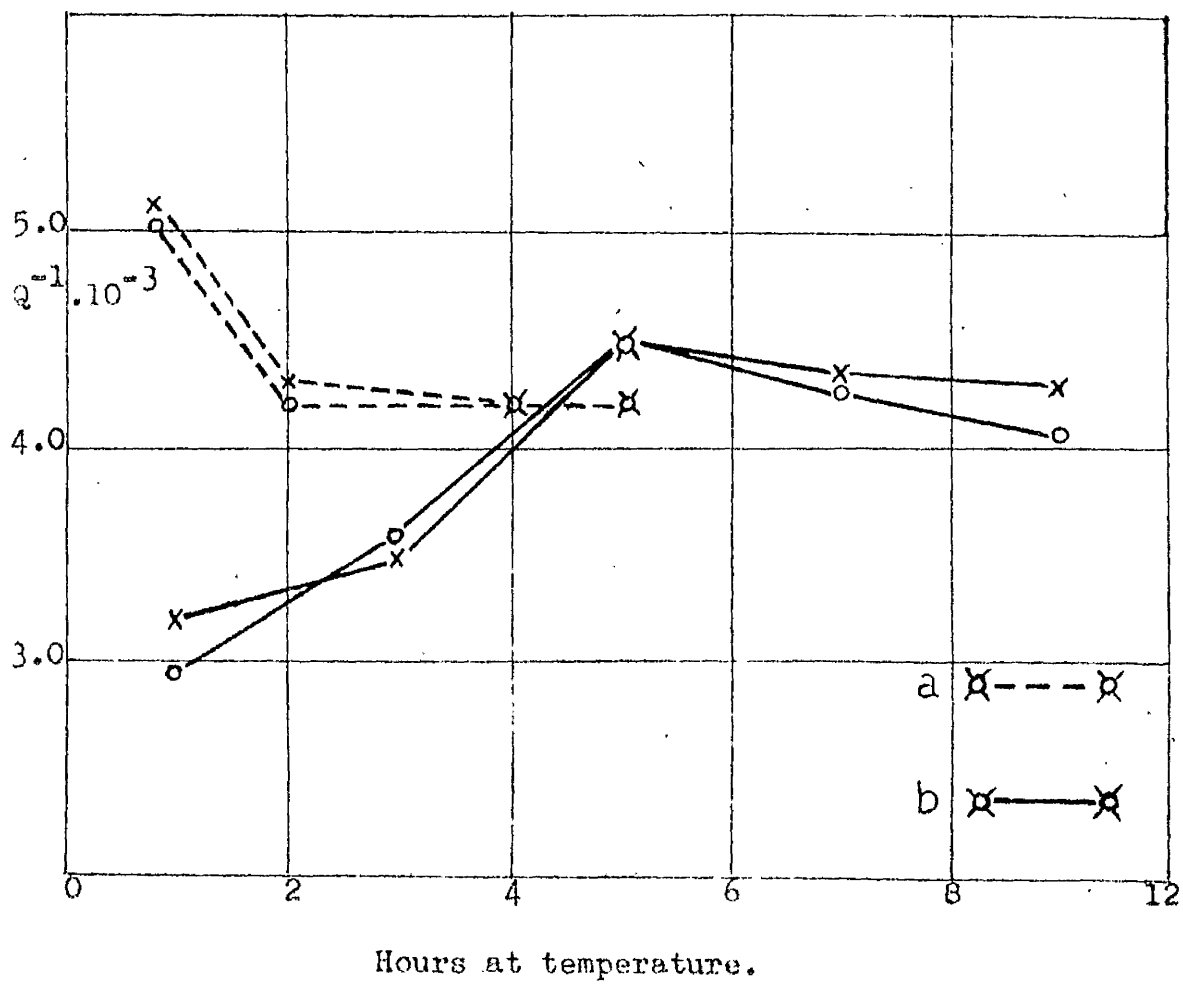


FIG.16. Limits of solid solubility as a function of absolute temperature (a) below 590°C (b) above 590°C.

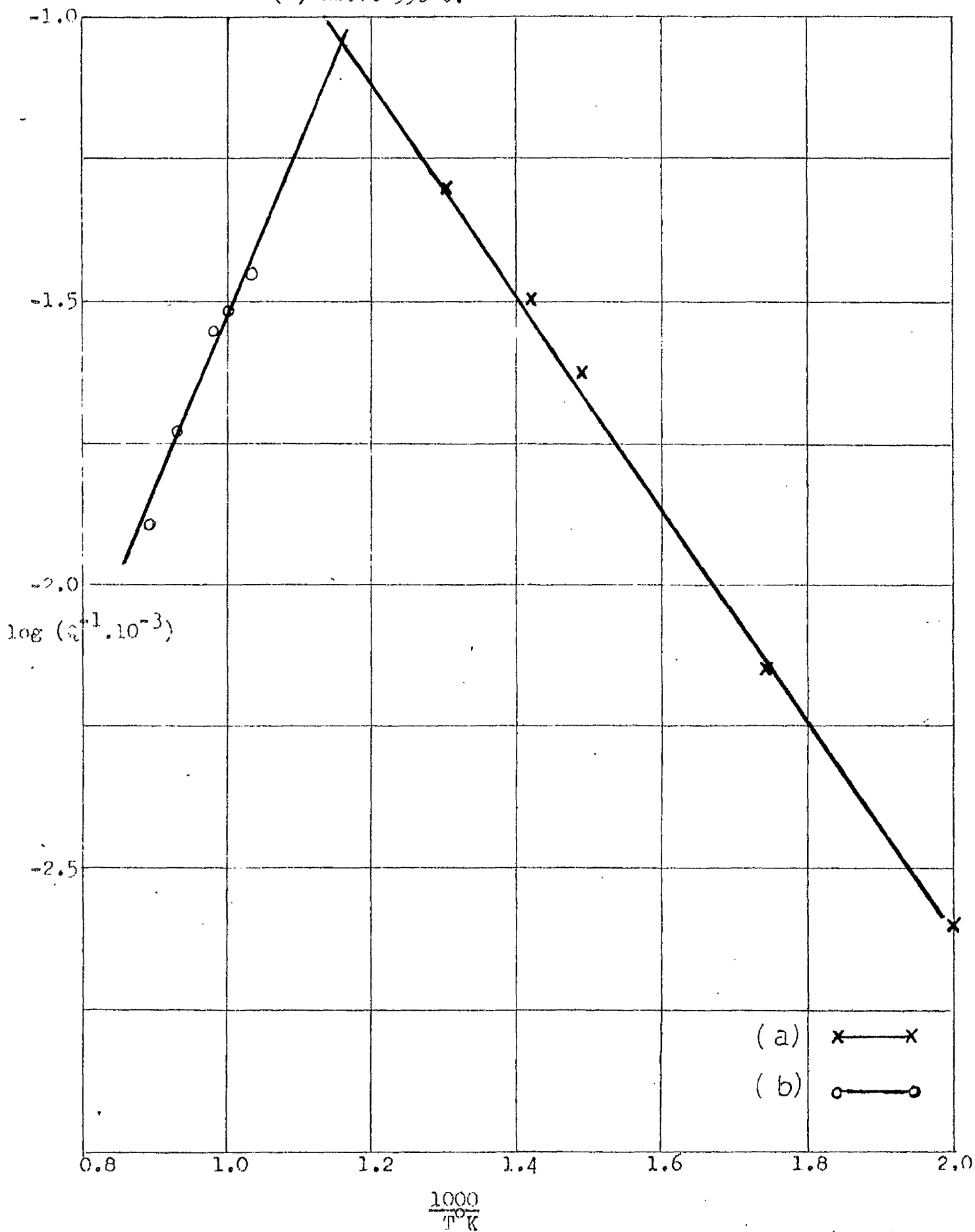


FIG.17. Solid solubility of nitrogen in alpha-iron as determine (a) by Dijkstra<sup>21</sup> and (b) this present work

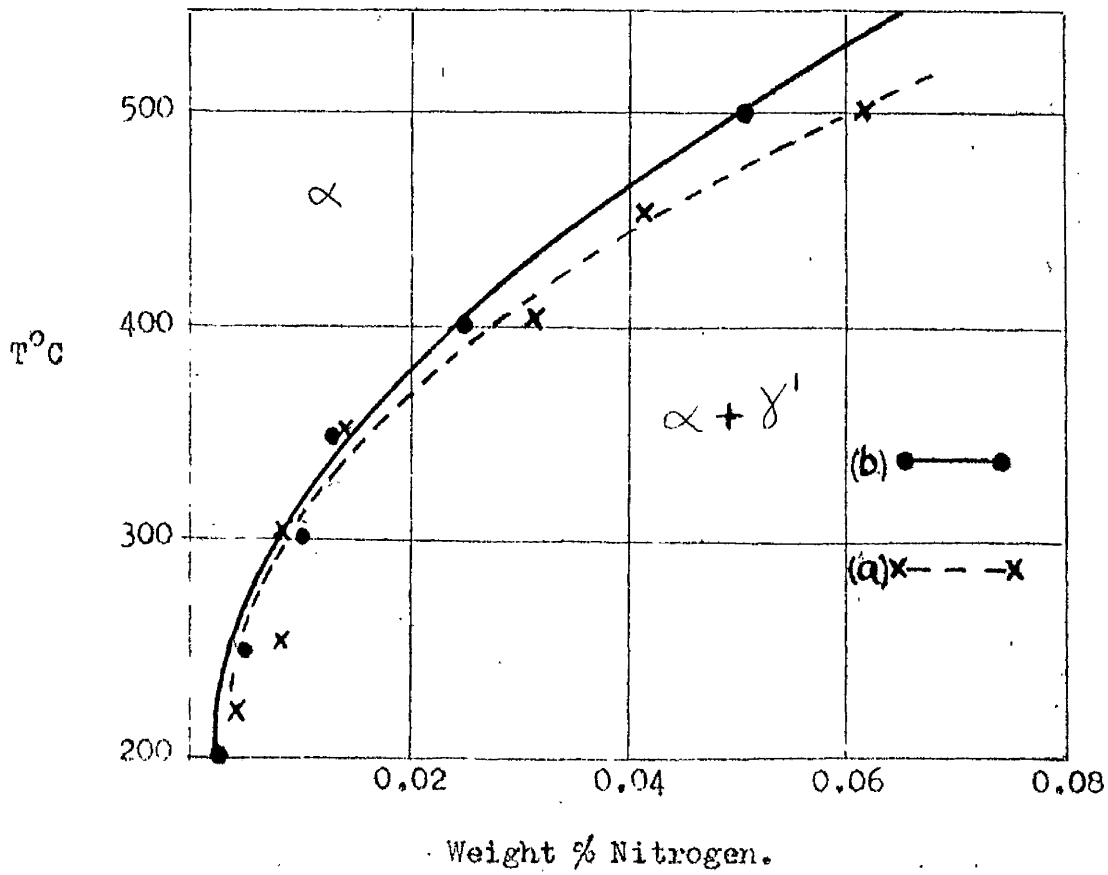


FIG.18. Solid solubility of nitrogen in alpha-iron as determined (a) by Rawlings and Tambini<sup>48</sup> and (b) this present work.

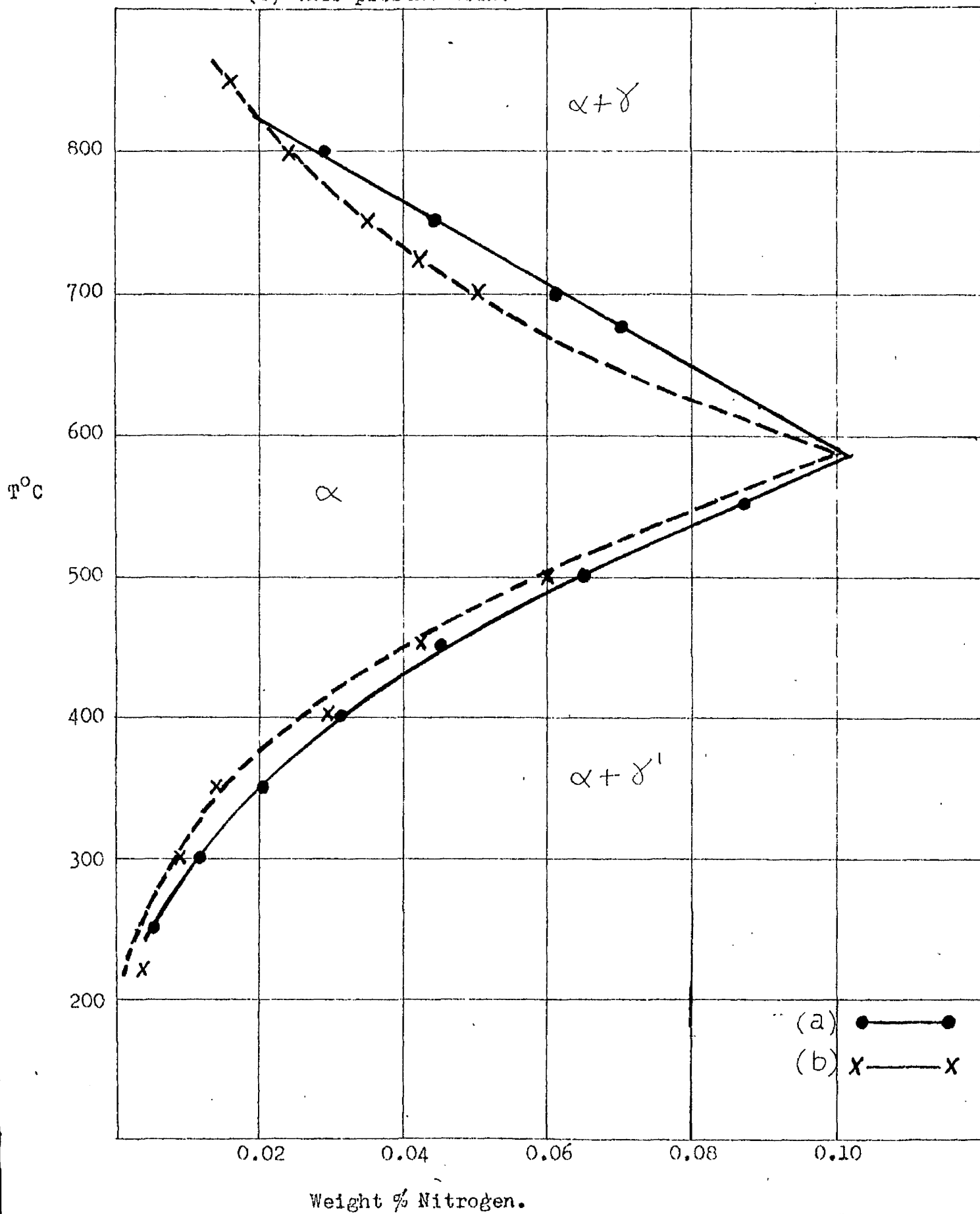


FIG.19. Solid solubility of nitrogen in alpha-iron as determined (a) by Paranjpe et al.<sup>51</sup> and (b) this present work.

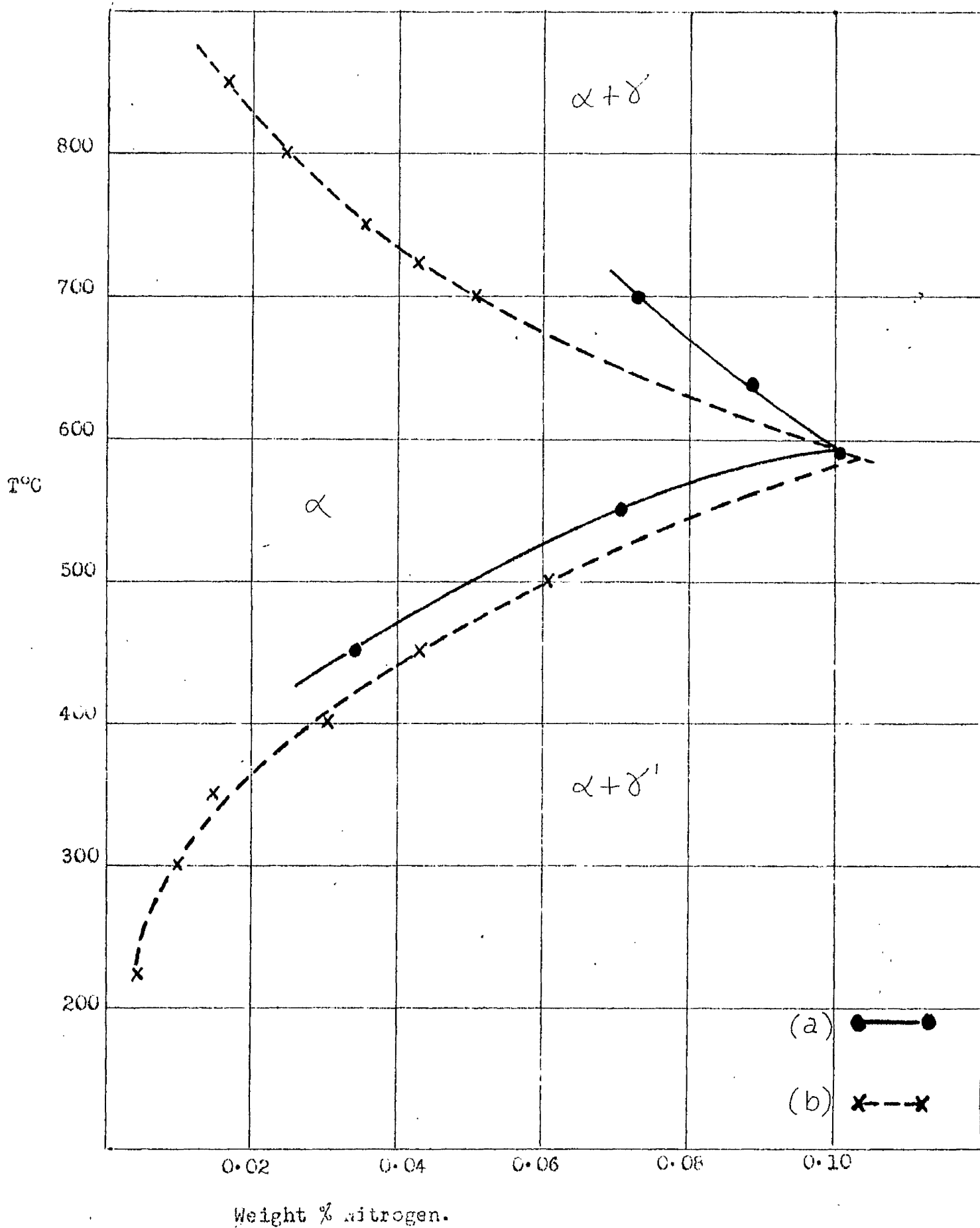


FIG. 20. Damping curve for 0.09% Al.alloy nitrided at 590°C for ½ hr. in 6% ammonia mixture.

(a) Experimental curve (b) Nitrogen Snoek peak

(c) Subsidiary peaks,  $C = (a - b)$ .

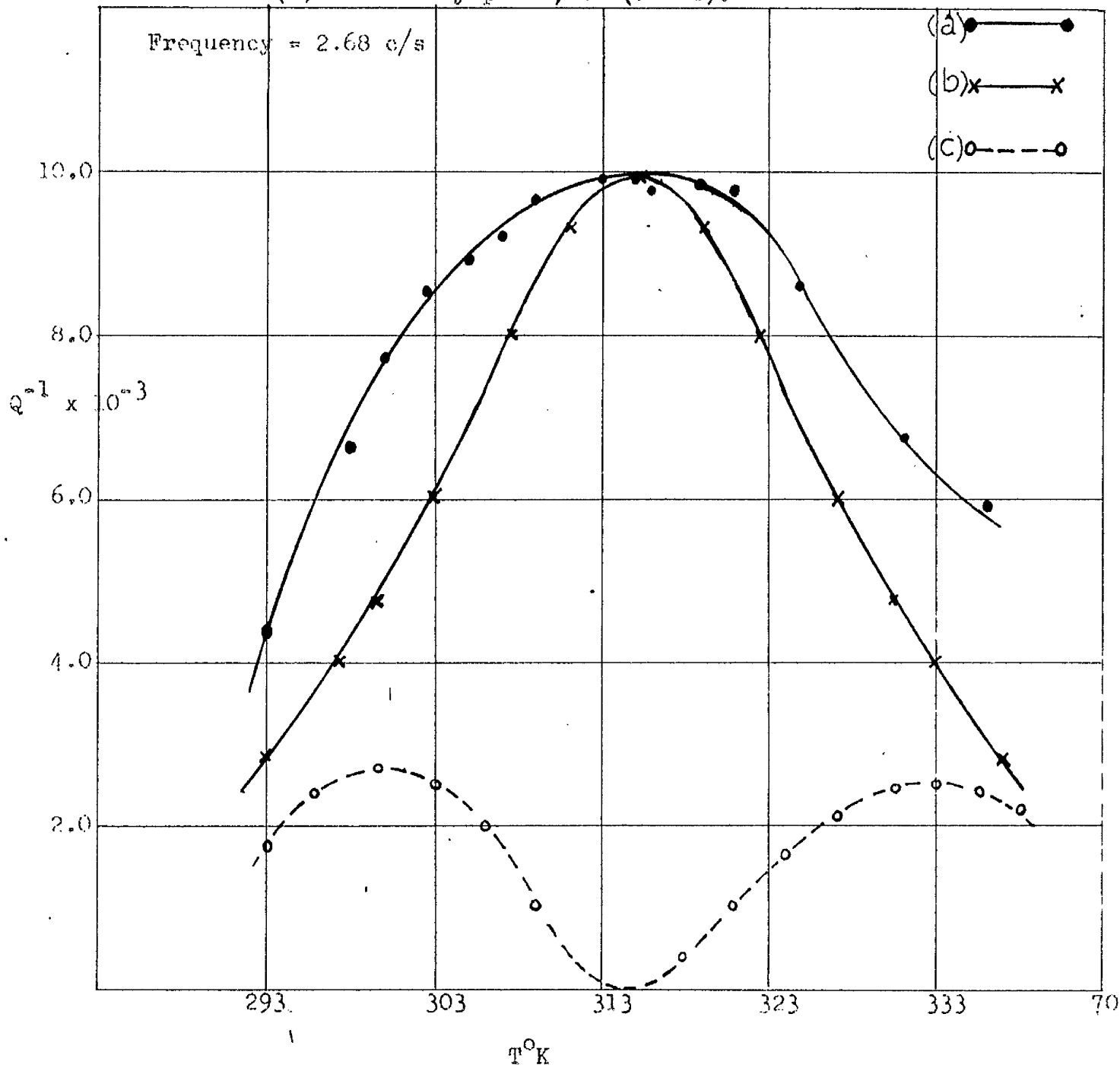


FIG.21. Damping curve as for Fig.20. (a) Experimental curve (b) Nitrogen Snoek peak (c) Subsidiary peak,  $C = (a - b)$ .

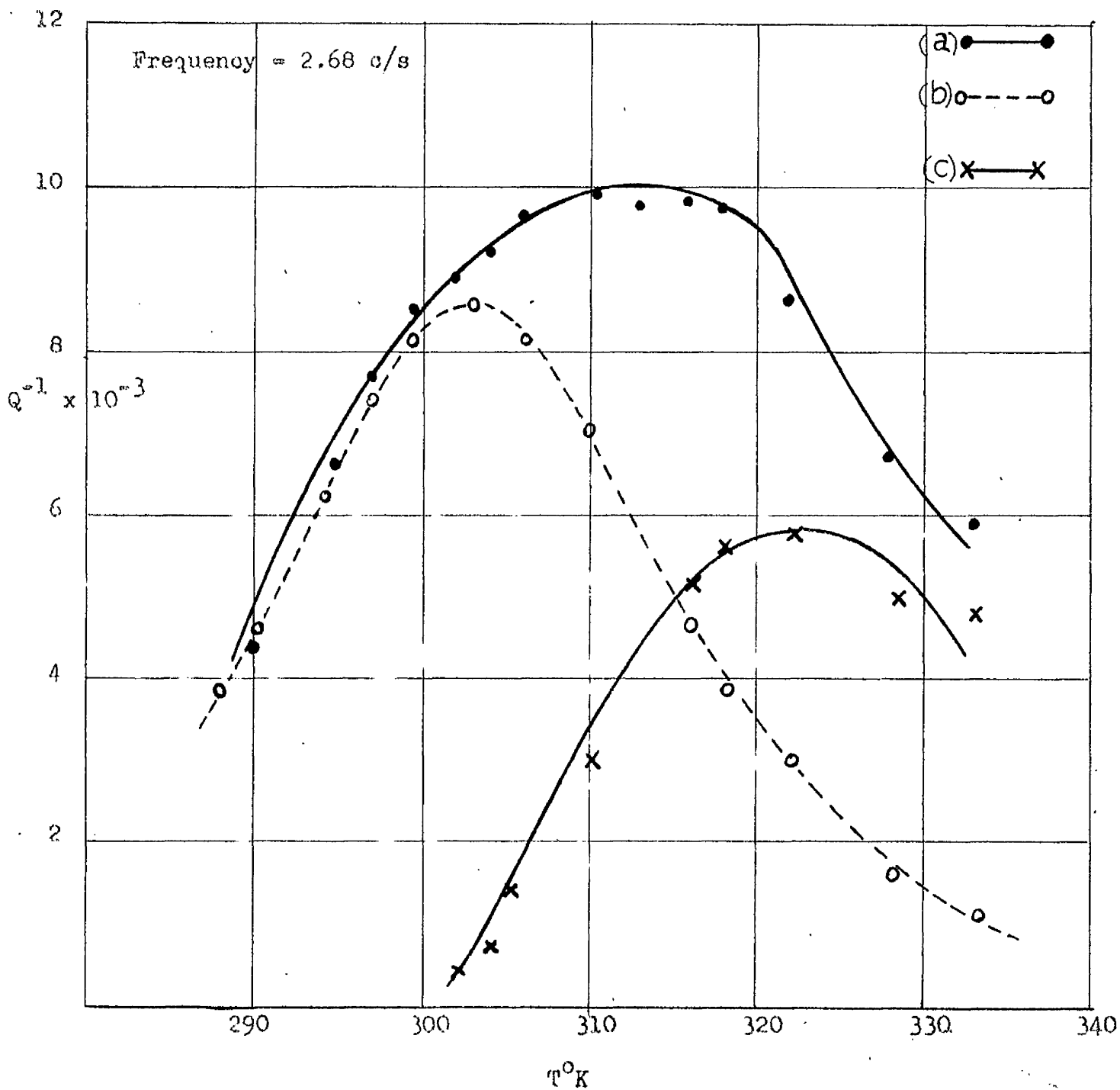


FIG.22. Damping curve for 0.9% Al alloy nitrided at 590°K for 1/2 hr. in 6% ammonia mixture.

(a) Experimental curve (b) Theoretical Snoek peak.

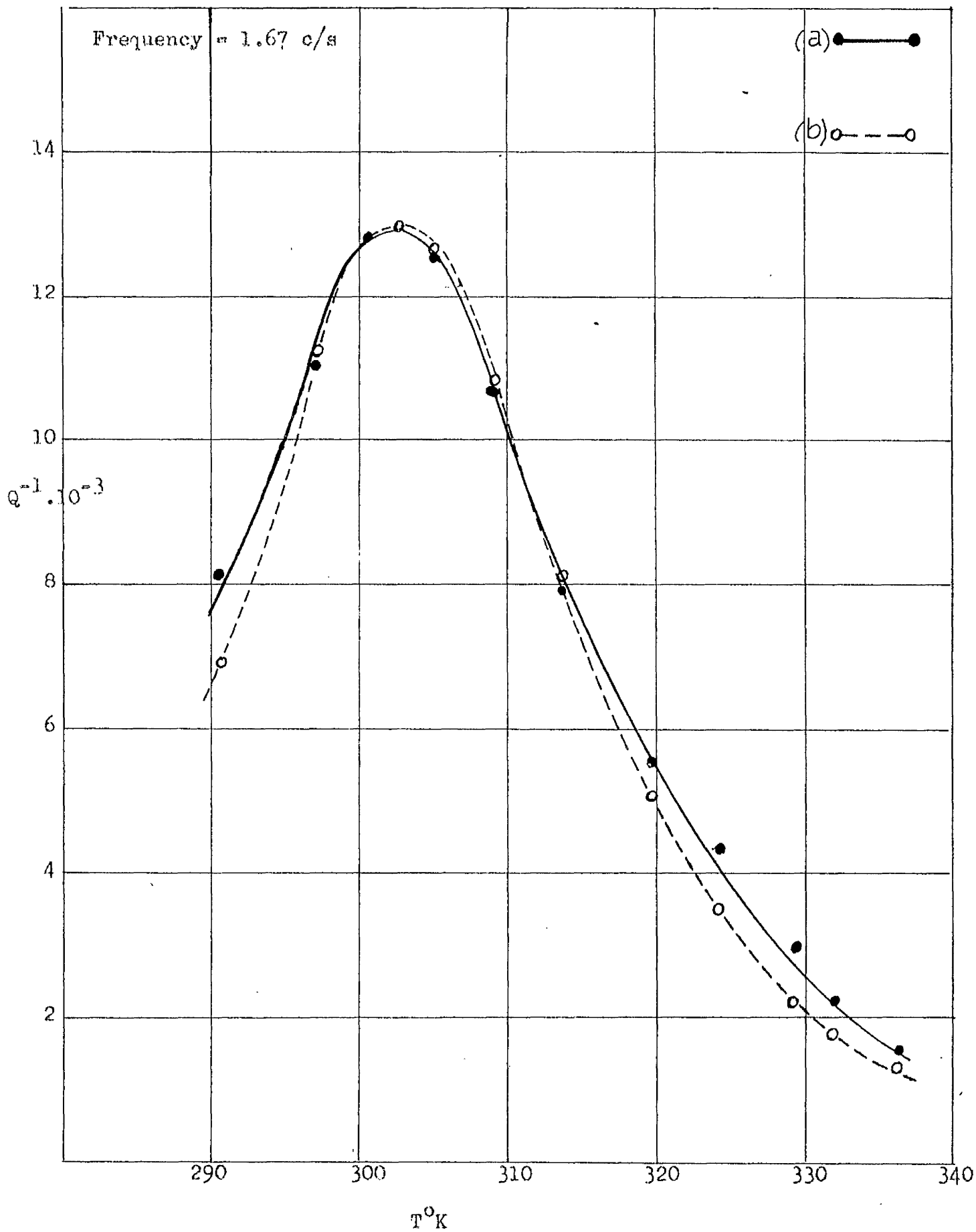


FIG. 23. Damping curve for 0.36% Al. alloy according to Laxar et al.<sup>24</sup>. (a) Experimental curve (b) Theoretical Carbon Snoek peak (c) Subsidiary peaks  $c = (a - b)$ .

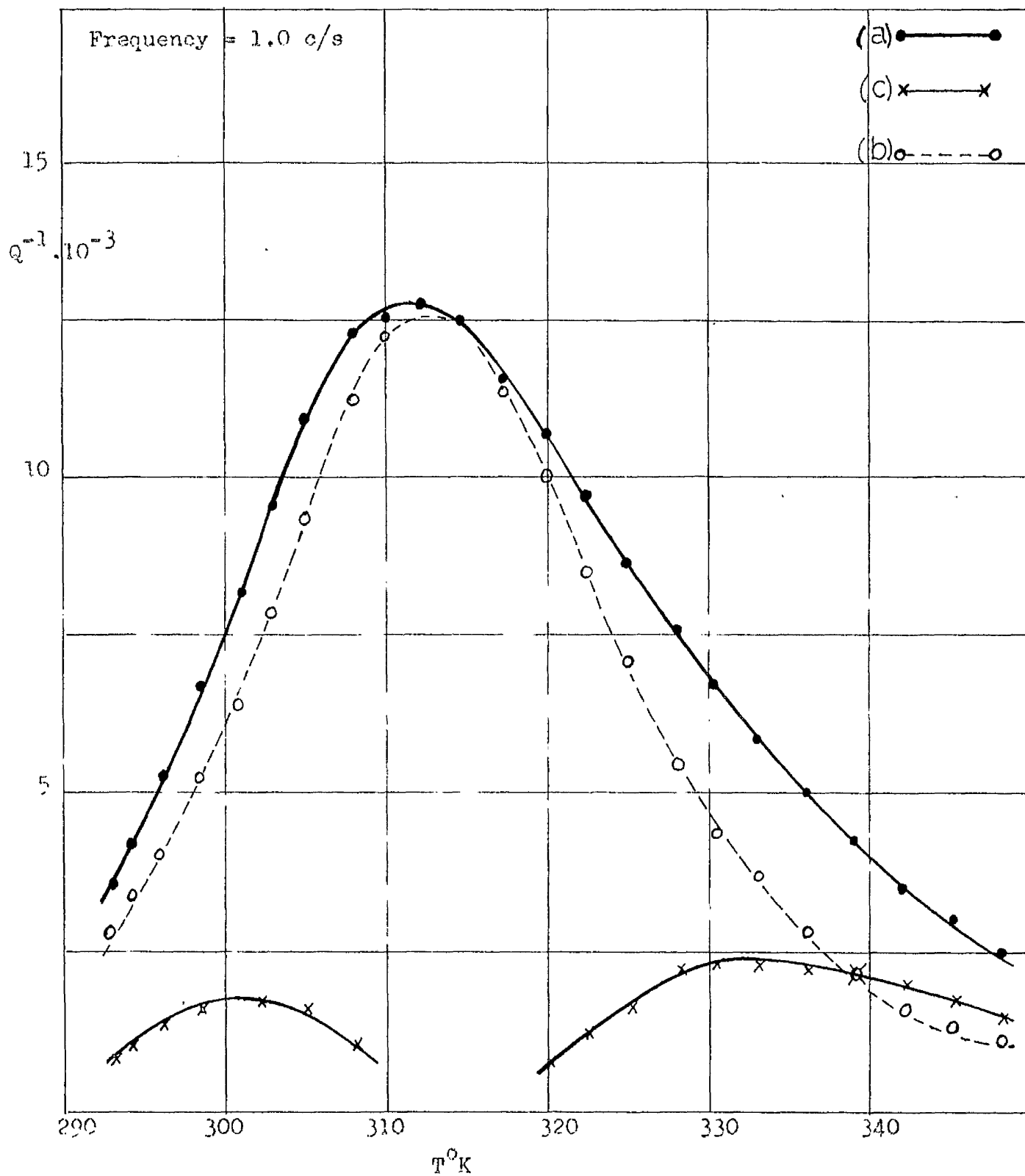


Fig. 24. Damping curve for 0.3% Al alloy carburised for 1 hr at 720°C in toluene vapour (a) Experimental curve, (b) Theoretical Carbon Snoek peak (c) Subsidiary peaks  $C = (a - b)$ .

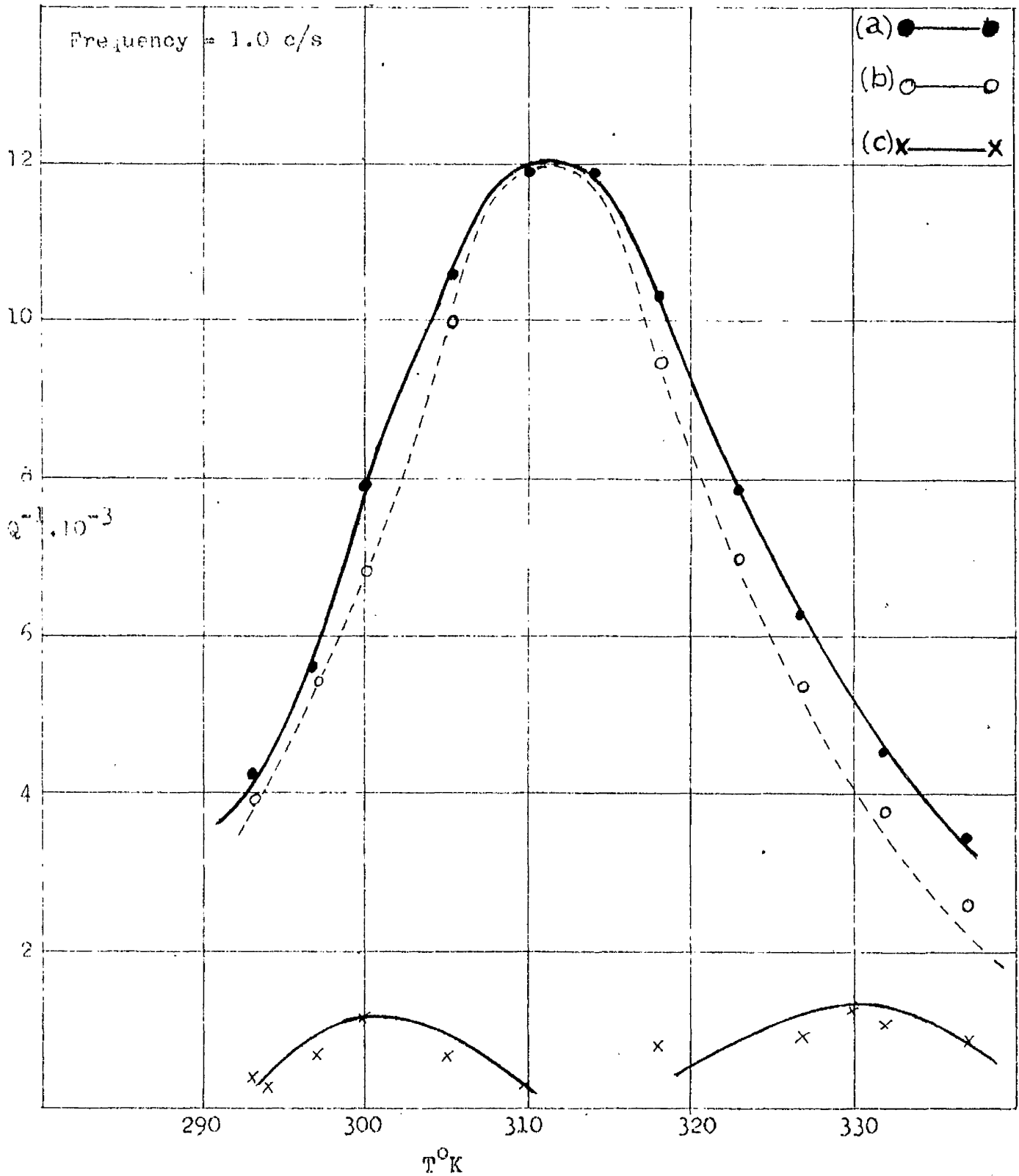


FIG.25. Damping curve for 0.3% Al nitrided at 590°C for 1/2 hr. in 6% ammonia mixture, unhomogenised  
(a) Experimental curve (b) Theoretical Nitrogen Snoek peak (c) Subsidiary peak c = (a - b).

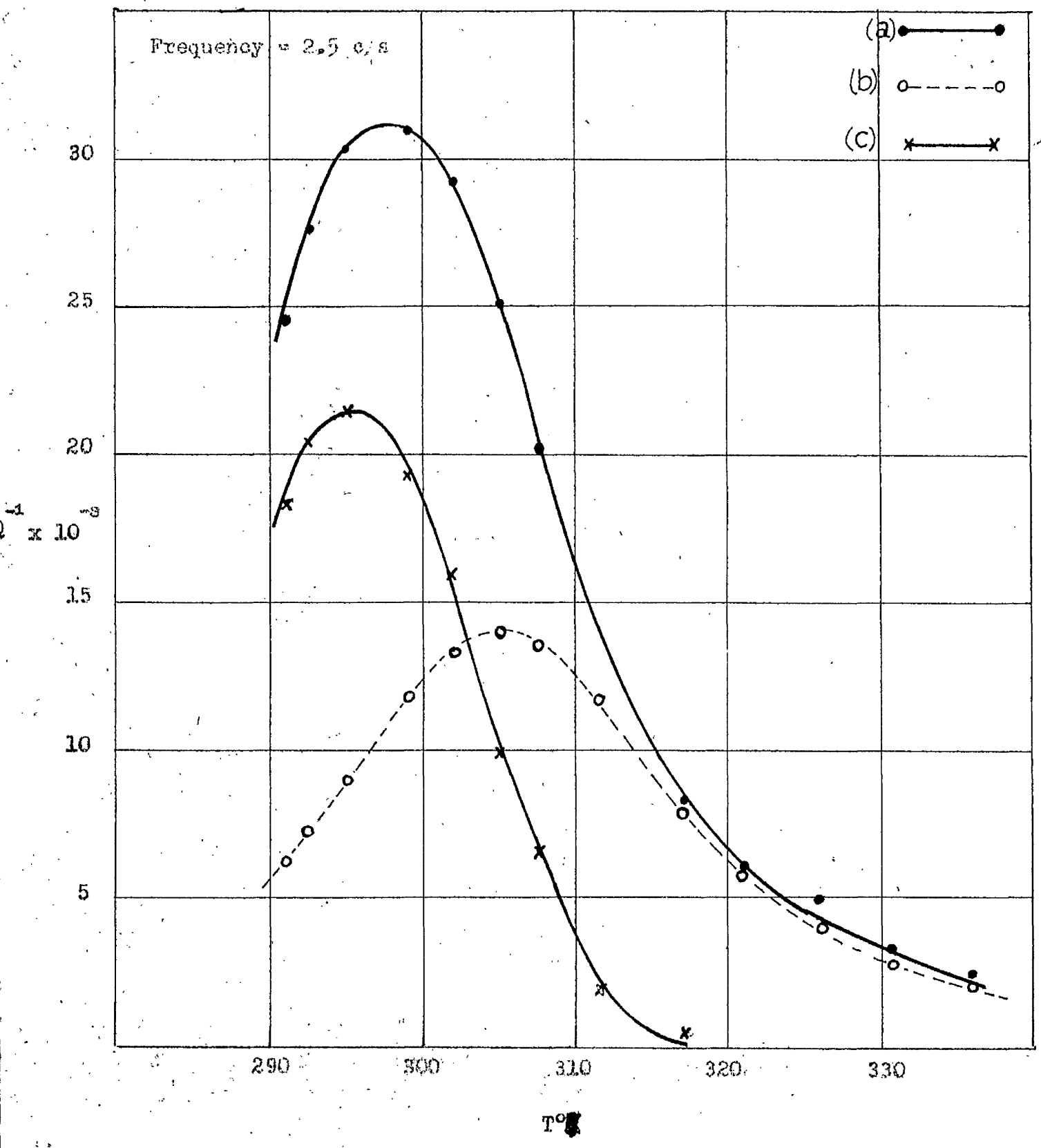


FIG. 26. Damping curve for 0.09% Al alloy nitrated for  $\frac{1}{2}$  hr. in 6% ammonia mixture, unhomogenised. (a) Experimental curve (b) Theoretical Nitrogen Snoek peak (c) Subsidiary peak.  $c = (a - b)$ .

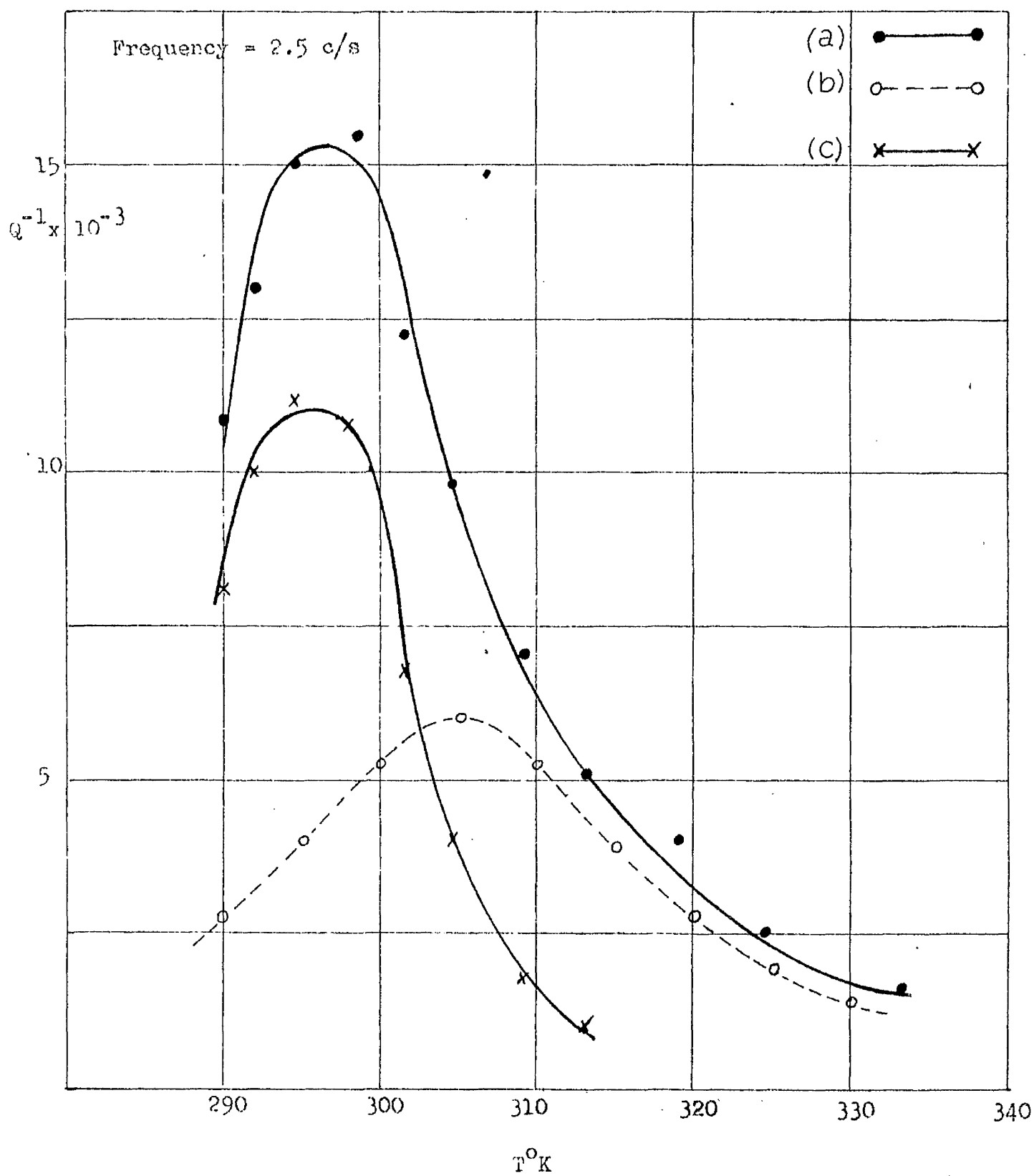


FIG. 27. Damping curve for 0.068% Al alloy nitrided for  $\frac{1}{2}$  hr. in 6% ammonia mixture, unhomogenised.  
 (a) Experimental curve (b) Theoretical Nitrogen Snoek peak. (c) Subsidiary Peak.  $c = (a - b)$ .

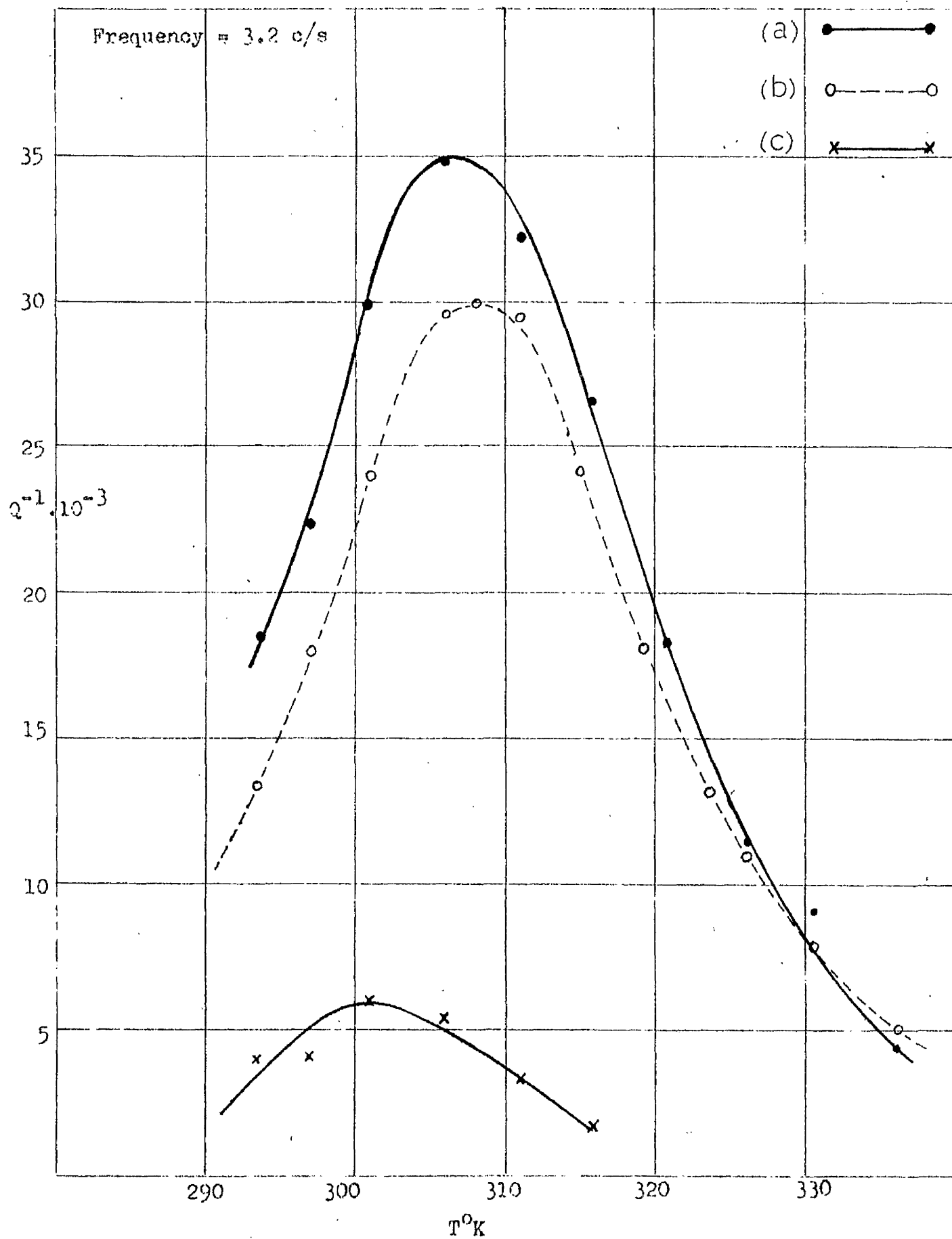


FIG. 28. Damping curve for 0.044% Al alloy nitrided for  $\frac{1}{2}$  hr. in 6% ammonia mixture, unhomogenised (a) Experimental curve (b) Theoretical Nitrogen Snoek peak. (c) Subsidiary peak C = (a - b).

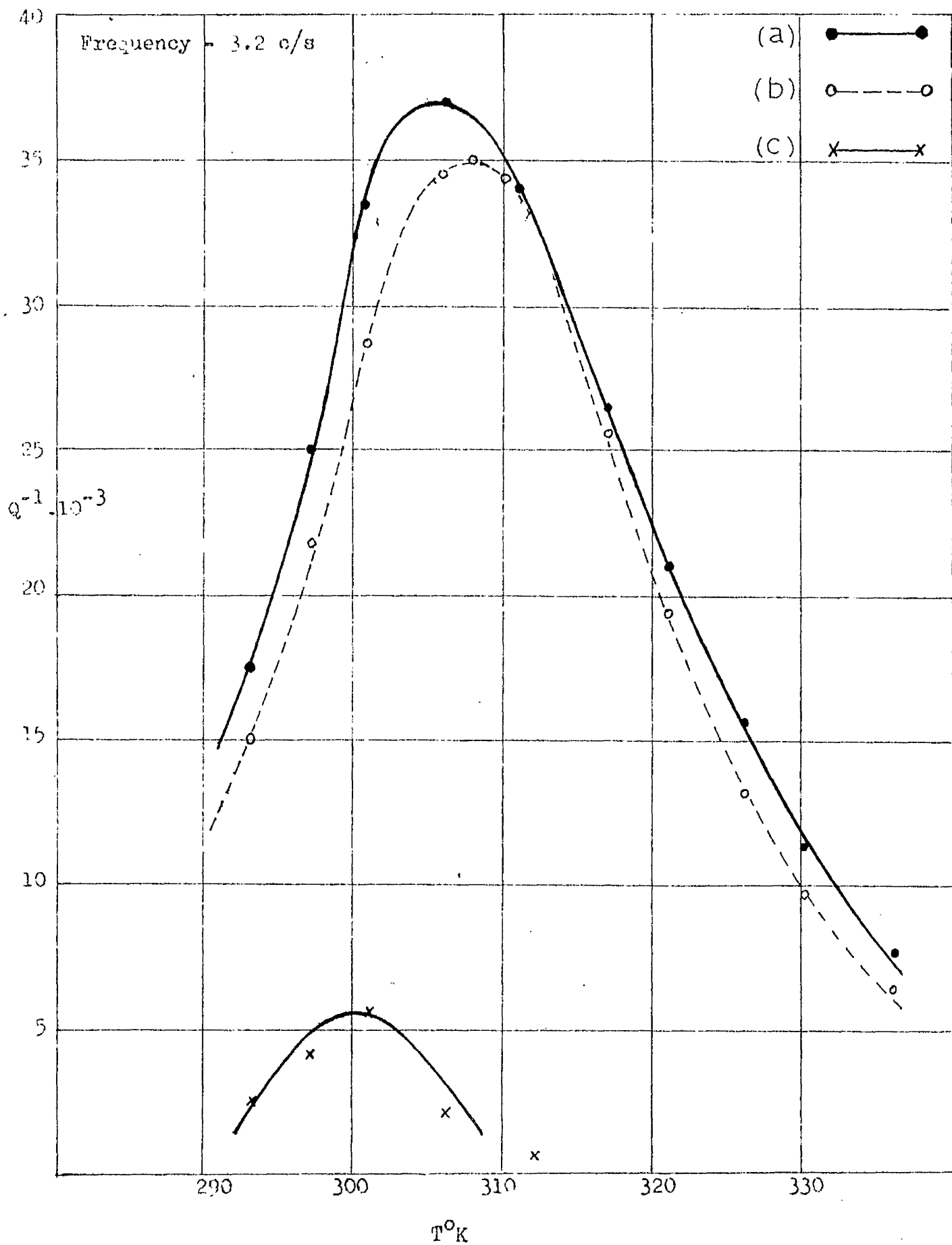


Fig.29. Damping curve for 0.015% Al.alloy nitrated for  $\frac{1}{2}$  hr. in 6% ammonia mixture, unhomogenised (a) Experimental curve (b) Theoretical Nitrogen Snoek peak. (c) Subsidiary peak  $C = (a - b)$ .

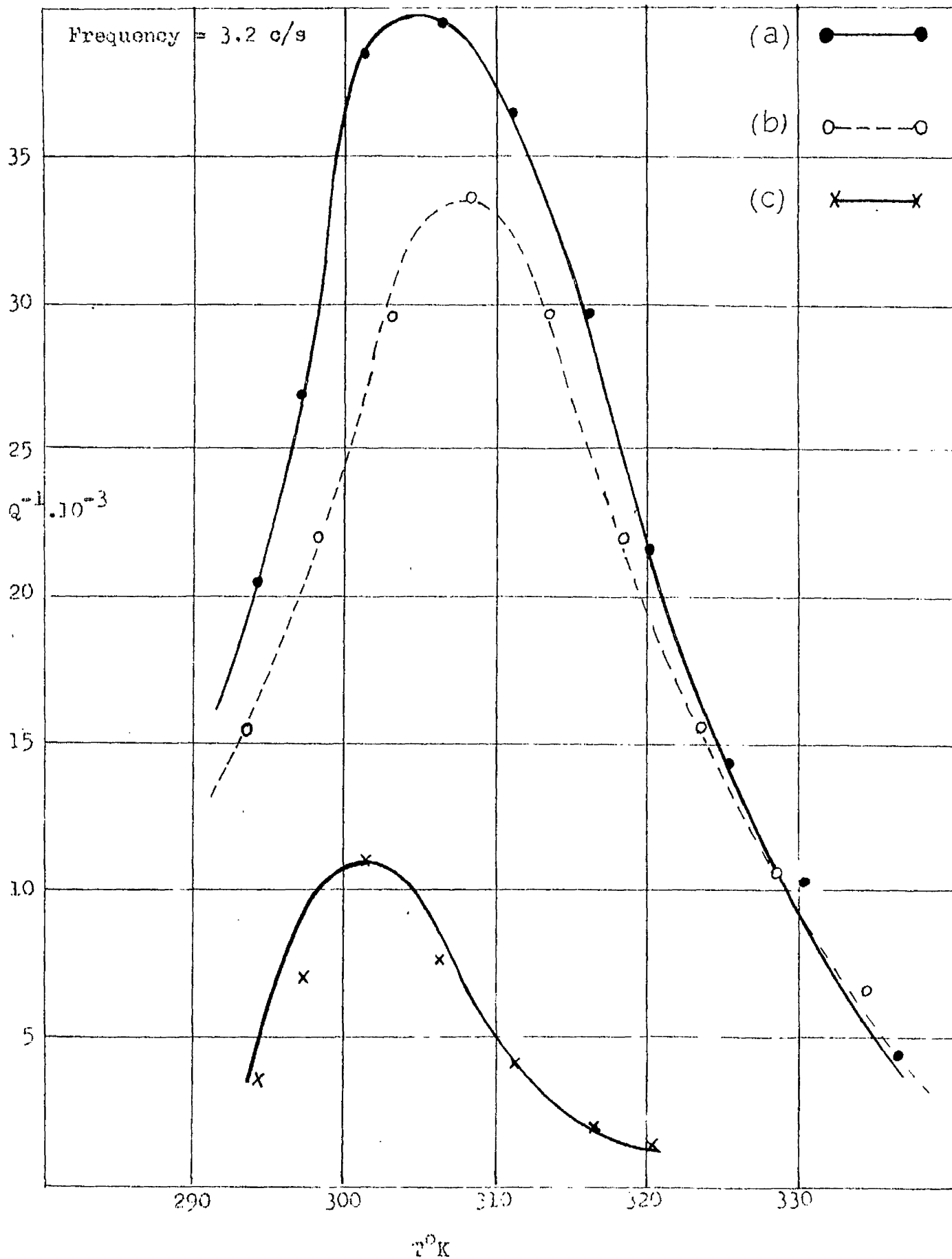


FIG. 30. Damping curve for 0.3% Al alloy nitrated for  $\frac{1}{2}$  hr. at 590°C in 6% ammonia mixture and homogenised 2 hrs at 590°C (a) Experimental curve. (b) Theoretical Nitrogen Snoek peak. (c) Subsidary peak  $C = (a - b)$

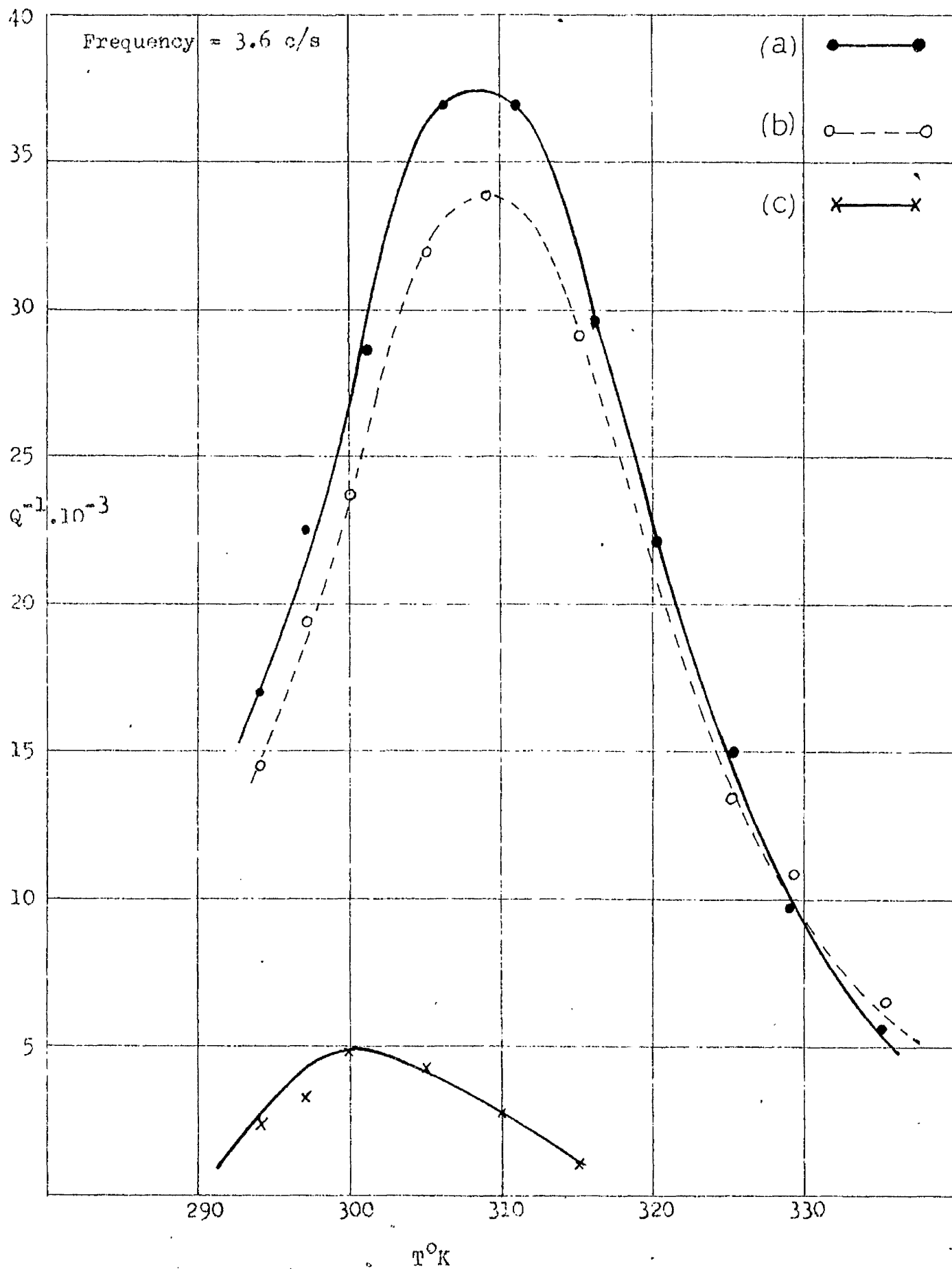


FIG. 31. Damping curve for 0.09% Al alloy nitrated for  $\frac{1}{2}$  hr. at  $590^{\circ}\text{C}$  in 6% ammonia mixture and homogenised 2 hrs. at  $590^{\circ}\text{C}$   
(a) Experimental curve (b) Theoretical Nitrogen Snoek peak.  
(c) Subsidiary peak  $C = (a - b)$ .

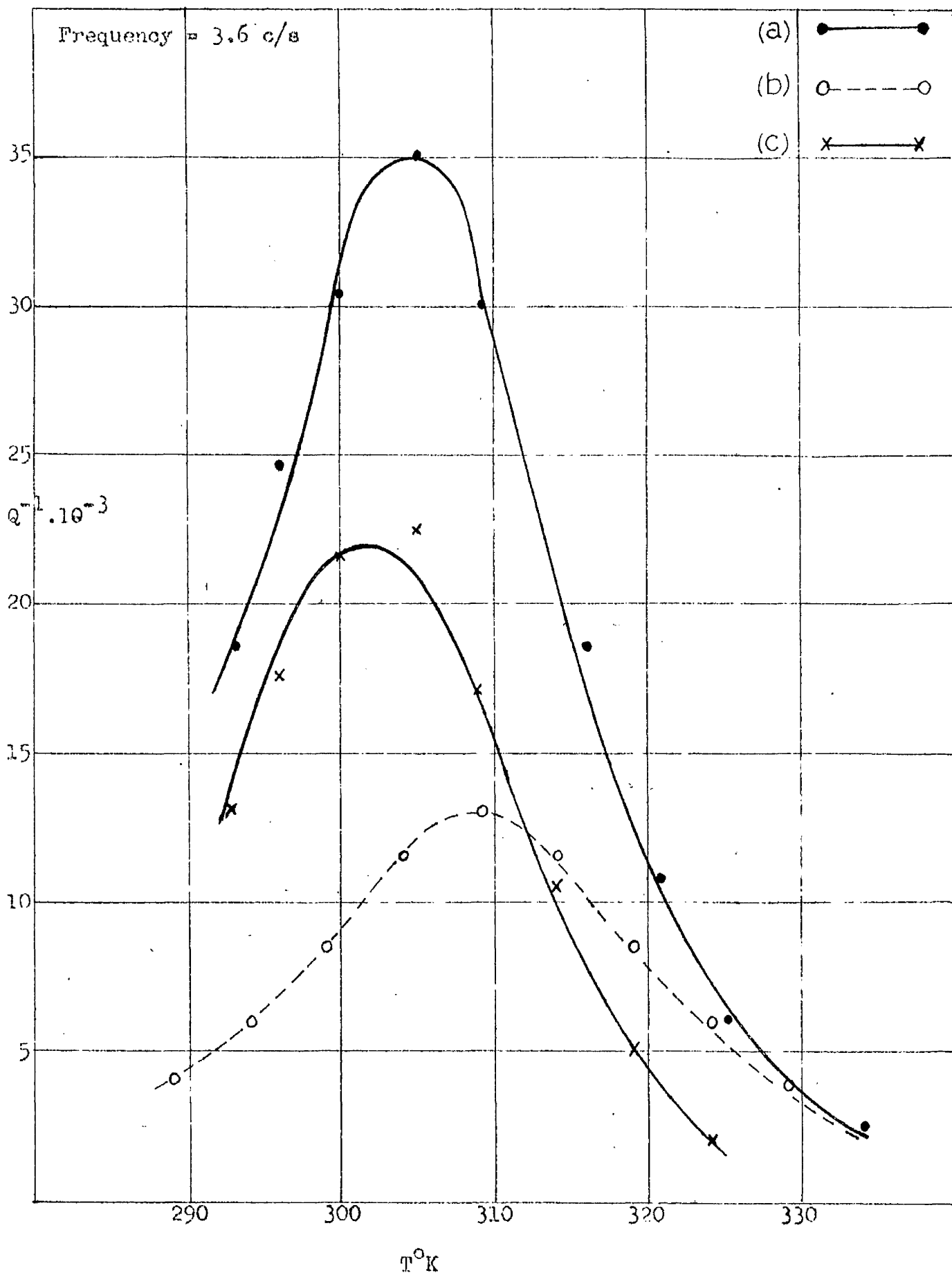


FIG. 32. Damping curve for 0.3% Al alloy as for Fig. 25, aged and re-solutioned at 590°C.

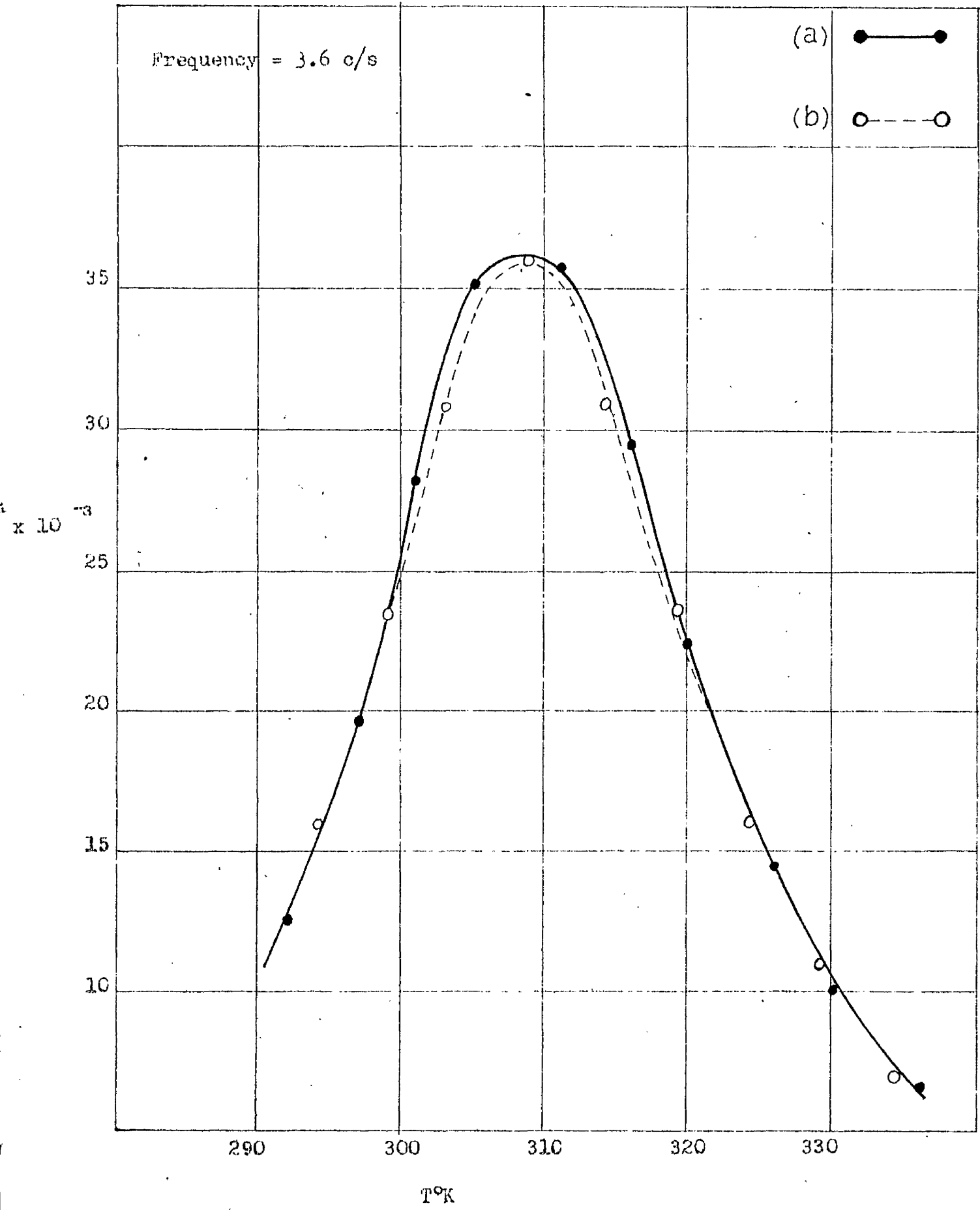
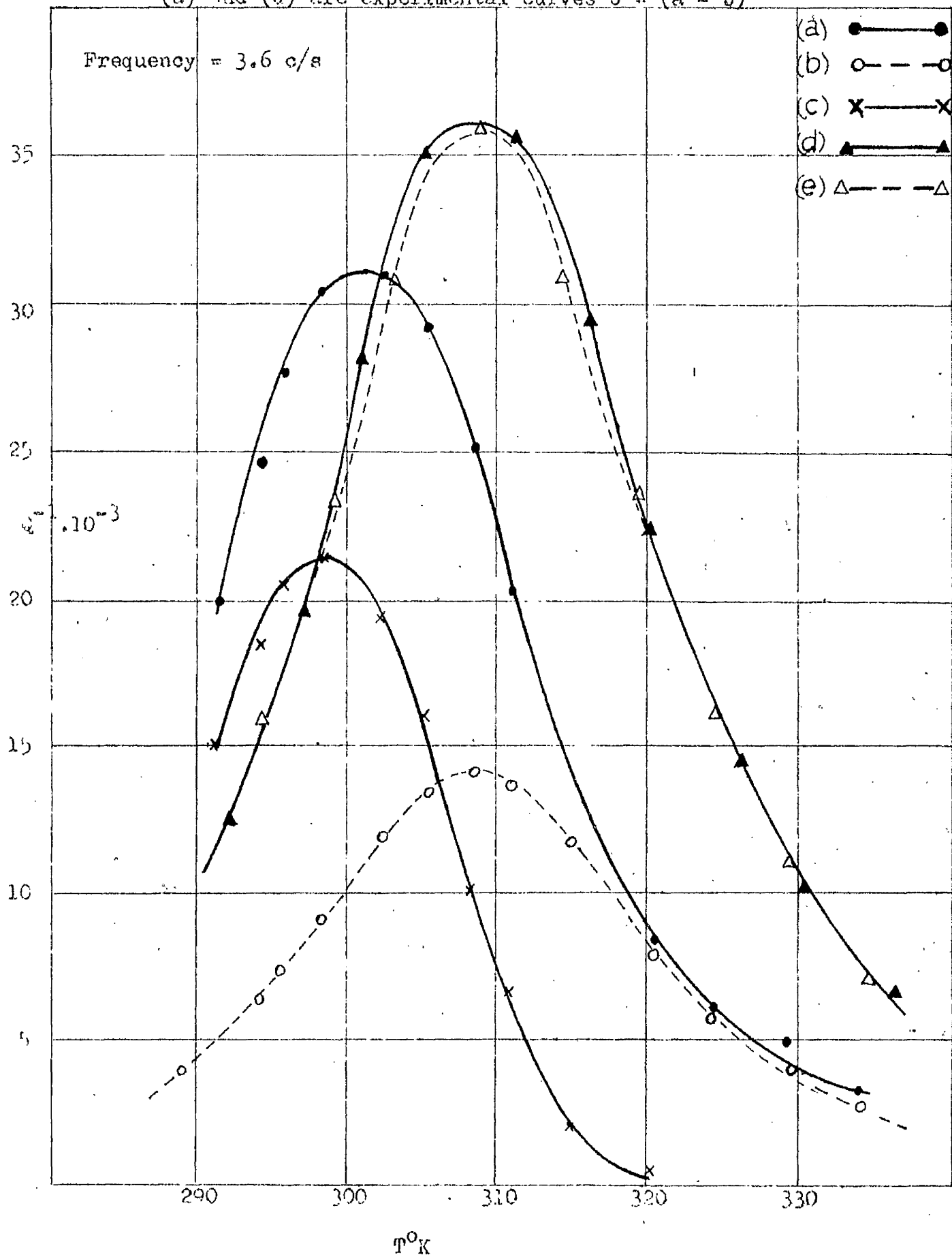
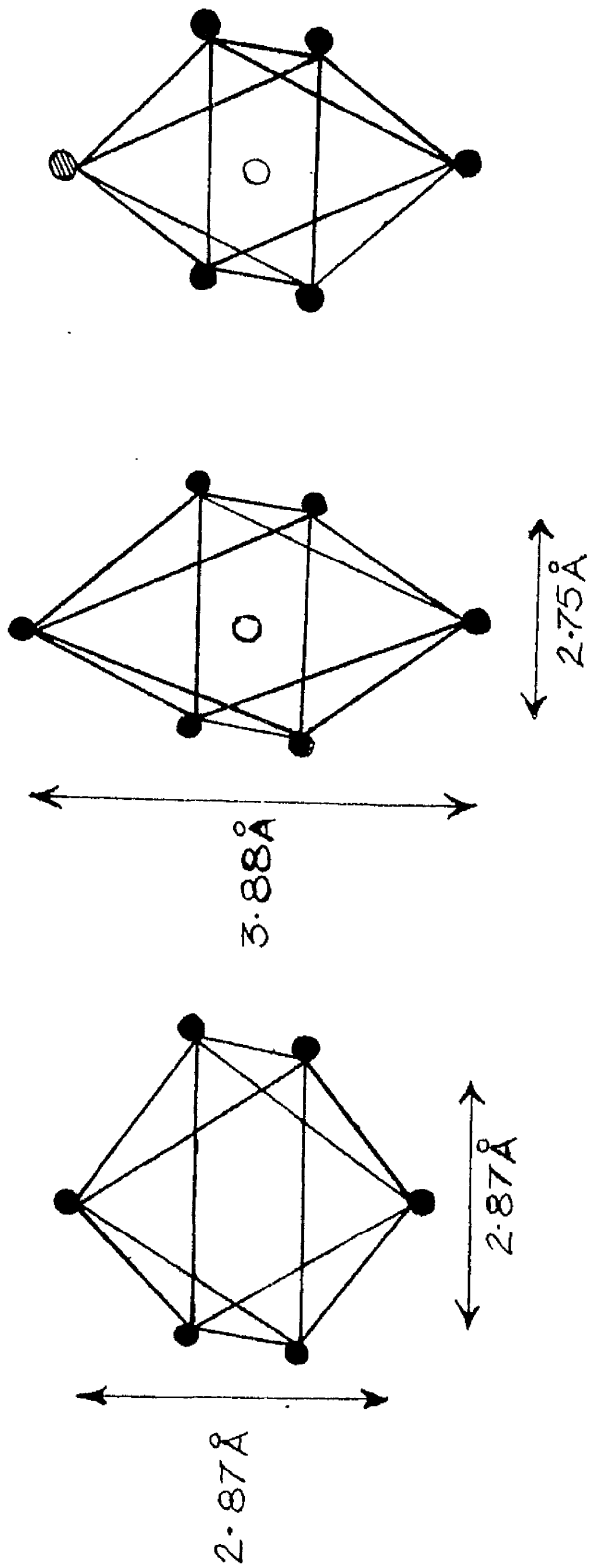


FIG. 33. Comparison of Figs. 25 and 32. (a), (b) and (c) as nitrated and quenched (d) and (e) as nitrated, quenched, aged and re-resolution treated. Dotted lines are theoretical Snoek peaks (c) is the subsidiary peak (a) and (d) are experimental curves  $C = (a - b)$



● — Fe atoms  
 ○ — N " "  
 ⊙ — Al " "



(a.) (b.) (c.)

FIG. 34. Distortion produced in alpha-iron by interstitially dissolved nitrogen.

FIG. 35. Damping curves for 0.3% Al alloy nitrided for  $\frac{1}{2}$  hr. at  $590^{\circ}\text{C}$  in 6% ammonia mixture. (a) Experimental curve (b) Theoretical Nitrogen Snoek peak (c) Subsidiary peak  $C = (a - b)$ .

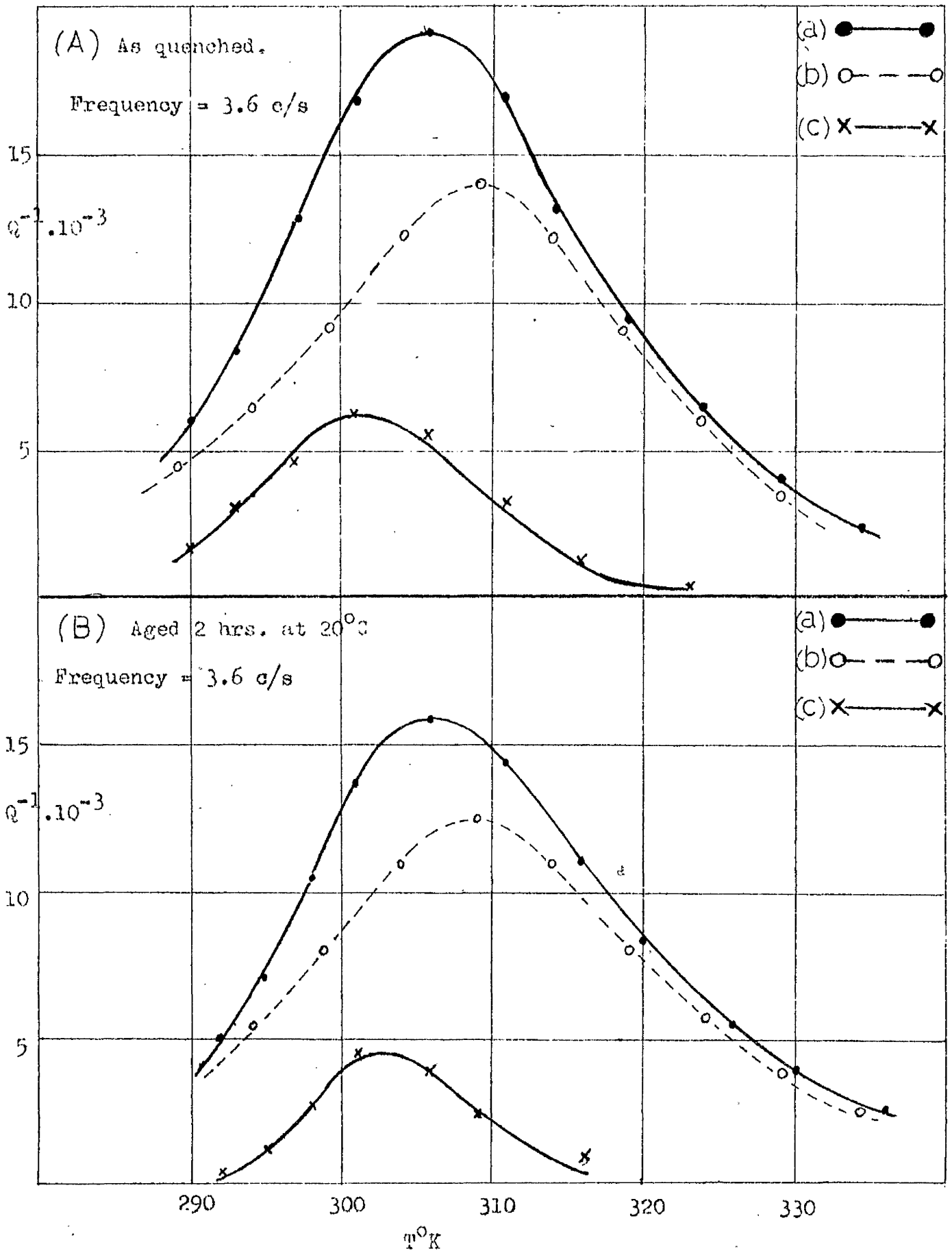


FIG. 36. Damping curves for 0.3% Al alloy nitrided for  $\frac{1}{2}$  hr. at 590 C in 6% ammonia mixture. (a) Experimental curve. (b) Theoretical Nitrogen Snoek peak (c) Subsidiary peak  $C = (a - b)$ .

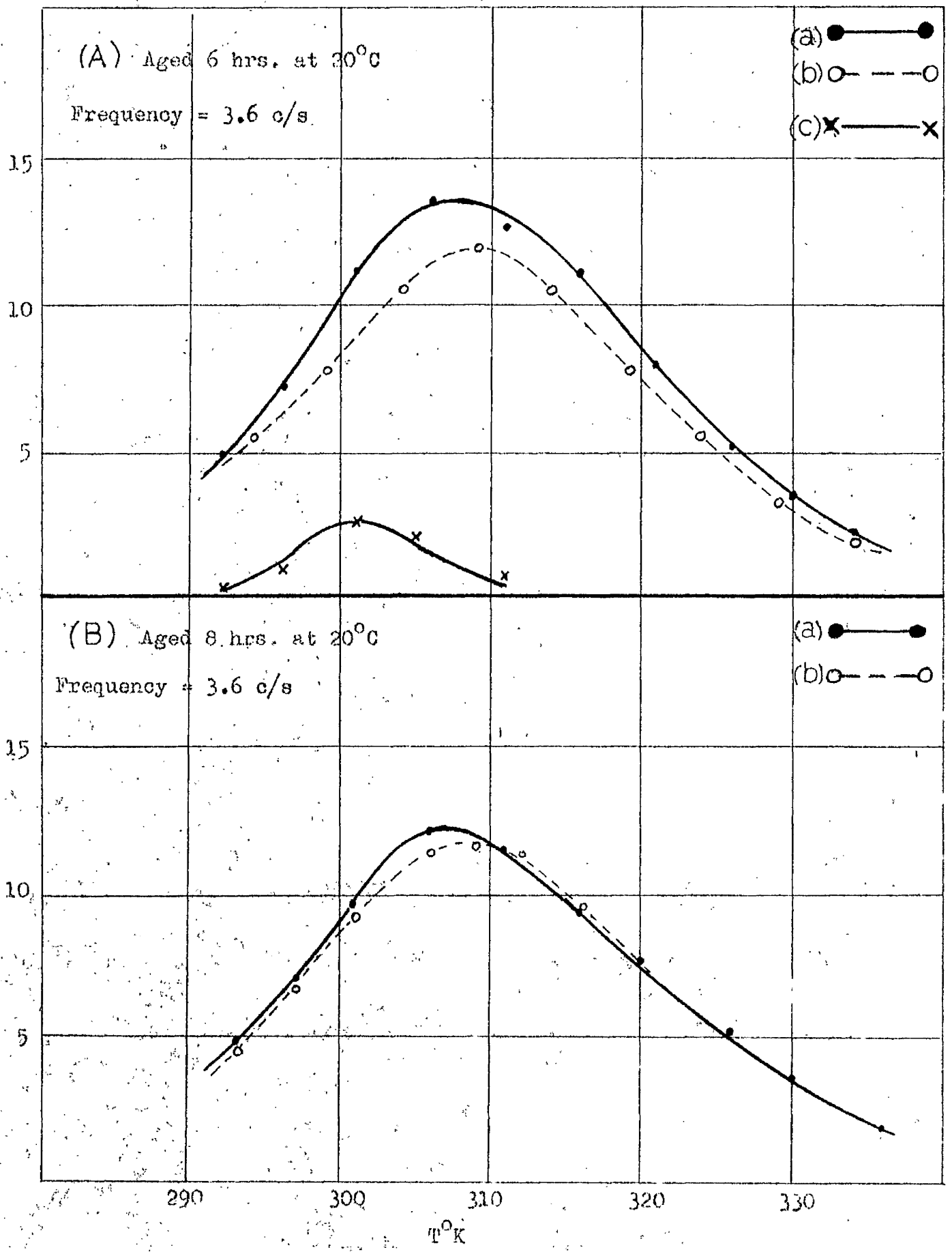
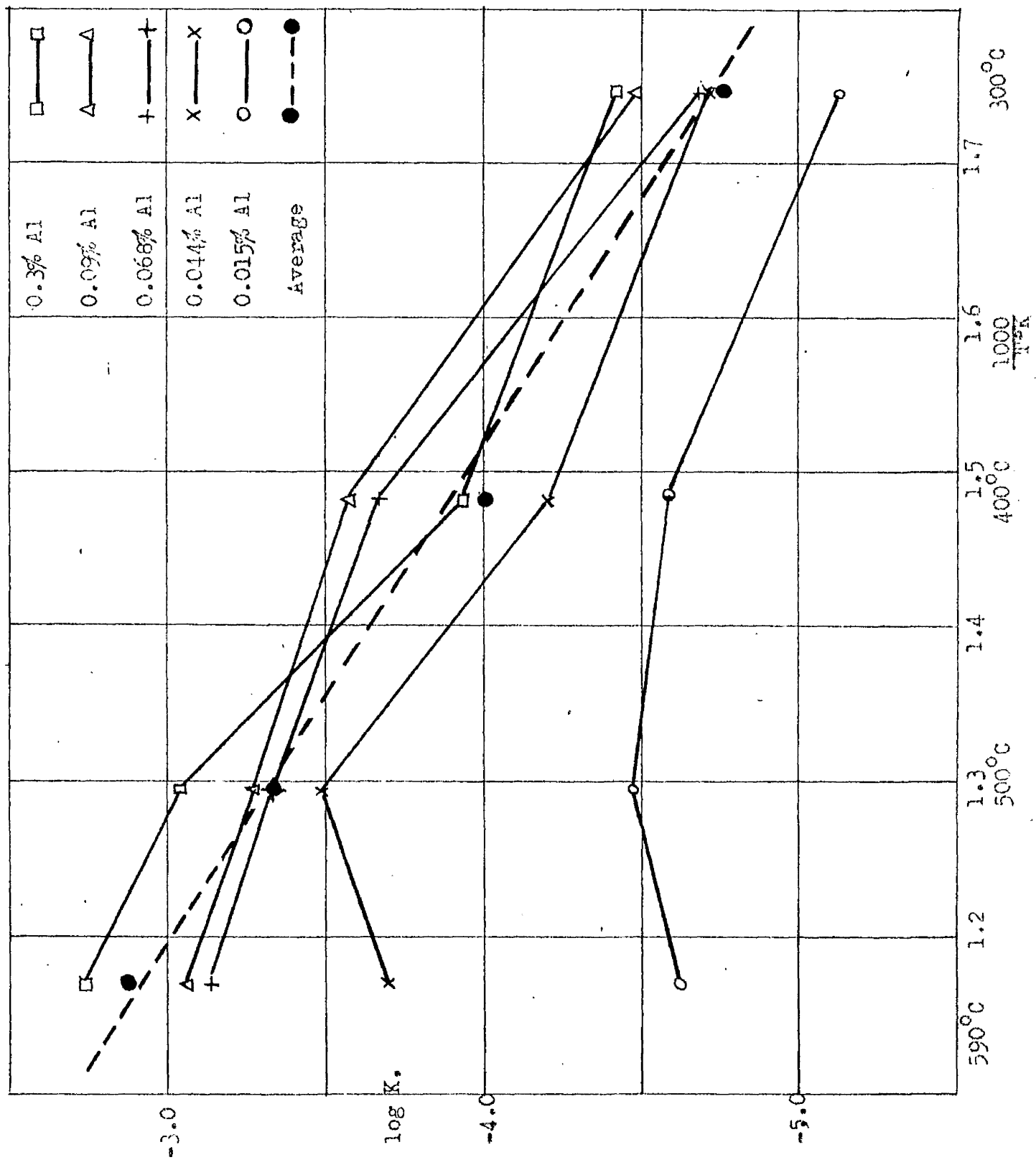


FIG. 37. Solubility product ( $K = [Al\%][N\%]$ ) as a function of the absolute temperature.



PART 5. DISCUSSION OF RESULTS.

Section 5.1

Introduction.

From the review in Section 1.3 of the work done on nitrogen in iron alloys by internal friction methods it is apparent that no comprehensive investigation has been made of the iron-aluminium-nitrogen system.

The most important single point in question is the existence of a second peak in addition to the Snoek peak. Fast has reported that no such peak is to be found in an alloy containing 0.5 atomic per cent of aluminium. On the other hand, Laxar et al reported secondary peaks in iron-aluminium-carbon alloys which at least indicates the possibility of similar peaks existing in the nitrogen system since carbon and nitrogen generally produce comparable effects when in solid solution in the same metal.

In order to have a basis for comparison of the information gathered from a study of the aluminium alloys it was decided, as a first step in this present investigation, to re-establish the data obtained by other workers on the damping characteristics in iron-nitrogen alloys.

cont'd...

Section 5.2 - The Snoek Peak in Iron-Nitrogen Alloys.

Several pure iron specimens were nitrided for short periods at 590°C quenched and the damping measured between 15°C and 65°C at different testing frequencies. Three of these curves are shown in Fig.13 and the  $Q^{-1}$  values are given in Table 4. The activation energy for diffusion of nitrogen was calculated by using the equation,

$$\ln \left( \frac{f_2}{f_1} \right) = \frac{dH}{R} \left( \frac{T_2 - T_1}{T_1 \cdot T_2} \right) \quad (6)$$

where  $f_1$  and  $f_2$  are linear frequencies of vibration and  $T_1$  and  $T_2$  are the corresponding temperatures at which the maximum damping for these frequencies is observed. The average  $dH$  value was 18.19 Kcals/mole of nitrogen (Table 5) although the calculated values varied from 16.9 to 19.39 Kcals/mole. From equation (6) it can be seen that the  $dH$  value obtained in this manner depends critically on the temperature difference between the peaks, this difference being the divisor in the equation,

$$dH = \frac{R \ln \left( \frac{f_2}{f_1} \right) T_1 \cdot T_2}{T_2 - T_1}$$

Assuming the error in placing the peak temperature to be the same for each peak it becomes apparent that the smaller the difference between  $T_2$  and  $T_1$  in the above equation the larger becomes the percentage error in the calculated  $dH$  value. Thus the most accurate value should be that from the peaks furthest apart and this in fact leads to a  $dH$  of 18.26 which agrees well with the value most quoted for the diffusion of nitrogen in alpha-iron. With an estimated

cont'd...

error of  $\pm 0.5^{\circ}\text{C}$  in measuring the temperature the error for a temperature range of  $11^{\circ}$  is  $\pm 10\%$  at the best. The activation energy may then be quoted as  $18.2 \pm 2$  Keals/mole of nitrogen.

Each of the three curves of Fig.13 was processed by computer using Programme 2 as described in Section 3.5 and the results are summarised in Table 6. This alternative method of calculating  $dH$  depends basically on the shape of the damping curve and therefore takes into account the  $Q^{-1}$  values determined experimentally over a range of temperatures rather than the position of the peak maximum. The results were processed both with and without a correction being made for background damping since this has a slight effect on the shape of the curve. The background damping was determined over the range of experimental temperatures on a fully decarburised specimen prior to nitriding and was found to  $5.10^{-4}$  on average. This value of  $5.10^{-4}$  is the contribution to damping due to frictional losses in the apparatus and the other factors which have been discussed previously in Section 3.4 and which are assumed to be constant and unaffected by nitriding. Strictly speaking to evaluate the damping produced by nitrogen alone the background damping should be subtracted from each experimental  $Q^{-1}$  value. This is borne out by the fact that the  $dH$  value closest to the generally accepted one of 18.2 is the 17.6 Keals/mole calculated from the results to which the background damping correction has been applied. As a method of determining the  $dH$  value the computer technique is probably more accurate than the method of using equation (6) when the peaks are separated by less

cont'd...

than  $10^{\circ}$ . The two methods are nevertheless in good agreement and throughout this work the value of  $dH$  used is 18.2 Kcals/mole.

cont'd...

### Section 5.3 - Diffusion of Nitrogen in Alpha-Iron.

The theory of the calculation of diffusion coefficients from internal friction peaks has been outlined in Section 1.3. The diffusion coefficient may be stated thus:-

$$D = \frac{a^2 \pi f}{10} \text{ cm}^2/\text{sec.}$$

where  $a$  is the lattice parameter,  $2.866^{\circ}\text{A}$  in the case of alpha-iron and  $f$  is the linear frequency of testing. In all six specimens were nitrided and their peaks determined at different frequencies. Three of the wires were those referred to in the calculation of the  $dH$  value. In each case the value of  $D$  was calculated (Table 7) and this was plotted against the reciprocal of the absolute temperature at which the peak occurred (Fig.14). The plot gives a straight line relationship. This observation is in fact expected from the classical expression for the diffusion coefficient  $D = D_0 \exp \frac{-dH}{RT}$  where  $D_0$  is a constant,  $dH$  is the activation energy for diffusion,  $T$  the temperature in  $^{\circ}\text{K}$  and  $R$  the gas constant. It is possible therefore to find both  $D_0$  and  $dH$  from Fig.14.  $D_0$  was found to be  $1.3 \cdot 10^{-2}$  and  $dH$  to be 19 Kcals/mole. Fast and Verrijp<sup>44</sup> report  $6.6 \cdot 10^{-3}$  and 18.6 while Wert<sup>20</sup> gives  $3 \cdot 10^{-3}$  and 18.2. In fact these large differences in  $D_0$  produce very small variations in the values of  $D$  for a given temperature within the experimental range. Hence the agreement between results obtained from this investigation and of those of the others quoted is quite good.

cont'd...

#### Section 5.4 - Solid Solubility of Nitrogen in Alpha-Iron.

Determination of the limits of solid solubility of nitrogen in alpha-iron has been the object of many investigations both by internal friction and more conventional methods. Rawlings and Tambini<sup>48</sup> determined the phase boundaries in alpha-iron using a damping technique. They increased the time of nitriding of wire specimens at a given temperature until the amount of nitrogen in solid solution, as measured by a damping peak, reached a maximum. Partially cracked ammonia was used as a nitriding medium and the ammonia potential in equilibrium with the specimens could be altered by varying the temperature of the cracking furnace. The peak  $Q^{-1}$  values so obtained were then multiplied by a factor of 1.28 to convert them to weight per cent nitrogen. These solubility results are plotted against temperature in Fig.18.

In repeating this investigation the author employed a different method of approaching the equilibrium between nitrogen in solid solution and  $Fe_4N$ . With the method used by Rawlings and Tambini<sup>48</sup> it is possible to be nitriding at an ammonia potential which either is not capable of achieving equilibrium or is capable of over-nitriding the specimen in the manner indicated in Section 3.3. To be absolutely sure of achieving equilibrium by the method of Rawlings and Tambini it would be necessary to nitride with a considerable range of ammonia potentials. The technique used in this work was to nitride the specimens at  $590^{\circ}C$  for a short period at an ammonia potential which experience

cont'd...

had shown would over-nitride if the time were not carefully controlled. In this way it was ensured that enough nitrogen was present to give an equilibrium between interstitial nitrogen and  $\text{Fe}_4\text{N}$  at temperatures other than the eutectoid.

Usually four specimens were nitrided at a time two of these being used to approach the equilibrium from above and two from below the temperature in question. All the specimens were homogenised for eight hours at  $590^\circ\text{C}$ . Two were furnace cooled to (say)  $300^\circ\text{C}$ , held for a period of time, quenched and the  $Q_{\text{Fe}_4\text{N}}$  value found. This procedure was followed with increasing periods of time until a constant value was obtained. The other two wires were left for several days to age and were then heated to  $300^\circ\text{C}$  and held for increasing periods until again a constant value was obtained. In the first case the treatment precipitates nitrogen from solid solution to establish equilibrium and in the second the nitrogen previously precipitated as  $\text{Fe}_4\text{N}$  is taken into solid solution. Agreement between the two methods is very good as is shown in Fig.15 and Table 8. The values obtained from the four specimens were averaged for each temperature. These are quoted in Table 9(a) over a range of solution temperatures from  $215^\circ\text{C}$  to  $650^\circ\text{C}$ . In the case of values established for temperatures above the eutectoid the approach to equilibrium was that of precipitating nitrogen from solid solution at the eutectoid, i.e. by heating the specimens from room temperature, not by cooling them from a higher temperature. This was necessary because the

cont'd...

furnaces used could not easily operate above 950°C making the approach to equilibrium by taking nitrogen into solid solution difficult to achieve.

The  $Q^{-1}$  values given in Table 9 are the equilibrium values obtained by quenching and measuring the damping at room temperature. The testing frequency was adjusted such that the peak occurred at room temperature which is a convenient one for rapid testing after quenching. The logarithm of this value is plotted against the reciprocal of the absolute temperature in Fig.16. Two straight lines result, one for subeutectoid temperatures with a negative gradient and another for temperatures above the eutectoid with a positive gradient. Both are of the form

$$Q^{-1} = A \exp. \frac{dH}{RT} \text{ or}$$

$$\ln Q^{-1} = \ln A + \frac{dH}{RT} \text{ or}$$

$$\log Q^{-1} = \log A + \frac{dH}{2.3 RT}$$

where A is a constant, T the temperature, in °K, R the gas constant and dH the heat of activation of the reactions involved above and below the eutectoid temperature.

The gradients of the lines are in fact  $\frac{dH}{2.3R}$ . The results plotted in Fig.16 for the subeutectoid temperatures give a dH value for the reaction  $4Fe + [N] \rightleftharpoons Fe_4N$  as - 8500 Kcals/mole of nitrogen and  $Q^{-1} = 13 \exp. - \frac{8500}{RT}$  as the expression connecting the solubility with temperature. The dH values found by Rawlings and Tambini<sup>48</sup>, Fast and Verrijp<sup>33</sup> and Peranjpe et al<sup>51</sup> are 7.54, 8.3 and 8.96 Kcals/mole respectively. The author's result is closer to that

of those workers using internal friction techniques than to the values obtained by Paranjpe et al.<sup>51</sup> based on chemical analysis of nitrated carbonyl powder which had been previously decarburised.

For temperatures above the eutectoid the  $dH$  value is 14,100 Kcal/mole of nitrogen and the related equation is  $Q^{-1} = 2.3 \cdot 10^{-5} \exp. \frac{14,100}{RT}$ . The  $dH$  value is that for the chemical reaction  $[N\alpha] \rightleftharpoons [N\gamma]$ . These results agree quite closely the 13,500 Kcal/mole and  $Q^{-1} = 4.6 \cdot 10^{-5} \exp. \frac{13,450}{RT}$  found by plotting the results of Rawlings and Tambini<sup>48</sup> in a similar manner.

The two lines of Fig.16 intersect at 589°K and give a  $Q^{-1}$  value of  $8.9 \cdot 10^{-2}$  for that temperature. Taking the eutectoid temperature as 590°C the results of Fast and Verrijp give the solubility as 0.097% nitrogen while the value is 0.108% for the same temperature according to Rawlings and Tambini. Using the conversion factor of Fast and Verrijp (1.26)<sup>33</sup> on the author's figure of  $8.9 \cdot 10^{-2}$  the solubility would be 0.112%, while that using the factor of Rawlings and Tambini (1.28) would give 0.114%. Dijkstra<sup>21</sup> using a factor of 1.26 reports the solubility at 590°C as 0.107%. The agreement shown by these various results is of quite a high order, when it is pointed out that damping values corresponding to the solubilities reported for 590°C all lie in the range  $(8.5 \pm 1) \cdot 10^{-2}$ .

Fig.17 illustrates graphically the difference between the results of Dijkstra<sup>21</sup> and those of the author. (In this graph

Dijkstra's factor of 1.26 is used on the author's results). Dijkstra's values are consistently lower above 350°C. Indeed Dijkstra's determinations are consistently lower than those obtained by any other workers using damping methods. A direct comparison of the alpha-phase boundaries as determined in this present work (using a factor of 1.28) and as determined by Rawlings and Tambini<sup>48</sup> is to be found in Fig.18. There is a fair measure of agreement below the eutectoid but the discrepancies to be found above the eutectoid are larger. They are greatest at temperatures approaching 590°C and Rawlings and Tambini's results are consistently higher throughout. In the present work a specimen 0.03 inches in diameter was used while that used by Rawlings and Tambini was only 0.02 inches in diameter. With such a thinner specimen a more effective quench could be obtained especially from higher temperatures and it is possible that not all of the nitrogen was retained in solid solution in this present work so that the damping peak would be correspondingly lower. This is confirmed to some extent by the fact that agreement is better between the two studies at the highest temperatures where there is less nitrogen in solid solution and the rate of precipitation would be slower.

The results of Paranjpe et al<sup>51</sup> are plotted in Fig.19 together with the present results (again multiplied by a factor of 1.28) and show a considerable divergence especially above the eutectoid temperature. The discrepancy is not consistent and the methods of determination are not comparable but it is interesting to note

cont'd...

that the work of Paranjpe et al would indicate a much greater solid solubility above the eutectoid than do the internal friction results. It is possible that  $Fe_4N$  is present in the cases of the determinations at  $650^{\circ}C$  and  $700^{\circ}C$  which would account for the high values obtained by chemical analysis.

It is appreciated that the method used by the author to determine the equilibrium values of interstitial nitrogen cannot be checked by chemical analysis since  $Fe_4N$  is present in all cases. However the method used has been proved acceptable since the  $Q^{-1}$  values found agree well, within the limits of experimental error, with the results of other workers. The value of  $dH$  found for the solution of  $Fe_4N$  is unaffected by this factor and also agrees closely with previously determined values. Smit and Van Bueren<sup>36</sup> have calculated theoretically that in a specimen of randomly orientated crystals the proportionality constant is 1.33. It is considered however that the factor of 1.28 found by Rawlings and Tambini<sup>48</sup> is the most reliable and the author's results using this agree well with the established solubility values.

Consequently it has been adopted in the present work to calculate the weight per cent nitrogen.

These results obtained with nitrogen in pure iron wires were very encouraging since they showed that the nitriding technique and the methods of recording and measuring the internal friction were fully acceptable and that the apparatus built was capable of producing accurate results. The results also helped confirm the work done previously as well as providing the author with useful experience in manipulating the apparatus before proceeding

cont'd...

to examine the iron-aluminum-nitrogen system.

cont'd...

Section 5.5 - Damping in Iron-Aluminium-Nitrogen Alloys.

Having established the Snoek peak in iron-nitrogen system steps were taken to study the iron-aluminium-nitrogen system. To this end three specimens from the alloy containing 0.09% aluminium by weight were nitrided and the damping curve determined between 15° and 65°C. In each case the curve established was considerably broader than the Snoek peak and the maximum was less sharply defined as is illustrated by the example given in Fig.20. Here the experimental curve is compared with the theoretical Snoek peak calculated from equation (5).

$$Q^{-1} = \frac{Q_m^{-1}}{\cosh \frac{dH}{R} \left( \frac{1}{T} - \frac{1}{T_m} \right)}$$

with a  $T_m$  of 42°C and with a  $dH$  value of 18.2 Kcal/mole for the same height of peak maximum as the experimental curve. The experimental peak is very much broader indicating the presence of one or more damping peaks in addition to the Snoek peak.

By assuming that the theoretical peak corresponds exactly to the experimental peak in height and temperature and by subtracting it from the experimental curve there is an indication that there are possibly three peaks present (Fig.20). The earliest attempts at resolving this peak into its components therefore were based on the assumption that there were in fact three peaks present.

It was hoped to compile a computer programme which by a reiterative process of continuous approximations would define the peaks present in terms of their peak heights ( $Q_m^{-1}$ ), their

peak temperatures ( $T_m$ ) and the activation energy ( $dH$ ). In order to accomplish this approximate  $dH$  values had to be assigned to the secondary peaks on either side of the arbitrarily placed Snoek peak. This was done by the graphical methods outlined in Section 3.5. It was not possible to calculate the  $dH$  value from equation (6) since it was only in the case of one frequency (Table 10) that both the secondary peaks were completely defined since the three peaks stretch over a larger temperature range than it was possible to test with the apparatus of this investigation. The  $dH$  values were calculated from the individual  $Q_m^{-1}$  values of these secondary peaks using the method of plotting the natural logarithm of the relaxation time against the reciprocal of the temperature. In this way the  $dH$  value for the lower peak at  $27^\circ\text{C}$  (Fig.20) was calculated as 15.5 Kcals/mole and that for the upper peak at  $60^\circ\text{C}$  as 19.2 Kcals/mole.

Preliminary calculations with these values indicated that the computer programme might well produce results in the manner expected. The programme was designed to take the values of  $Q_m^{-1}$ ,  $T_m$  and  $dH$  fed into it for each curve and vary them with respect to each other until a constant value was reached for each one. Although the  $Q_m^{-1}$ ,  $T_m$  and  $dH$  were known for the Snoek peak inaccurate values were deliberately fed into the computer so that if the computer eventually produced the established values for this peak then the programme would have proved itself. The computer programme was designed to provide a  $Q_m^{-1}$ ,  $T_m$  and  $dH$  value for each peak by using the experimental values of  $Q_m^{-1}$ . Unfortunately

the values produced were unacceptable in terms of the experimental curve as, instead of converging on certain values for the required constants successive cycles produced increasingly divergent results and eventually gave  $Q_m^{-1}$  values many times higher than the highest experimental  $Q^{-1}$ . It became apparent that not enough precise information had been given to the computer and that with so many variables no single mathematical solution could be found which explained the experimental curve in terms of three  $Q_m^{-1}$ 's,  $T_m$ 's and  $dH$ 's.

A change of approach to the problem was necessary. It was decided to reduce the number of variables by specifying all the known information about the Snoek peak. The first step was to establish the exact position of the Snoek peak for the testing frequency used. This was done by using the data of Fast and Verrijp in conjunction with equation (6). For the frequency used in drawing up Fig.20, i.e. 2.7 cycles/sec. and for a  $dH$  value of 18.2 Kcals/mole it was found that Snoek peak was at  $33^{\circ}\text{C}$  and not  $42^{\circ}\text{C}$ . On calculating a theoretical peak with its  $T_m$  at  $33^{\circ}\text{C}$  and subtracting it from the experimental curve it became apparent that there was only one other peak (Fig.21 and Table 11) and not two as had been previously surmised. This elimination of one of the secondary peaks is based on the assumption that the form-nitrogen Snoek peak is completely unaffected by the presence of another relaxation process. It remained then to determine the characteristics of this other peak which occurs at  $52^{\circ}\text{C}$  for 2.7 cycles/sec.

cont'd...

Using equation 6 on the secondary peak so obtained for the three specimens  $\Delta H$  values ranging from 14 to 23 Kcals/mole were found which had an average value of 19.7 Kcals/mole. On processing the results, obtained by the subtraction of the Snoek peak from the experimental one, in Programme 2 in the computer an average value of  $\Delta H$  for the three secondary peaks was found to be 19.5 Kcals/mole (Table 12(a)).

The  $\Delta H$  values obtained for the secondary curve are very close to that reported by many workers for the damping caused by interstitial carbon in alpha-iron. The suspicion that this peak was in fact due to carbon was strengthened by the fact that the  $T_m$  value of  $51^\circ\text{C}$  given by the computer programme for the peak shown in Fig.21 is only  $1^\circ\text{C}$  higher than that which would be expected from carbon at the same frequency (Taking a  $\Delta H$  value of 20 Kcals/mole and a  $T_m$  of  $40^\circ\text{C}$  for a frequency of one cycle a second the  $T_m$  for carbon at a frequency of 2.7 cycles/sec is  $50^\circ\text{C}$ ). The peak temperatures given by the computer for the other two frequencies agree well with the theoretical values for carbon at these frequencies. On the basis of this evidence it was concluded that the secondary peak was not due to nitrogen interacting with aluminium but was the Snoek peak for carbon in alpha-iron.

Two features of importance emerge from this conclusion. Firstly it appeared that the decarburisation of the specimens was not complete in the 72 hours treatment given to them. It had been appreciated earlier that the dry hydrogen process used to prevent oxidation of aluminium was not a very efficient decarburising

cont'd...

agent with which to effect the removal of soluble carbon. Yet tests conducted to determine the background damping before nitriding had given no indication of the presence of a carbon peak of the order of  $6.10^{-3}$  as found in these three specimens. Explanation is to be found in the formation of aluminium carbide. The reaction for the formation of  $Al_4 C_3$  has a high negative free energy and it is even less readily removed by hydrogen than interstitial carbon. The presence of carbon as precipitated carbide would not produce a damping peak and this would account for the low background damping found in the temperature range where a carbon peak would have been expected. Although  $Al_4 C_3$  is a stable compound aluminium nitride is even more stable. The negative free energies of formation are 37 and 55 Kcal/mole respectively at  $600^{\circ}C$ . The following reaction would take place

$$Al_4 C_3 + 4N \rightleftharpoons 4 Al N \quad (\Delta H = -185,000 \text{ Kcal/mole at } 600^{\circ}C \text{ indicating that the reaction would go to the right as written) and carbon would be liberated to contribute to damping. This would explain the appearance of a carbon peak where none had been found previously. With reference to the work of Laxer et al.<sup>24</sup> it is possible that the secondary peak found is in fact composed of two peaks; the Snock due to carbon and a subsidiary peak some  $14^{\circ}$  lower in temperature of rather smaller peak height. This subsidiary however would be disguised by the much larger nitrogen peak.$$

The height of the carbon peak was  $6.10^{-3}$  which is equivalent to approximately  $8.10^{-3}$  weight per cent of carbon and in an attempt to remove it the decarburising time was doubled. A specimen

cont'd...

decarbured in this manner and from the same alloy (0.09% aluminium) was nitrated and the damping curve determined as shown in Fig.22. As can be seen there is very good agreement between the experimental peak and the theoretical Snoek peak for nitrogen in iron. There is some slight divergence between 320°K and 330°K where the carbon peak would be expected to fall. This is the final piece of corroborating evidence for the explanation that the second peak found in Fig.21 is due to the presence of interstitial carbon. Prolonging the treatment to more than six days did not generally provide much improvement in agreement between the experimental and theoretical peak and it is possible that specimens picked up carbon from hydrocarbon impurities in the hydrogen although every precaution was taken to exclude these (See Section 3.3). In general it was found extremely difficult to remove the carbon entirely and usually a very small allowance had to be made for it in analysing experimental curves in the computer.

The second point is with regard to the usefulness of the computer programmes. Although the second peak could not be attributed directly to the presence of aluminium the time devoted to developing the computer programmes was not mis-spent. Applying the principles outlined in Section 3.5 for just such a case as this the computer had been successfully used to analyse a composite peak containing one completely unknown relaxation process. Good agreement was obtained between the three examples with respect to the  $\Delta H$  value found. The very good agreement between the  $T_m$  values given by the

computer and the theoretical  $T_m$  values for carbon was later substantiated by the decarburising experiments as being evidence that the secondary peak was due to carbon. It is doubtful if the peak would have been as convincingly demonstrated to be due to carbon without the computer programmes which are fully vindicated by this example.

Laxar et al<sup>24</sup> reported as many as three other peaks in addition to the Snoek in an aluminium-carbon system containing 2.36% aluminium. They also give results for alloys containing 0.04 and 0.36% aluminium which are similar in composition to two of the alloys made for the present investigation.

In order to establish whether or not the peaks reported for 2.36% aluminium were present in alloys containing only 0.04 or 0.36% Laxar's curves for these alloys were subjected to the computer analysis devised for this investigation. Very little variation was found from the theoretical carbon peak in the case of the 0.04% alloy. With the 0.36% alloy however significant differences were observed when a theoretical calculated Snoek peak was subtracted from the experimental results (Fig.23). Small peaks of the order of  $1.5 \cdot 10^{-3}$  and  $2.5 \cdot 10^{-3}$  were found at approximately the same temperatures as those reported by Laxar et al for two of their secondary peaks in the 2.36% alloy. As the aluminium content increases Laxar et al find that the heights of the secondary peaks rise at the expense of the Snoek peak. It would appear therefore that the height of the peak is dependent on alloy content and that any peak there may be in the iron-aluminium-

nitrogen system will be most obvious in the alloy containing the maximum aluminium (0.3%) in this series and that below this composition the secondary peak would be too small to be readily detected.

Before further nitriding experiments were undertaken, it was decided to carry out some experiments in an attempt to confirm the work of Laxar et al on the iron-aluminium-carbon system. When 0.3% aluminium specimens of this present series of alloys were carburised the presence of the two peaks, illustrated in Laxar et al's work in Fig.23, was confirmed (Fig.24). Laxar et al find their peaks at  $301^{\circ}\text{K}$  and  $340^{\circ}\text{K}$  in their higher alloys. The author's analysis of their peak for 0.36% aluminium has the secondary peaks at  $301^{\circ}$  and  $335^{\circ}\text{K}$  while the author's own work gives the peaks at  $300^{\circ}$  and  $331^{\circ}\text{K}$ . Agreement is good for the lower peak but not quite so good for the higher peak which lies at the upper temperature limit of the apparatus used in this present work. The heights of the peaks recorded differ again at the higher temperature but by and large the present work confirms that of Laxar et al. To ascertain if similar effects could be obtained in the iron-aluminium-nitrogen system three specimens of the 0.3% aluminium alloy were nitrided for thirty minutes in a 6% ammonia, ammonia/hydrogen mixture, quenched and the damping curve established as illustrated in Fig.25.

Previous calculations using equation (6) had established that the Snoek peak for this frequency (2.5 cycles/second) would lie at  $305^{\circ}\text{K}$  ( $32^{\circ}\text{C}$ ). In actual fact the experimental peak lay

cont'd...

considerably below this temperature at  $296^{\circ}\text{K}$  ( $23^{\circ}\text{C}$ ) indicating that the experimental peak was a compound of two or more peaks. When the experimental results were processed in computer Programme 1 they yielded the Snoek and secondary peak shown in Fig.25. Similar analysis on the two other experimental curves gave comparable results. The secondary peaks, as determined graphically by subtraction lay between 7 and  $10^{\circ}$  below the Snoek peak. By using equation (6) two  $\text{dH}$  values were calculated to be 21 and 30.8 Kcals/mole. No great reliance can be placed on these values as this graphical method positioned the secondary peak at the same temperature for two different frequencies. When the values for the secondary peaks arrived at by subtraction were processed in computer Programme 2,  $\text{dH}$  values were found which gave a mean value of 24.6 Kcals/mole. The  $T_{\text{m}}$  values so found varied from  $8^{\circ}$  to  $11^{\circ}$  below the Snoek peak and the ratio of the secondary peak to the Snoek peak was 1.5. In summary it may be stated that this 0.3% alloy when nitrided gives an additional damping peak which lies approximately  $9^{\circ}\text{C}$  below the Snoek peak, is usually one and a half times the height of the Snoek peak and has a  $\text{dH}$  value of 24.6 Kcals/mole.

Since this peak is of a regular shape and has a  $\text{dH}$  value a little higher than that for the diffusion of nitrogen in iron it would appear that it arises from a single relaxation process. The general characteristics of a compound peak are an irregular shape, such as those found by Dijkstra<sup>21</sup>, Laxer et al.<sup>24</sup> and others and a low  $\text{dH}$  value. The activation energies for the diffusion of

interstitial or substitutional atoms in metals are usually of the order of several tens of thousands of calories per mole of interstitial or substitutional atoms. For example the diffusion of carbon in iron has a  $\Delta H$  value of 20 Kcals/mole and that of aluminium in iron is 56 Kcals/mole. Peaks with  $\Delta H$  values of approximately 10 Kcals/mole or less are, for the reason, suspected of being compound peaks. For example the  $\Delta H$  value found by the computer for the experimental curve given in Fig.25 is 8.6 Kcals/mole. There is no precise scientific basis for deciding whether or not a peak is a single relaxation process or a combination of two or more. If a curve exhibits the general characteristics of a single process i.e. regular shape and high  $\Delta H$  value, then it can usually be regarded as a single process. If on the other hand a curve is irregular and has a low  $\Delta H$  value then the possibility exists that it is a compound of several processes and it should be analysed as such. Generally these assumptions are justified. It could be argued that a  $\Delta H$  value of 24.6 Kcals/mole as found here could be produced by two processes of even higher  $\Delta H$  e.g. the 56 Kcals/mole  $\Delta H$  value for the diffusion of aluminium in iron. However the regular shape of the curve tends to discount the theory that it is composed of two peaks as does the fact that the diffusion of aluminium in iron is negligible at room temperature.

A similar nitriding treatment carried out on the other alloys of the series gave the results tabulated in Tables 17-20 and illustrated in Figs. 26,27,28 and 29. In each case a secondary peak was obtained and the  $\Delta H$  values calculated by computer were

all in the range  $24 \pm 2$  Kcals/mole. As can be seen however the peaks heights show no definite dependence on aluminium content and the ratio of the peak heights is not constant and in no case agrees with the value of 1.5 found in the case of the 0.3% alloy referred to in Table 17.

All of the above mentioned secondary peaks had been found by the examination of unhomogenised wires that is to say the specimens had been nitrided quenched and the damping curve determined immediately. There had been no anneal at  $590^{\circ}\text{C}$  to allow nitrogen to diffuse through the wire and establish equilibrium with the aluminium in solution. When homogenisation was carried out at  $590^{\circ}\text{C}$  for two hours the secondary peak disappeared in all but the 0.09% and 0.3% alloys where it was considerably reduced in magnitude (Figs. 30 and 31 and Tables 11 and 12.) In the case of the 0.3% alloy the secondary peak fell to one seventh of the value of the Snoek peak whereas it had been 1.5 times as large as the Snoek peak when the wire was unhomogenised. With the 0.09% alloy the Snoek peak in the homogenised specimen was approximately equal to the secondary peak in height whereas before homogenisation it had been only half the height of the secondary peak. After 3 hours homogenisation the secondary peak had disappeared in both these alloys. All of this suggests that the mechanism to which the peak is attributable depends on a metastable association of atoms.

In order to investigate this metastable peak the three wires referred to with respect to Fig. 25 were given a resolution treatment at  $590^{\circ}\text{C}$  for one hour. They were then quenched and the damping

curve determined as is exemplified in Fig.32. It is assumed that, in the intervening period the nitrogen had precipitated and that the re-solution treatment would have taken the nitrogen of  $Fe_4N$  back into solid solution. Computer analysis showed these curves to be Snoek peaks with no secondary or abnormal peaks. At this stage there appeared to be a distinct relationship between the combined heights of the Snoek and secondary peaks, as found in the unhomogenised specimens, and that of the Snoek after solution treatment (Fig.33.) The sum of the heights of the two peaks of Fig.25 is very nearly equal to the height of the Snoek peak of Fig.32 i.e.  $3.8 \cdot 10^{-2}$ . This close numerical relationship was found with the other two wires. The specimen of Fig.30 from the same alloy, given the same nitriding treatment but homogenised for two hours has a Snoek peak of  $3.4 \cdot 10^{-2}$  and a secondary peak of  $4.5 \cdot 10^{-3}$  to give a very similar total of  $3.85 \cdot 10^{-2}$  as the sum of the peaks. The indications are therefore, that ageing and re-solution or homogenising increase the Snoek peak at the expense of the secondary peak by approximately the amount by which the secondary peak falls. It is only the non-equilibrium conditions which apply in unhomogenised wires that produce the secondary peak and a possible mechanism may be assigned to the peak from a study of these conditions.

cont'd...

Section 5.6 - Mechanism for the Secondary Peak.

The characteristics of the secondary peak are that it occurs at a temperature  $9^{\circ}$  lower than that of the Snoek peak due to nitrogen and it has a  $\Delta H$  value 6.4 Kcals/mole higher. These facts immediately eliminate carbon interactions as the possible cause since the Snoek peak due to carbon lies some  $20^{\circ}$  higher for the same frequency and Laxar et al.<sup>24</sup> report no secondary peak for aluminium-carbon interactions at the temperature of the secondary peak found here.

The fact that the secondary peak appears at a lower temperature than the Snoek and yet has a higher  $\Delta H$  value would at first sight appear to be in conflict with the views of Wert<sup>19</sup>, who has found a simple straight line relationship between the  $\Delta H$  for a process and the temperature at which it occurs. Interpretation of his graph drawn from the damping of different interstitials in various body centre cubic lattices gives a direct relationship such that the higher the value of  $\Delta H$  the higher the temperature at which the peak occurs for a given frequency. It is apparent however that this relationship does not hold for secondary peaks caused by the presence of alloys. For example Dijkstra and Sladek<sup>54</sup> found all of their secondary peaks with various alloy additions to have  $\Delta H$  values very close to the 18 Kcals/mole for the Snoek peak except in the case of Molybdenum where the reported  $\Delta H$  was 16 Kcals/mole for a secondary peak which lay  $53^{\circ}$  above that of the Snoek peak.

As discussed in Section 1.2 the occurrence of the damping peak

cont'd...

is due to the fact that at a certain temperature the cycle of oscillation of the interstitial atom is comparable to the period of vibration of the pendulum when operating at a certain frequency. Thus it is probably more accurate to say that the temperature at which the peak occurs for any given process is dependent on the relaxation time of the process rather than the  $dH$  value. The relaxation time is given by the equation  $T = T_0 \exp. \frac{dH}{RT}$  where  $T_0$  is a constant. The exact physical interpretation of  $T_0$  is not clear but it must be dependent on such factors as the chemical affinity between the solute and solvent atoms, on the relative sizes of the solute and solvent atoms and on the elastic properties of the solvent. The energy required to make an interstitial diffuse will depend on the physico-chemical conditions which  $T_0$  embodies and  $T_0$  will be altered by the introduction of an alloy atom which will undoubtedly effect all of the above factors. There is no reason to suppose that the relationship which Wert<sup>19</sup> found between  $T_m$  and  $dH$  should apply if the introduction of an alloying element produces variation in  $T_0$ .

Various mechanisms have been suggested to account for the appearance of subsidiary peaks due to interstitials in body centre cubic alloys<sup>54,58</sup>. All of these postulate a different type of jump process associated with interstitial sites adjacent to substitutional solute atoms in which the activation energy and mean time of stay of the interstitial differ from that in a normal site. Preferential association of the interstitial with such an interstice may result from a mechanism of the type suggested by Leak et al<sup>58</sup> for the

iron-silicon-nitrogen system. Jack<sup>46,12</sup> has shown that interstitial nitrogen in alpha-iron causes a distortion of the cubic cell resulting in an expansion along the diad axis (Fig.34(a) and 34(b) ). According to Leak et al<sup>58</sup>, if a silicon atom occupies one of the sites of the octahedron as shown in Fig.34(c) with an interstitial nitrogen atom at the centre then the resulting lattice distortion should be smaller than in Fig.34(b) since silicon tends to contract the lattice. The energy for the system would be lower and hence a nitrogen atom would prefer to be in an octahedron containing a silicon atom. This would introduce atom jumps between iron-iron and iron-silicon interstices with a resultant damping peak in addition to the Snoek peak.

Such a geometrically favourable position however cannot be responsible for the subsidiary peak reported in the presence of manganese in iron by Dijkstra and Sladek<sup>54</sup> since manganese, unlike silicon, expands the iron lattice. These latter authors postulate that lower energy interstitial sites are produced by manganese, chromium, molybdenum and vanadium without attempting to explain why this should be the case. The chemical affinity between the substitutional and interstitial atoms however must be an important factor in determining the relative distribution of the interstitial between iron-iron and iron-alloy sites. In the present case where aluminium is the substitutional solute it would be expected that the chemical affinity factor would be the dominant one since aluminium expands the iron lattice and does not create a geometrically suitable site. It is probably more accurate to describe the reasons for a

nitrogen atom preferring iron-manganese, iron-silicon or iron-aluminium sites to iron-iron sites in terms of both relative chemical affinity and the relative geometry of the pure iron and alloy lattice. It is extremely difficult to evaluate what contributions these two factors make in the case of aluminium or indeed any other alloying elements.

If an explanation of the secondary peak is to be sought in terms of an interaction between aluminium and nitrogen atoms there are several possible mechanisms as detailed below:-

- (a) Jumps between iron-iron and iron-aluminium sites.
- (b) Jumps between iron-aluminium and iron-aluminium sites.
- (c) Jumps between iron-aluminium and aluminium-aluminium sites.
- (d) Jumps between aluminium-aluminium and aluminium-aluminium sites.
- (e) Jumps in strained interstices in the lattice, for example round a coherent precipitate.

Consideration of these possible mechanisms may lead to the conclusion as to which is the most likely process. Mechanisms (b), (c) and (d) all imply the presence of pairs of aluminium atoms or at least aluminium atoms in such close juxtaposition that iron-aluminium to iron-aluminium jumps are possible. It is unlikely however that pairs of aluminium atoms will occur to any great extent in alloys as dilute as those used here. Laxar et al.<sup>24</sup> consider pairing unlikely in their aluminium alloys even up to 2.36 weight per cent. Further since the presence of aluminium expands the lattice and increases the strain energy locally it is

cont'd...

even more unlikely that pairs of aluminium atoms are the cause of this secondary peak in the case. Mechanisms (b), (c) and (d) are therefore excluded on these grounds.

There seem to be adequate reasons why mechanism (a) could not account for the secondary peak found in alloys of this present work. Firstly thermodynamic data indicates that aluminium nitride is a very stable compound the negative free energy of formation of which is 60 Kcal/mole at 600°C, the nitriding temperature. In view of the high chemical affinity between the two elements it would appear unlikely that nitrogen and aluminium would be found together in solid solution under equilibrium conditions.

Darken et al.<sup>17</sup> give the following relationship for the solubility product  $K = [Al\%][N\%]$  for the reaction  $[Al] + [N] \rightleftharpoons AlN$  in gamma-iron,  $\log K = -7,400/T + 1.95$ . On extrapolating this to 590°C (ignoring the effect of the phase change from gamma to alpha-iron) the K value is of the order of  $10^{-7}$ . The height of the Snoek peak in the alloys containing 0.3 per cent aluminium is approximately  $3.8 \cdot 10^{-2}$  after homogenisation. This is equivalent to approximately  $5 \cdot 10^{-2}$  weight per cent nitrogen in solid solution which would be in equilibrium with  $2 \cdot 10^{-6}$  weight per cent aluminium in solid solution. The work of Leslie et al.<sup>39</sup> gives similar results and the  $[Al]$  level is so low that no interaction effect between aluminium and nitrogen atoms could be observed by internal friction techniques. This is of course in agreement with the fact that the peak is not observed under equilibrium conditions since it disappears on homogenising. However it could be suggested that measurable solubilities of  $[Al]$  and  $[N]$  might occur under conditions in which

AlN had difficulty in nucleating at temperatures where diffusion of aluminium is limited. In fact could this happen it would follow that homogenisation would allow precipitation of aluminium nitride and subsequent solution treatment would only take the nitrogen of  $Fe_4N$  into solid solution. Thus supersaturation with  $[Al]$  and  $[N]$  could explain a transient secondary peak due to an interaction between  $[Al]$  and  $[N]$ , which subsequently precipitated. However the evidence of Figs. 30, 32 and 33 is that the nitrogen associated with the secondary peak returns to solid solution, when the secondary peak falls or disappears. If mechanism (a) applied the secondary peak would disappear on re-solution and the Snoek peak would remain unaltered. The secondary peak certainly disappears but the Snoek peak increases in height. On these grounds mechanism (a) is not considered to be the cause of the secondary peak.

Mechanism (e) therefore remains as the other possibility to be explored. That is to say the peak is caused by nitrogen jumps in strained interstices in the iron lattice. Several possible mechanisms might account for the presence of interstices which produce atom jumps which are distinguishable from the jumps of the Snoek mechanism e.g. the presence of a coherent precipitate, a high local concentration of interstitial solute, or a second phase. This latter possibility has been investigated thoroughly by East<sup>57</sup> who concluded that bulk precipitates of a second phases such as nitrides or carbides did not give rise to damping peaks. It is also possible that the nitriding conditions which do not allow time for diffusion of nitrogen to the centre of the wire, produce a

cont'd...

high local concentration of nitrogen atoms with resulting severe lattice distortion. However in previous cases, Fig.13 for example, pure iron wires have been subjected to just such nitriding treatments without producing secondary peaks. It is only in alloy specimens that these conditions produce a secondary peak. It would appear then that the nitriding conditions alone are not responsible. The likeliest possibility therefore seems to be the presence of a coherent precipitate and it remains to discuss whether such a mechanism could account for the experimental observations.

With regard to the composition of the alloys there are four main elements present, iron, aluminium, nitrogen and carbon so that the coherent precipitate is most likely to be either aluminium carbide, iron nitride or aluminium nitride. Any aluminium carbide present would be in the fully precipitated state having been formed in the molten alloy. Since iron nitride and aluminium nitride are the other two remaining possibilities efforts were made to distinguish between the two by studying the rate of decay of the secondary peak.

Here specimens from the 0.3% alloy were nitrided at 590°C quenched and the damping curve ascertained. The curve was re-determined at two hour intervals i.e. the damping was measured between 15°C and 65°C, such a way that after  $Q^{-1}$  value had been found at 65°C the chamber was cooled and exactly two hours after the first reading at 15°C the second reading at 15°C was taken. The results are graphed in Figs.35 and 36 and the  $Q^{-1}$  values are given in

Table 27. These graphs show that the secondary peak ages much more quickly at room temperature than the Snoek peak and although the thermal cycling over  $50^{\circ}\text{C}$  for four cycles is bound to have an effect on the rate of precipitation of the nitrogen associated with both peaks it serves as a means of comparison. As can be seen the height of the secondary peak drops from  $6.5 \cdot 10^{-3}$  in Fig.35(a) in the as quenched condition to  $4 \cdot 10^{-3}$  in four hours 35(b) and has virtually disappeared in eight hours as shown in Fig.36(b). On the other hand the Snoek peak falls only from  $1.4 \cdot 10^{-2}$  to  $1.15 \cdot 10^{-2}$  in the same period. It has only been shown that three hours homogenisation was sufficient to remove the secondary peak. It has been demonstrated however<sup>39</sup> that the rate of precipitation of aluminium nitride at  $590^{\circ}\text{C}$  is so slow that it is doubtful if a secondary due to the presence of a coherent precipitate of aluminium nitride would disappear at that temperature in three hours. It certainly would not disappear in eight hours at room temperature. None of these facts however are inconsistent with the possibility of the precipitation of a complex iron-aluminium nitride. Since due to a high local concentration of nitrogen, the lattice would be supersaturated with both  $\text{Fe}_4\text{N}$  and  $\text{AlN}$  there would be a tendency for such a phase to form during nitriding.

Conditions during precipitation in an alloy can be such that the alloying substitutional element participates in diffusion and precipitates are formed whose composition is different from the matrix. Such a case would be the precipitation of aluminium nitride from an iron-aluminium matrix. However in the iron-aluminium-nitrogen system the rates of diffusion of aluminium and nitrogen in iron are

widely different and as the work of Leslie et al<sup>39</sup> confirms little diffusion of aluminium occurs at 590°C and virtually none at all at room temperature. In such cases where the substitutional element does not have the opportunity to diffuse the precipitate derives its composition from the matrix. In the present case a complex iron-aluminium nitride would precipitate. Hultgren<sup>67</sup> designated this type of precipitation as para-precipitation. Such a para-precipitate would precipitate much more easily than aluminium nitride since it would only involve the diffusion of nitrogen atoms to the sites of aluminium atoms.

The mechanism envisaged for the secondary peak can be summarised as follows. During nitriding a high local surface concentration of nitrogen is produced. (It can be seen from Table 25 that the presence of aluminium results in a much more rapid absorption of nitrogen than obtained in a pure iron wire). Since the lattice is supersaturated in this surface region with respect to Fe<sub>4</sub>N and AlN a coherent precipitate of matrix composition is formed. The presence of this produces lattice strain and the secondary peak is considered to be due to nitrogen jumps associated with distorted interstices in such regions. If the wire is homogenised at 590°C diffusion of nitrogen towards the centre of the wire progressively reduces the height of the secondary peak (Fig.30) and increases the height of the Snoek peak. Similarly ageing and subsequent re-solution gives time for redistribution of nitrogen and removes the secondary peak. The ageing experiments at room temperature referred to above indicate that the secondary peak falls more rapidly than the Snoek

cont'd...

peak. In terms of the mechanism proposed this would be due to the greater degree of supersaturation around the coherent precipitates formed at the nitriding temperature whereas the Snoek peak is due to nitrogen in less supersaturated regions and precipitates normally. Diffusion of nitrogen away from the supersaturated region will also contribute to the more rapid fall in the secondary peak. These ageing rates are also in good accord with the fact that the mean time of stay of nitrogen atoms in the strained interstices responsible for the secondary peak is smaller (0.136 secs) than that for the Snoek peak (0.223 secs) at room temperature.

In conclusion it may be stated that the appearance of a secondary peak is a condition of the non-equilibrium nitriding technique employed and that the peak is a metastable one which is not found in fully homogenised iron-aluminium alloys.

Section 5.7 - Solubility of Aluminium Nitride in Iron.

Examination of the damping characteristics in iron-aluminium-nitrogen alloys in equilibrium conditions has shown that there was no detectable internal friction peak due to the interaction of aluminium and nitrogen atoms. It was not possible therefore to assess the quantity of nitrogen associated with aluminium in solution directly in terms of a damping peak. In order to study the reaction between aluminium and nitrogen in alpha-iron i.e.

$[Al] + [N] \rightleftharpoons AlN$  an indirect method was adopted for calculating the equilibrium constant or solubility product, K. K is given by the expression  $K = [Al\%] [N\%]$  i.e. the product of the percentage of aluminium and the percentage of nitrogen in solution at equilibrium.

From the knowledge gained from the study of the damping curves of iron-aluminium-nitrogen alloys it would appear that any nitrided iron-aluminium alloy contains the amount of nitrogen indicated by the height of the damping peak and the amount of nitrogen equivalent to that necessary to form aluminium nitride with the aluminium of the alloy. This assumption is made in calculating the equilibrium constant K from the percentage nitrogen in solid solution as determined by the height of the damping peak and the total nitrogen content of the wire as determined by chemical analysis. This latter figure provides a means of calculating the value of Al%

The height of the damping peak multiplied by a factor of 1.28 gives the weight per cent nitrogen in solid solution. If it is

cont'd...

assumed that the remainder when this figure is subtracted from the total nitrogen is nitrogen present as aluminium nitride, then it is possible to calculate the percentage of aluminium which has combined to form aluminium nitride. This in turn when subtracted from the total aluminium of the specimen will give the quantity of aluminium in solution and K can be calculated as shown below:-

$$K = [Al\%] [N\%]$$

$$\text{where } [N\%] = 1.28 \times QM^1$$

$$\text{and } [Al\%] = (\text{Weight \% Al in alloy}) - \frac{27}{14} (\text{Total \% N} - [N\%])$$

As indicated in Section 1.3 no work has been published on the reaction of aluminium and nitrogen in alpha-iron below 800°C although Darken et al.<sup>37</sup> and Leslie et al.<sup>39</sup> have done so above this temperature and by methods involving chemical analysis. It was decided therefore to study the equilibrium between 300°C and 600°C. To this end the following technique was employed. Wires from each of the aluminium alloys were nitrided at 590°C for thirty minutes and homogenised at that temperature in pure nitrogen for sixteen hours. The specimens were then furnace cooled to whatever temperature was required and held for two hours before quenching and measuring the damping. The wires were then analysed for total nitrogen content, by the method given in Appendix 2, and K was calculated in the manner shown above.

The values so obtained are given in Table 25 and graphed as a plot of  $\log_{10} K$  against the reciprocal of the absolute temperature in Fig.37. As can be seen there is a very wide scatter

cont'd...

of K values at each temperature with a marked dependence on aluminium content. If these results are averaged they give a straight line relationship of the type  $K = A \exp. \frac{dH}{RT}$  where A is a constant, dH the heat of formation of aluminium nitride from aluminium and nitrogen in solid solution, T the absolute temperature and R the gas constant. On this basis the dH value found from this graph is 14,700 Kcals/mole and the corresponding equation is  $\log K = \frac{-3200}{T} + 0.78$ .

This does not compare favourably with the equation given by Darken et al.<sup>17</sup>,  $\log K = \frac{-7400}{T} + 1.95$  or that found by Leslie et al.<sup>39</sup>  $\log K = \frac{-6770}{T} + 1.03$  which corresponds well with that of Darken et al. The dH value found by Darken et al is 33,800 Kcals and that by Leslie et al, 31,000 Kcals. On allowing 15,000 Kcals for the solution of aluminium and 7,200 Kcals for the solution of nitrogen in iron thermodynamic data indicates that a dH value of approximately 33,000 Kcals would be expected. This is very close to the values found by both Darken et al and Leslie et al. Extrapolation of the results of both these groups of workers gives K values which are several powers of ten smaller than those calculated here as is shown in Table 26. All of these facts combine to suggest that the results obtained in this present work are seriously in error.

There are three possible reasons why the K values found are as high. Firstly it is entirely possible that complete equilibrium was not achieved especially at the lower two temperatures and that holding at temperature for two hours is not sufficient time to

cont'd...

achieve this equilibrium. If this were the case it would result in high values of  $Q_{Al}^1$  and hence high K values. Secondly it is possible that part of the aluminium in the specimen is present as aluminium carbide unaffected by decarburisation or nitriding treatments. This would have the effect producing apparently high values of  $[Al\%]$  as at least some of the aluminium not combined as nitride would be present as aluminium carbide and not as aluminium in substitutional solid solution. Thirdly the accuracy of both the aluminium and nitrogen analyses are doubtful. The aluminium contents were obtained from the original cast analysis and even slight variations in the aluminium content of individual wires could produce considerable errors. The nitrogen analyses were performed on the small sample weights available from single wires and are thus subject to a fairly large error.

However the marked dependence of K values on aluminium content (Fig.37) might be interpreted as the result of more aluminium carbide being formed in wires of higher aluminium content pointing to this factor as the main source of error.

cont'd...

### Section 5.8 - Summary of Conclusions.

It is now necessary to attempt to assess what the present investigation has achieved.

On the purely practicable side a certain amount of reliable and efficient apparatus has been designed and put into commission. This apparatus has allowed the author to confirm most of the reported information to be gained from the study of the internal friction due to stress-induced diffusion of interstitial nitrogen in alpha-iron.

The iron-aluminium-nitrogen system has been investigated and a metastable peak discovered. This has been attributed to the interaction of nitrogen atoms with distortions in the lattice due to a coherent precipitate of iron-aluminium nitride. Otherwise the observation of Fast<sup>57</sup>, that there is no damping peak due to interaction of aluminium and nitrogen atoms in fully homogenised iron specimens at equilibrium, is confirmed. Consideration of the solubility product for the reaction  $[Al] + [N] \rightleftharpoons AlN$  indicates why no secondary peak is to be found under equilibrium conditions. The internal friction technique can accurately measure nitrogen solubilities to the order of about  $10^{-3}$  but no lower than this. That is to say if the solubility product is of the order of  $10^{-6}$  or less when the nitrogen solubility is  $10^{-3}$  or less then the internal friction technique as used in this investigation is not sensitive enough to indicate the presence of a secondary damping peak. At  $590^{\circ}C$  Darken et al.<sup>17</sup> give  $K$  as  $2.10^{-7}$  which would indicate

cont'd...

indicate that if there was enough nitrogen in solid solution to be measurable i.e.  $10^{-3}$  there would be too few aluminium atoms in solution i.e.  $10^{-4}$  to cause the interaction between aluminium and nitrogen atoms necessary to give rise to a secondary peak. Conversely if there were more than  $10^{-3}$  aluminium atoms in solution there would not even be enough nitrogen in solution to cause a Snoek peak. However at temperatures above  $1100^{\circ}\text{C}$  the solubility product is of the order of  $10^{-4}$  according to Darkey et al.<sup>17</sup> and it might be possible to produce a Snoek and a secondary peak in iron-aluminium-nitrogen alloys by nitriding and quenching from above this temperature.

Attempts to calculate the solubility of aluminium nitride in alpha-iron did not prove successful because equilibrium was not achieved and because of the presence of aluminium carbide. In fact had equilibrium been fully established the indications are that the internal friction technique would not have been adequate as a method of measuring nitrogen solubility. From this point of view the technique cannot be used to establish solubilities or a ternary diagram for iron-aluminium-nitrogen.

As indicated above, studies of the solubility of reasonably stable nitrides, necessitate the use of very low ammonia potentials if measurable equilibrium solubilities of the substitutional atom are to remain in equilibrium with the nitride. Indeed the ammonia potentials in many cases have to be so small as to be impossible to measure or control accurately. The method of nitriding used here could not be so controlled although it is possible that very

cont'd...

small nitrogen potentials could be achieved by soaking pure iron wires in contact with a metallic nitride at elevated temperatures.

In view of the interference of carbon in the present experiments it would be advisable to deoxidise the alloy melts with hydrogen in future where there is the possibility of the formation of a stable carbide of the alloying element. To do so may not be as practicable or as thermodynamically efficient as deoxidation by carbon but would be beneficial in the long term. However the appearance of a carbon peak after nitriding where none had manifested itself previously is a phenomenon of some interest. Since the presence of nitrogen and carbon in solid solution are of great importance in determining the mechanical properties and in particular high temperature creep properties of steels, the interaction of nitrides and carbides of various alloys over a range of temperatures might usefully be studied using an internal friction technique.

Of particular interest are the computer techniques developed to analyse complex damping curves. These have justified themselves and the effort expended on their development by the manner in which they identified carbon in one of the initial complex peaks, referred to in the preceding paragraph. These techniques may prove themselves important in future work in the field of internal friction studies.

Section 5.9 Bibliography.

1. C.E. Stromeyer, J.I.S.I., 1907, V.73, 200.
2. P.D. Merica, Trans. A.I.M.M.E, 1932, V.99, 13.
3. W. Koster, Arch. Eisenhüttenwesen, 1930, V.3, 637.
4. C. Zener, "Elasticity and Anelasticity of Metals", University of Chicago Press, 1948.
5. R.H. Randall, F.C. Rose, and C. Zener, Phys. Rev., 1939, 56, 343.
6. C. Zener and R.H. Randall, Trans. A.I.M.E., 1940, 137, 41.
7. T.S. Ke, J. App. Phys., 1948, 19, 285.
8. G. Richter, Ann. Physik Leipzig, 1937, 26, 605.
9. G. Richter, Ann. Physik Leipzig, 1938, 32, 683.
10. J.L. Snoek, Physica, 1939, 6, 591.
11. J.L. Snoek, Physica, 1941, 8, 711.
12. K.H. Jack, Proc. Roy.Soc., 1948, A195, 34.
13. R.H. Frazier, F.W. Boulger and C.H. Loxig, Ship Structure Committee Report, Serial No. SSC/53, 1952.
14. G.W. Geil, N.L. Carwile and T.G. Edgges, J. Research. Nat. Bureau of Standards, 1952, 46, 193.
15. I.E. Kontorovich, Fizika Metallov i Metallovidenie, 1956, 3, 553.
16. H. Schrader, H. Wiester and H. Siepmann, Arch. Eisenhüttenwesen, 1950, 21, 21.
17. I.S. Darken, R.P. Smith and E.W. Filer, Trans. A.I.M.M.E., 1951, 191, 1174.
18. L.J. Dijkstra, Phillips. Res. Rep., 1947, 2, 357.

19. C. Wert and J. Marx, *Acta Met.*, 1953, 1, 113.
20. C. Wert, *Phys. Rev.*, 1950, 79, 601.
21. L.J. Dijkstra, *Trans. A.I.M.M.E.*, 1949, 185, 252.
22. J.D. Fast and M.B. Verrijp, *Acta Met.*, 1955, 3, 203.
23. T.S. Ke, *Phys. Rev.*, 1947, 71, 533.
24. F.H. Laxar, J.W. Frame, and D.J. Blickwede, *Trans. A.S.M.*, 1960, 53, 683.
25. C.Y. Ang and C. Wert, *J of App. Phys.*, 1954, 25, 1061.
26. L-C Cheng and M. Gensairex, *Acta Met.*, 1953, 1, 483.
27. M.E. Fine, *Trans. A.I.M.M.E.*, 1950, 188, 1322.
28. S. Pearson, Ministry of Supply, R.A.E. Report, Met. 67, 1951.
29. J.P. Burden, "Nature", 1960, 188, 221.
30. "Vacuum Metallurgy", Rheingold Publishing Corporation New York, 1958.
31. M.J. Spendlove, "Vacuum Metallurgy Symposium", p.192, Electrochemical Society Publications, 1954.
32. F.C. Langenberg, *J. Metals*, 1956, 1099.
33. J.D. Fast and M.B. Verrijp, *J.I.S.I.*, 1955, 180, 337.
34. D. Polder, *Phillips Res.Rep.*, 1946, 1, 5.
35. M.E. Hirsch, M. Polanya and K. Weissenberg, *Z. Physik*, 1921, 7, 161.
36. J. Smit and H.G. Van Bueren, *Phillips Res. Rep.*, 1954, 2, 460.
37. C.S. Barrett, "The Structure of Metals", McGraw-Hill. Book. Coy, Inc., New York, 1952, p.489.
38. G. Lagerberg and A. Josefsson, *Acta Met.*, 1955, 3, 236.
39. W.C. Leslie, R.L. Rickett, C.L. Dotson and C.S. Walton, *Trans. A.S.M.*, 1954, 46, 1470.

40. L.S. Darken and R.W. Gurry, "Physical Chemistry of Metals"  
McGraw-Hill Book Coy. Inc., New York.
41. C.J. Smithells, "Metals Reference Book", Butterworth and  
Coy. Ltd., London, 1962.
42. C. Wert and C. Zener, Phys. Rev., 1949, 76, 1169.
43. C. Wert, J. of App. Phys., 1950, 21, 1196.
44. J.D. Fast and M.B. Verrijp, J.I.S.I., 1954, 176, 24.
45. G. Borelius, S. Berglund and O. Avasan, Arkiv Fysik,  
1950-51, 2, 551.
46. K.H. Jack, Proc. Roy. Soc., 1951, A208, 216.
47. W. Wepner, Arch. Eisenhüttenwesen, 1956, 27, 449.
48. R. Rawlings and D. Tambini, J.I.S.I., 1956, 184, 302.
49. H.U. Astrom, Ark Fysik, 1954, 8, 495.
50. H.U. Astrom and G. Borelius, Acta Met., 1954, 2, 547.
51. V. Paranjpe , M. Cohen, M.B. Bever and C.F. Floe, Trans.  
A.I.M.M.E., 1950, 188, 261.
52. A. Sieverts, G. Zapfend and H. Moritz, Z. physik Chem.,  
1939, A183, 19.
53. N.S. Corney and E.T. Turkdogan, J.I.S.I., 1955, 180, 344.
54. L.J. Dijkstra and R.J. Sladok, Trans. A.I.M.M.E., 1953, 197, 69.
55. J.D. Fast, Iron and Coal Trades Review, 1950, 837.
56. J.D. Fast and J.L. Meijering, Phillips. Res. Rep. 1953, 8, 1.
57. J.D. Fast, Metaux, Corr. Indus, 1961, 36, 383 and 431.
58. D.A. Leak, W.R. Thomas and G.M. Leak, Acta Met., 1955, 3, 501.
59. R. Rawlings and F.M. Robinson, J.I.S.I., 1961, 197, 211.

cont'd...

60. P.H. Emmett, S.B. Hendricks and S. Brancener, J. Amer. Chem. Soc., 1930, 52, 1456.
61. E. Kula and A. Joseffson, Trans. A.I.M.M.E., 1952, 194, 161.
62. P. Flament, Rev. de Met, 1957, 54, 537.
63. G. Collette, Comptes Rendues, 1960, 251, 2017.
64. T.S. Ke, Trans. A.I.M.M.E., 1948, 176, 448.
65. C. Zener, Proc. Phys. Soc., 1940, 52, 152.
66. E. Lehrer, Z. Elektrochem, 1930, 36, 383.
67. A. Hultgren, Trans. A.S.M., 1947, 39, 915.

### ACKNOWLEDGEMENTS.

The author wishes to express his gratitude to Dr. R. Kennedy for his interest and advice in directing this research.

The author would also wish to thank Professor E.C. Ellwood for his interest and Mr. R.M. Jamieson for his practical assistance.

The research was undertaken in the Department of Metallurgy of the Royal College of Science and Technology while the author was in receipt of a research grant from the Department of Scientific and Industrial Research.